# New Stationary Phases for High-Performance Liquid Chromatography of Biomolecules

By

**Mohammad Talebi**

A thesis submitted in fulfilment of the requirements for the degree of

**Doctor of Philosophy**


UNIVERSITY OF TASMANIA

**School of Chemistry**
**Hobart campus**

**Submitted May 2013**

## Declarations

I hereby declare that this thesis contains no material which has been accepted for the award of any other degree or diploma in any tertiary institution, and to the best of my knowledge contains no copy or paraphrase of material previously published or written by any other person, except where due reference is made in the text of the thesis.

**Mohammad Talebi**

This thesis may be made available for loan and limited copying in accordance with the *Copyright Act* 1968.

**Mohammad Talebi**

University of Tasmania

Hobart

## Acknowledgements

This project was supported by a PhD scholarship from the Pfizer Analytical Research Centre (PARC), Australian Centre for Research on Separation Science (ACROSS) and University of Tasmania. The tuition fee was covered by a grant from the State Government of Tasmania, Department of Economic Development and Tourism.

This work would have not been possible without the kind support of the following people:

First of all, I would like to express my sincere gratitude and appreciation to my supervisors who kindly provided me this opportunity, Prof Emily Hilder and Prof Paul Haddad, for their patience, time and their continuous support throughout my PhD and thereafter.

My co-supervisors at Pfizer Inc., USA, Dr Nathan Lacher and Dr Qian Wang are acknowledged for their time, support and invaluable comments during this project.

I thank all my friends, labmates and members of ACROSS for their friendship, collaboration and advice, including Jason Hon, Lea Mauko, Tom Kazarian, Cameron Johns, Joe Hutchinson, Éadaoin Tyrrell, Esme Candish, Tim Causon, Oscar Potter, Jeremy Deverell, and A/Prof Joselito Quirino. I specially thank Dr Anna Nordborg and Dr Dario Arrua for contributing many valuable ideas and useful discussions to this work.

Prof Pavel Nesterenko is thanked for his useful advice and comments, and A/Prof Greg Dicinoski for providing me the teaching opportunity as a demonstrator for KRA336.

All past and present staff of the School of Chemistry are acknowledged for their endless support, including Anthony Malone, Murray Frith, Andrew Grose, Brendon Schollum and Clodagh Moy.

The staff of Central Science Laboratory (CSL) are thanked for their excellent technical support, including Dr Karsten Gömann, for his kind assistance and expertise in using the scanning electron microscope facilities, Dr Thomas Rodemann for providing the access to the FT-IR instrument, and Peter Dove in Central Mechanical Workshops for his expertise and efforts.

I wish to acknowledge all my friends in Hobart for their true friendship and company and for all the great times and memories that I've had with them, including Manish Khandagale, András and Kriszta Gáspár, and Joan Isherwood.

And finally, I would like to dedicate this work, first and foremost, to my wife, Mitra, who not only accepted all difficulties in my passion for the academic life, but also encourages me to pursue my dreams with continuous love and support; and second, to our families in Iran, for their patience and emotions. I appreciate the sacrifices they all made en route to completion of this undertaking.

## Abbreviations

| | |
|---|---|
| ACN | Acetonitrile |
| AIBN | 2,2′-Azobisisobutyronitrile |
| AMH | Ammonium hydroxide |
| BACM | 4-[(4-aminocyclohexyl)methyl] cyclohexylamine |
| BSA | Bovine serum albumin |
| CE | Capillary electrophoresis |
| CEX | Cation-exchange |
| CF | Chromatofocusing |
| cIEF | Capillary isoelectric focusing |
| 2D | Two dimensional |
| DBC | Dynamic binding capacity |
| DEA | Diethylamine |
| EDA | Ethylenediamine |
| EDMA | Ethylene dimethacrylate |
| ESI | Electrospray ionisation |
| GLT | Glass-lined tubing |
| GMA | Glycidyl methacrylate |
| HIC | Hydrophobic interaction chromatography |
| HILIC | Hydrophilic interaction liquid chromatography |
| IEC | Ion-exchange chromatography |
| IEX | Ion-exchange |
| Lys-C | C-terminal lysine |
| mAb | Monoclonal antibody |

| | |
|---|---|
| MD | Multi-dimensional |
| MPD | Median pore diameter |
| MW | Molecular weight |
| PEA | *O*-Phosphorylethanolamine |
| PEG | Polyethylene glycol |
| PETA | Pentaerythritol triacrylate |
| p*I* | Actual isoelectric point |
| $pI_{app}$ | Apparent isoelectric point |
| RPLC | Reversed-phase liquid chromatography |
| SCX | Strong cation-exchange |
| SEA | 2-Aminoethyl hydrogen sulfate |
| SEC | Size exclusion chromatography |
| SEM | Scanning electron microscopy |
| TEA | Triethylamine |
| TOF-MS | Time of flight-mass spectrometer |
| UHPLC | Ultra high pressure liquid chromatography |
| WAX | Weak anion-exchange |
| WCX | Weak cation-exchange |

# Publications

## Papers in peer-reviewed journals:

1) *M. Talebi, A. Nordborg, A. Gaspar, N.A. Lacher, Q. Wang, X.Z. He, E. F. Hilder, P.R. Haddad;* Charge heterogeneity profiling of monoclonal antibodies using low ionic strength ion-exchange chromatography and well-controlled pH gradients on monolithic columns. *Submitted to* ***Journal of Chromatography A*** (chapter 3).
2) *M. Talebi, R. D. Arrua, A. Gaspar, N.A. Lacher, Q. Wang, P.R. Haddad, E.F. Hilder;* Epoxy-based monoliths for capillary liquid chromatography of small and large molecules. ***Analytical and Bioanalytical Chemistry****, 405 (2013) 2233-2244* (chapter 5).
3) *R. D. Arrua, M. Talebi, T. Causon, E.F. Hilder;* Review of recent advances in the preparation of organic polymer monoliths for liquid chromatography of large molecules. ***Analytica Chimica Acta****, 738 (2012) 1-12* (chapter 1).

## Conferences:

1) *M. Talebi, N. A. Lacher, E. F. Hilder, P. R. Haddad; W*ell-controlled pH gradient cation-exchange chromatography-mass spectrometry for charge heterogeneity profiling of monoclonal antibodies. *24th Australia and New Zealand Society for Mass Spectrometry Conference (ANZSMS24),* 2-6 Feb **2013**, Melbourne, Australia, *(oral communication).*

2) *M. Talebi, E.F. Hilder, P.R. Haddad, N.A. Lacher, Q. Wang;* Epoxy-based monolithic columns for capillary liquid chromatography of small and large molecules. *38th International Symposium on High Performance Liquid Phase Separations and Related Techniques (HPLC 2012),* 16-21 Jun **2012**, Anaheim, CA USA *(poster presentation).*
3) *M. Talebi, E.F. Hilder, P.R. Haddad, N.A. Lacher, Q. Wang;* Polymeric cation-exchange monolithic columns for capillary liquid chromatography of proteins. *11th Asia-Pacific International Symposium on Microscale Separations and Analysis (APCE2011),* 27-30 Nov **2011**, Hobart, Australia *(poster presentation).*
4) *M. Talebi, A. Nordborg, E.F. Hilder, P.R. Haddad, N.A. Lacher, Q. Wang, J. Wang;* Polymeric monolithic ion-exchange stationary phases in combination with pH gradient for the separation and purity profiling of monoclonal antibodies.
    - *International Symposium on Drug Analysis (Drug Analysis 2010),* 21-24 Sep **2010**, Antwerp, Belgium *(Invited lecture).*
    - *18th Annual RACI Research & Development Topics Conference,* 5-8 Dec **2010**, Hobart, Australia (*oral communication*).
5) *Nordborg, M. Talebi, E.F. Hilder, P.R. Haddad, B. Zhang, J. Wang,* Polymeric monolithic ion-exchange stationary phases for the separation and purity profiling of biopharmaceuticals, *29th International Symposium on the Separation of Proteins, Peptides &*

*Polynucleotides.* 25-28 Oct **2009**, Delray Beach, Florida, USA *(oral communication).*

6) *E.F. Hilder, A. Nordborg, M. Talebi, P.R. Haddad, B. Zhang, J. Wang;* High performance ion-exchange phases for the separation of therapeutic proteins. *24th International Symposium on Microscale Bioseparations,* 19-22 Oct **2009**, Dalian, China *(invited lecture).*
7) *E.F. Hilder, A. Nordborg, M. Talebi, P.R. Haddad, B. Zhang, J. Wang,* High performance ion-exchange stationary phases for the separation of therapeutic proteins and oligonucleotides, *International Ion Chromatography Symposium-IICS.* 21-24 Sep **2009**, Dublin, Ireland *(invited lecture).*

## Statement of Co-Authorship

The following people and institutions contributed to the publication of work undertaken as part of this thesis:

- *Candidate:* Mohammad Talebi, Pfizer Analytical Research Centre (PARC), ACROSS, School of Chemistry, UTAS
- *Author 1:* R. D. Arrua, ACROSS, School of Chemistry, UTAS
- *Author 2:* T. Causon, ACROSS, School of Chemistry, UTAS
- *Author 3:* A. Gaspar, ACROSS, School of Chemistry, UTAS
- *Author 4:* A. Nordborg, ACROSS, School of Chemistry, UTAS
- *Author 5:* E.F. Hilder, ACROSS, School of Chemistry, UTAS
- *Author 6:* P.R. Haddad, ACROSS, School of Chemistry, UTAS
- *Author 7:* N.A. Lacher, Analytical R&D, Pfizer BioTherapeutics Pharmaceutical Sciences, Chesterfield, MO, USA
- *Author 8:* Q, Wang, Analytical R&D, Pfizer BioTherapeutics Pharmaceutical Sciences, Chesterfield, MO, USA
- *Author 9:* X.Z. He, Analytical R&D, Pfizer BioTherapeutics Pharmaceutical Sciences, Chesterfield, MO, USA

**Author details and their roles:**

**Paper 1: Review of recent advances in the preparation of organic polymer monoliths for liquid chromatography of large molecules.**
*Located in chapter 1 (Note: Only a section of this paper is included in this thesis)*
*Candidate was the second author (25%) and with author 1 (40%), author 2 (15%) and author 5 (20%) wrote sections of the review article. Author 5 contributed to the refinement and final corrections, and author 1 contributed to the submission.*

**Paper 2: Epoxy-based monoliths for capillary liquid chromatography of small and large molecules**
*Located in chapter 5*
*Candidate was the first author (50%) and contributed to designing and performing experiments, and writing. Author 1 (8%) contributed to designing and performing an experiment. Author 3 (7%) assisted with an experiment. Author 5 (15%) contributed to concepts, proof reading, refinement and submission. Author 6 (10%) with author 7 (5%) and 8 (5%) contributed to the proof reading and corrections.*

**Paper 3: Charge heterogeneity profiling of monoclonal antibodies using low ionic strength ion-exchange chromatography and well-controlled pH gradients on monolithic columns**

*Located in chapter 3*
*Candidate was the first author (45%) and contributed to designing and performing experiments, and writing. Author 3 (10%) contributed to designing and assisted with an experiment. Author 9 (10%) contributed to designing and performing an experiment. Author 5 (10%) and author 6*

*(10%) contributed to designing, proof reading, refinement and submission. Author 4 (5%), with author 7 (5%) and author 8 (5%) contributed to the proof reading and corrections.*

We the undersigned agree with the above stated "proportion of work undertaken" for each of the above published (or submitted) peer-reviewed manuscripts contributing to this thesis:

Signed: _____ _____

*Prof. Emily Hilder*
*Supervisor*
*School Of Chemistry*
University of Tasmania

*A/Prof. Greg Dicinoski*
*Head of School*
*School of Chemistry*
University of Tasmania

Date: 20/02/13

## Abstract

This work presents a study on the preparation and application of polymer monoliths for the liquid chromatography of biomolecules with a focus on the ion-exchange (IEX) mode.

As one important application of polymer monoliths in bioanalysis, charge heterogeneity profiling of monoclonal antibodies (mAbs) in different biopharmaceuticals was performed by developing an elution approach based on shallow pH gradient, generated using single component buffer systems as eluents through cation-exchange (CEX) monoliths as stationary phases. A useful selection of small molecule buffer species is described that can be used within very narrow pH ranges (typically 1 pH unit) defined by their buffering capacity for producing controlled and smooth pH profiles when used together with porous polymer monoliths. The results obtained appeared to be consistent with those obtained by imaged capillary isoelectric focusing (iCE) in terms of both resolution and separation profile. The retention mechanism based on the trends observed for proteins at pH values higher than the electrophoretic p*I*, as well as the high resolution gains, were discussed using applicable theories. Very low ionic strength eluents also enabled direct coupling of the ion-exchange chromatography (IEC) to mass spectrometer for further characterisations of mAbs. Although there are few reports of IEC-MS technique for small proteins in which the IEX column is directly interfaced to the mass spectrometer, the employment of a linear pH gradient elution scheme directly interfaced to

mass spectrometer for the analysis of large proteins such as mAbs is also unique in the present work.

New polymer monoliths were prepared in 100 µm i.d. capillaries by thermally-initiated co-polymerisation of glycidyl methacrylate as reacting monomer and pentaerythritol triacrylate as a hydrophilic cross-linker. The monolith recipe and polymerisation conditions were optimised to obtain a homogeneous monolith with good mechanical stability and characteristics suitable for separation of biomacromolecules. Nevertheless, shrinkage of the material prevented making monoliths in a column with conventional dimensions. Post-polymerisation modification of the monolith was performed *via* optimised reaction conditions in order to incorporate weak cation-exchange (WCX) or strong cation-exchange (SCX) functionalities using amine reagents respectively containing phosphoric acid or sulforic acid groups. Dynamic binding capacities up to 15.1 mg/mL were measured using lysozyme as a standard probe, which is comparable or greater from some of the commercially available columns. Compared to monoliths reported previously for the same purpose, the developed monoliths also demonstrated negligible hydrophobicity with separation efficiency of approximately 55,000 plates/m in isocratic separation of sample proteins.

A versatile epoxy-based monolith was synthesised in 100 µm i.d. capillaries by polycondensation polymerisation of glycidyl ether 100 with ethylenediamine using a porogenic system consisting of polyethylene glycol, *MW* = 1000, and 1-decanol. Polymerisation was performed at 80 °C for 22 h. The resultant monolith possessed hydrophilic properties

originating from the incorporation of hetero-atoms in the monolith skeleton which was further strengthened by simple acid hydrolysis of residual epoxides, resulting in a mixed diol-amino chemistry. The modified column was used successfully for hydrophilic interaction liquid chromatography (HILIC) of small molecule probes, such as nucleic acid bases and nucleosides, benzoic acid derivatives, as well as for peptides released from a tryptic digest of cytochrome c. The mixed mode chemistry allowed both hydrophilic partitioning and IEX interactions to contribute to the separation, providing flexibility in selectivity control. Residual epoxide groups were also exploited for incorporating a mixed IEX chemistry. Alternatively, the surface chemistry of the monolith pore surface rendered hydrophobic *via* grafting of a co-polymerised hydrophobic hydrogel. The inherent hydrophilicity of the monolith scaffold also enabled high performance separation of proteins under IEX and hydrophobic interaction (HIC) modes and in the absence of nonspecific interactions.

## Table of Contents ..... Page

# *Chapter 1*

# Literature review

## 1.1 Overview

The developments in molecular and cell biology in the last quarter of the 20th century led to new technologies for the production of complex biomolecules being divided into two main categories: proteins and nucleic acids [1]. Biopharmaceuticals have the potential to assist in human health care in the areas of diagnostics, prevention and treatment of diseases. In 1982 the Food and Drug Administration (FDA) approved human insulin synthesized in *Escherichia coli* as the first recombinant therapeutic product in the United States. Advances in biotechnology have broadly expanded the variety of therapeutics, including hormones, cytokines, vaccines, and monoclonal antibodies (mAbs). Among these developing therapeutics, mAbs are particularly attractive as they can be designed to selectively target tumour cells and elicit a variety of responses once bound. Until 2005, more than 206 unique therapeutic mAbs have been studied in clinical trials for a variety of cancer indications worldwide [2, 3]. These advances of recombinant proteins were made possible by the development of efficient and reproducible production and purification systems that permit manufacture of these

complex molecules in large amounts with consistent quality suitable for human use [4]. Simultaneous with this growth has been the proliferation of biotechnology companies. There are about 1300 companies competing for this market [3]. In 2000, annual sales of biopharmaceuticals in the United States alone comprised approximately 10% ($8 billion) of all therapeutic sales in the country [3].

Control of the quality of biopharmaceuticals is crucial not only during large scale manufacturing but also during the research and development phases, as impurities and contaminants have to be characterized and reduced to acceptable levels. Hence, the increased attention toward biotechnology products in the last three decades has challenged both the regulatory authorities responsible for approving new drugs and the biotechnology industries, which must consistently produce a definable and safe product.

There is an overwhelming interest in the separation of biological molecules by chromatographic techniques, for example, in pharmaceuticals or for medical diagnostics. In particular, the application of high-performance liquid chromatography (HPLC) to the separation of both biomacromolecules and their related small molecules has increased considerably over the last two decades. Whereas reversed-phase chromatography (RPLC) is the most commonly used mode of separation for peptides and small molecules, the three-dimensional structure of proteins can be sensitive to the often harsh conditions employed in RPLC. Preferably, IEC, size-exclusion chromatography (SEC) and hydrophobic

interaction chromatography (HIC) are the most commonly used modes for the separation of bio(macro)molecules when preserving the native structure of the biomolecule is also of interest [5, 6].

## 1.2 IEC of biomolecules

IEC is a method of separating proteins based on differences in their net charge. IEC can be a highly selective chromatographic technique, being able to resolve, for example, proteins which differ by only a single charge [7]. Due to the orthogonality of separation mechanism to RPLC, IEC is often used as the first dimension in two dimensional (2D) separations. For example, on-line IEC-RPLC was developed for automated shotgun proteome analysis [8]. IEC is advantageous in providing fast separation of biomolecules with high recoveries and resolving power. Also, buffer components are non-denaturing and IEC can be used as a preconcentration step to recover proteins from a dilute solution [9]. Compared with HIC, lower salt concentration is used in IEC, thus precipitation of biomolecules due to the high salt concentration can be avoided [9].

The disadvantages of IEC are few, but include 1) the sample must be applied to the IEC column under conditions of low ionic strength and controlled pH, which sometimes requires an extra step of buffer exchange to be conducted, 2) chromatographic instrumentation should be resistant to salt-induced corrosion, and 3) post-chromatographic preconcentration of dilute solutions of recovered proteins can result in high salt

concentrations (typically more than 1 M), which is unsuitable, for example, in biological assays unless buffer exchange is carried out [10].

Based on the classical net charge theory the separation process in IEC relies upon the formation of electrostatic interactions between the charged groups on biomolecules (typically, amines, carboxylic acids, sulfonic acids and phosphoric acids), and an ion-exchange sorbent carrying the opposite charge. Non-bound biomolecules (i.e., neutral molecules which do not carry any electrical charge or molecules carrying the same charge as the ion-exchanger) are not retained in the column, and bound biomolecules are recovered by elution with a buffer of either higher ionic strength, or altered pH. The basic concepts involved in this theory imply that 1) at their isoelectric point (p*I*) proteins will not be retained because the net charge is zero, 2) proteins will be retained on positively (negatively) charged anion (cation) exchangers when the pH of the eluent is greater (lower) than their p*I* because they have a net negative (positive) charge, and 3) there is a functional relationship between the net charge and retention time of proteins [11].

Lesins and Ruckenstein [12] indicated, along with others [13, 14], that the net charge theory is an over-simplification of protein adsorption on charged sorbents. This is because of two reasons: significant retention in IEC may occur at the p*I*, where correlation between net charge and retention is poor [11]. These authors suggested that charge localization on the protein surface that is quite different from the net charge of the molecule may occur. Regnier emphasized the importance of

heterogeneity on the protein surface and its relation to protein adsorption [15]. Lesins and Ruckenstein [12] indicated that if there is a non-uniform charge distribution on the protein surface, it is not necessary for the net charge of the protein to be opposite to that of the ion-exchanger for adsorption due to electrostatic interactions to occur; instead the occurrence of oppositely charged patches is all that is necessary. These charged patches and the subsequent heterogeneity in the protein-ion exchanger contact region would significantly affect the conformational changes encountered by proteins during the separation process.

### 1.2.1 pH gradient elution

In the classic mode of IEC, proteins are eluted using a salt gradient (most often NaCl) with the eluent pH being nearly constant. While the resolving power of IEC by this approach is high, the same can be said regarding the amount of effort required to fully optimise a method. The design of an optimal IEC process is not straightforward due to the involvement of numerous interrelated parameters such as, type of stationary phase, dimension of the column, amount of sample loaded, loading and eluting buffer (type, concentration and pH), mode of elution (isocratic, gradient or stepwise), and slope of the gradient elution profile [16]. Besides, once the method development is completed, a method is usually product-specific with very limited robustness; eg., eluent pH has shown a robustness tolerance as low as ±0.05 pH units around the optimised value [17]. It has also been shown that complex pH transitions occur in response to salt gradient [18-20]. Consequently, the retention and

separation efficiency are affected by the characteristics of both salt gradient and eluent pH [21].

Yamamoto and Ishihara observed that the resolution of β-lactoglobulin A and B in IEC is highest when the eluent pH is near the pI of proteins (5.1 and 5.2) [22]. This behaviour was related to the enhancement of adsorption affinity of these proteins near their isoelectric points. However, salt gradient IEC is generally operated at a fixed eluent pH, which cannot be generalised as the optimum pH when several proteins are being separated [23]. Finally, the chief deficit of salt gradient IEC is that proteins with the same number of effective charges will be eluted from the ion exchanger close to each other. This limits significantly the selectivity of IEC when complex protein mixtures are separated [24]. The situation will be even worse when protein charge variants are to be resolved. These variants arise from modifications of the amino- and carboxylic-termini and amino acid side chains [25]. While with small proteins, such as recombinant human growth hormone, separation of all charge species is possible, the number of possible charge variants increases when the size of proteins is increased [26]. As changes in charge from different modifications may be additive or subtractive, IEC becomes even more complex and the overall resolution of individual variants is likely to be lost. This is particularly a matter of concern for important large proteins, such as mAbs, for which their characterisation poses many challenges for therapeutic use in humans. For example, Rozhkova showed that even a 3% change in the pH of eluents or the

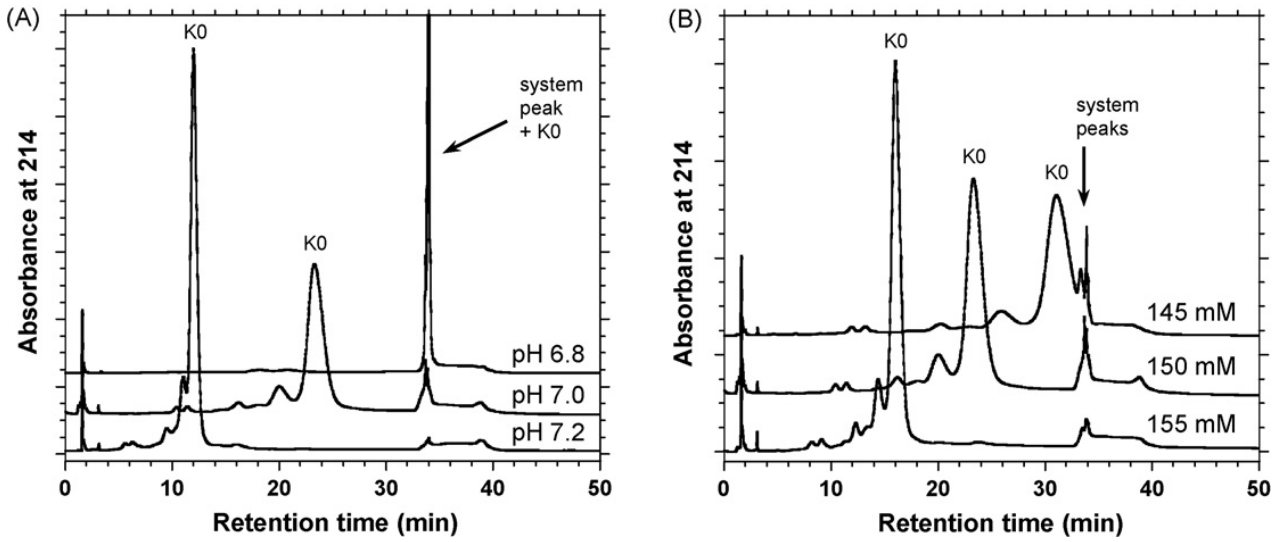


**Figure 1.1:** The sensitivity of CEX chromatography into the eluent pH (A) and the eluent concentration (B) in analysis of an mAb sample treated with Carboxypeptidase B prior to analysis (reprinted with permission from Ref. [21]).

concentration of strong eluent during cation-exchange (CEX) chromatography of a recombinant humanised mAb resulted in a significant shift in retention times (> 5 min) and also loss in resolution, as a result of co-elution of some species (see **Figure 1.1**) [21].

Internal pH-gradient or chromatofocusing (CF) is an IEC technique developed by Sluyterman and co-workers in the late 1970s for pH-based separation of proteins [27-31]. The technique most commonly utilises the buffering capacity of a weak-anion exchange (WAX) column to generate a (preferably) linear pH gradient inside the column. The column is equilibrated with a high pH buffer (equilibrating buffer), followed by loading of a protein sample. Retained proteins are then eluted in the order of their apparent isoelectric points (p$I_{app}$), which are in general close to their actual isoelectric points (p$I$), upon a step change to a

second buffer (focusing buffer) of lower pH. To obtain a linear pH gradient over a wide pH range (and hence larger peak capacity), the buffers traditionally contain mixtures of polyampholytes with a wide range of p$K_a$ values to produce an even buffering capacity over the chosen pH range.

As the focusing buffer descends through the column, various ampholyte components bind differentially to the stationary phase developing an internally retained pH gradient. Consequently, the protein is sequentially eluted from the stationary phase when the pH of the focusing buffer is slightly higher than the protein p*I* and is retained again when the buffer pH falls slightly below the p*I* [30]. This progressive titration of the stationary phase causes focusing of the protein band and generally results in high resolution separation of proteins when compared to salt gradient IEC [32, 33]. This approach, however, suffers from some limitations. Polyampholyte buffers tend to be expensive and due to the way they are manufactured, tend to exhibit batch-to-batch irreproducibility in composition [34, 35]. They are difficult to remove from isolated proteins due to the formation of association complexes, and also exhibit high UV absorption [32]. These limitations were addressed by a number of workers who investigated the use of a simple mixture of buffer species in the focusing buffer. Frey and his co-workers [23, 34, 36, 37] developed a model to accurately predict the separation in CF using buffers composed of only simple mixtures of amine buffering species for covering the desired pH range. Using this model, an optimised buffer composition was predicted to produce a linear pH gradient over a wide

pH range of 9.5 to 5.5 inside a diethylaminoethyl (DEAE)-WAX column. This buffer was composed of 2.4 mM Tris, 1.5 mM imidazole and 11.6 mM piperazine and demonstrated very good agreement between predicted and experimentally measured pH profiles. The performance of this buffer system was also demonstrated by CF separation of human hemoglobins $A_0$ and $S_1$ variants, and equine myoglobin [36].

An alternative to CF is the external pH-gradient approach proposed by Anderson *et al.* [33, 35, 38, 39] which utilises pump proportioning to generate a pH gradient prior to the column with minimal buffering capacity. Buffers are composed of simple amine species that have their p$K_a$ values evenly distributed over the desired pH range. Under such conditions, the contribution from the column itself to the delay of the pH-gradient is minimal, which allows for easier method development and optimisation, since the slope and profile of the pH gradient can be controlled by the pump with less dependence on column chemistry [17, 32].

pH-based IEC was employed by some workers for isolation of antibodies from biological samples. Waldrep and Schulte [40] employed a step pH gradient and a DEAE column for fractionation of four immunoglobulin G (IgG) subclasses (IgG1-4). A descending pH gradient was established from 9 to 6 using 20 mM Tris-acetate buffer. Buffers covering a wider pH range (3.8-10) were developed by Ahmed *et al.* [16] for selective isolation of a mAb from hybridoma cell culture supernatant.

Buffers were composed of 20 mM each of citric acid, sodium phosphate, Bicine, and N-Cyclohexyl-2-aminoethanesulfonic acid (CHES).

Profiling the charge-related heterogeneity of proteins, including mAbs, is one of the important applications of IEC. MAbs have gained significant attention as potential therapeutics due to their qualities, such as high degree of specificity in binding to target antigens, ability to initiate immune response to the target antigen and long serum persistence, which reduces the need for frequent dosing [41, 42]. For biopharmaceutical development, product consistency and long shelf life are important factors that provide flexibility in manufacturing. During manufacture, various forms of microheterogeneity in an antibody's size or charge can occur due to enzymatic processes or spontaneous degradation and modifications, including for example, deamidation, oxidation, isomerisation and fragmentation [43]. Almost all of these changes can alter the surface charge properties of the antibody either directly by changing the number of charged groups or indirectly by introducing structural alterations [42]. These variants need to be characterised, for example, for quality control purposes or improving formulations in order to minimise further degradation during storage of the purified antibody. While conventional salt gradient IEC is generally product-specific, i.e., requires several method parameters to be optimised for each individual antibody [44], recent reports on pH-based separation of mAbs have demonstrated the required multi-productivity, high-resolution and robustness against variations in sample matrix salt concentration and pH [17, 21, 44].

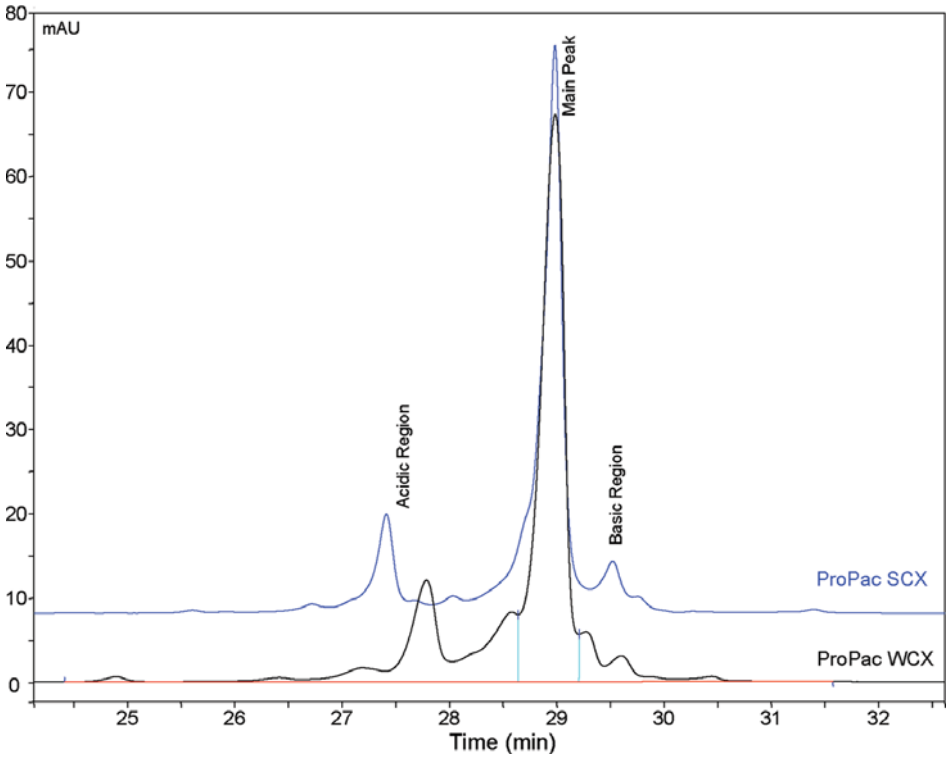


**Figure 1.2:** pH gradient CEX chromatography of a mAb sample using Dionex® particulate packed columns containing WCX or SCX chemistry (reprinted from Ref. [17]).

Farnan and Moreno [17] demonstrated a high-resolution separation of charge heterogeneity in a series of intact mAbs having p*I* values from 7.3 to 9.1 using a buffer system that originally was optimised by Kang and Frey [34] for CF of proteins (see **Figure 1.2**). Interestingly, while the buffer composition had been optimised for WAX chemistry under CF mode, an ascending gradient of buffers mixed externally and delivered into a ProPac WCX column also demonstrated a pH profile with the same linearity over a pH range of 6 to 9.5. The method was also validated following industry standard validation practices and demonstrated good robustness and precision being independent of sample matrix and composition [44].

Due to the large size of antibodies, suitable chromatographic resolution is usually hard to achieve. Generation of Fab and Fc fragments by papain digestion has been used to simplify the separation [42]. Regnier and co-workers used a strong CEX column for purification of Fab fragments (p*I* values 5.4, 5.5 and 5.8) generated from the papain digestion of an anti-cortisol IgG2B antibody [45]. Protein isoforms were separated by running a pH gradient from pH 4.5 to 6.4 generated using 10 mM N-Cyclohexyl-2-aminoethanesulfonic acid (MES). Despite incomplete resolution of the isoforms, up to 90% purity was determined for the collected fractions analysed by capillary electrophoresis (CE).

Analysis of individual fragments also allows determination of the location where heterogeneity has happened in the antibody. Typically, enzymatic digestion of the antibody followed by analysis of the resulting peptide fragments by liquid chromatography-mass spectrometry (LC-MS), referred to as peptide mapping, is performed to identify the modification. MS/MS study can also be performed to identify the precise position of the modification within the peptide [25, 42, 46]. As an example, a new form of mAb cysteine-related heterogeneity in the hinge region of an IgG2 was discovered by fractionation of an antibody sample using AEX chromatography followed by enzymatic digestion of fractions resulting in C-terminal lysine (Lys-C) variants [47]. MS/MS experiments uncovered the replacement of up to two disulfide bridges with a similar number of trisulfides in the antibody hinge region. AEX chromatography was performed on a ProPac WAX-10 column by running a pH gradient elution with a buffer system consisting of 2.4 mM 3-(N-

morpholino)propanesulfonic acid (MOPS), 1.4 mM imidazole and 11.6 mM piperazine at pH 7 and 5.5 as eluents A and B, respectively.

The external pH gradient approach also benefits from the flexibility in using a wide spectrum of buffer species. While mostly amine-based species are usually used as buffer components, the feasibility of common inorganic buffer species such as phosphate for pH-based separations of proteins has been also demonstrated by some workers. Different Lys-C variants generated *via* various enzymatic digestion methods in a recombinant mAb (human anti-tumour necrosis factor mAb D2E7) were successfully resolved using a ProPac WCX-10 column and a typical eluent composition used in CEX chromatography of proteins at different pH [48]. Accordingly, 10 mM phosphate buffer pH 7.5 was used as eluent A and 500 mM NaCl in 10 mM phosphate buffer pH 5.5 as eluent B. This system actually took advantage of combining both salt and pH gradient approaches. Capillary isoelectric focusing (cIEF) and LC-MS analysis were also performed for further characterisation of deglycosylated and reduced antibody fractions collected from CEX chromatography. More recently, Rozhkova demonstrated that resolving Lys-C variants with the same column chemistry is also feasible in the absence of a NaCl gradient [21]. Instead, the ionic strength of buffers was kept constant by adding 60 mM NaCl to both eluents (10 mM phosphate) and the pH gradient was established in a very narrow pH range of 6.7 to 7.5. For comparison, separation was also carried out under the salt gradient approach. Unlike the pH gradient, minor changes in phosphate buffer pH (± 0.2 pH unit) or NaCl

concentration in eluent B (± 5 mM) caused catastrophic effects on separation efficiency and resolution.

## 1.3 Monolithic columns: preparation and applications

To a great extent, the remarkable success of HPLC in bioseparations has been achieved as a result of advances in column technology centred mostly on increasing the separation capacity, enhancing the detection sensitivity and increasing the analysis throughput [49]. While particle packed-columns traditionally represent the most commonly used media in HPLC, their application for separation of macromolecules is particularly limited due to the slow diffusional mass transfer into the mobile phase presented in the pores of beads and also into the void between the packed particles [50]. Another limitation of packed-beads can be seen in high-throughput macro- and nano-scale separations [49]. According to Gidding's theory [51], resolution, efficiency and throughput of a separation in such scales benefit from sub-micrometre sized particles (< 2 μm). However, both preparation and application of these columns demand extraordinarily high back-pressures and necessitate employing costly equipment such as ultra-high pressure liquid chromatography (UHPLC) systems. These challenges have been well-addressed through recent advances in column technology, such as core-shell technology and also the development of a new generation of HPLC columns, namely monolithic columns (for which their preparation for bioanalysis is the main focus of the present study).

Separation using conventional packed columns is inherently slow due to the diffusional constraints, as they exhibit a rapid reduction in resolution and separation capacity with increasing eluent velocity [50]. On the other hand, the efficient isolation of labile biomolecules requires a fast and reliable separation process working under mild conditions in order to decrease losses due to biomolecule degradation.

Monolithic materials are characterised by their numerous interconnected cavities (pores) of different sizes and their structural rigidity which is secured through extensive crosslinking. Although the contribution of mobile phase in mass transfer (Cm term in the Van Deemter equation) of small molecules in monoliths is generally larger than that of packed columns, in the case of large molecules such as proteins, the Cm would be predominantly convective, rather than diffusive like particulate sorbents, and therefore prevents loss in separation efficiency at higher flow-rates [50, 52-54]. However, while for packed columns an increase in efficiency can be achieved by using particles of smaller size, the efficiency of monolithic stationary phases-particularly in separation of small molecules-can be maximised by optimising the domain size, i.e., the combined average size of the macropores and microglobules. The smaller domain size is favourable as it improves the efficiency by minimising both the C-term and the Eddy dispersion (the A term in the Van Deemter equation) [55].

Such a porous structure can be created from inorganic precursors, resulting in bimodal silica-based materials. Typical features

characterising this kind of monolith are a bicontinuous skeleton comprising flow-through pores or macropores (typically ~ 2 μm in size), along with skeletal pores or mesopores (typically 2-50 nm). Such a pore distribution provides a typical surface area around 300 $m^2/g$, depending on the preparation conditions [53]. Silica-based monoliths have proved to be well-suited for the separation of small molecules where their high surface area provides adequate retention for desired efficiency and selectivity. While quite successful for small molecule separations, the application of silica-based monoliths for efficient separation of large molecules is limited owing to the restricted diffusion of solutes into the monolith mesopores [56]. Other issues associated with silica-based monoliths include the radial inhomogeneity (comparable to the level seen in polymer monoliths), their limited pH tolerance, complicated and sensitive production procedures, and the limited number of monomers and solvents available for their preparation [53, 57].

Polymeric monoliths are the other main category of monolith materials developed in the late 1980s and early 1990s [58, 59]. From the very beginning this type of monoliths has proven to be well suited for the (fast) separation of proteins [59-61]. Simple and single step preparation from a wide variety of monomers also enables application of polymeric monoliths to be far beyond chromatographic demands in areas, such as microfluidics, preconcentration and solid-phase extraction units as well as catalytic supports [62-68].

Polymeric monoliths are usually prepared *via* a free radical polymerisation reaction from a mixture of initiator, monomers (including crosslinking monomer) and pore-forming solvents (porogens) that are polymerised *in situ* in a mould, for example a tube, capillary or the channels of a microfluidic device. A binary mixture of solvents is typically used as porogen to allow tuning of porous properties and morphology of the monolith. The type of initiator is also chosen in accordance with the fashion that the polymerisation reaction is triggered, which is usually thermal or photo-initiation [69].

Since their emergence about two decades ago, monolithic columns have been extensively investigated by many researchers leading to a significant impact of this concept on separation science [66]. The vast variety of methods enabling the preparation of monoliths as well as the wide spectrum of their applications has been well documented in numerous reviews, *eg.* see [53, 57, 66, 69-72]. Very recently, we also summarised in a review the recent developments in the preparation of polymeric monoliths for liquid chromatography of large molecules [73]. Therefore here, one important aspect of polymeric monoliths in bioseparations that has captured less attention, i.e., biocompatibility, is discussed with the focus on IEC as one of the most commonly used HPLC modes for bioseparation.

### 1.3.1 Biocompatibility in monoliths for bioseparation

The concept of biocompatibility has been transferred to chromatographic stationary phases, such as monoliths, by Li and Lee in 2009 [74]. According to their definition "a biocompatible stationary phase is a material that resists against non-specific adsorption of biomolecules (including peptides and proteins) and does not interact with them in a way that would alter or destroy their structures or biomedical functions."

The type of non-specific interactions actually depends on the mode of chromatography employed. For example, while protein denaturation is a common issue in RPLC of proteins due to the strong hydrophobic interactions involved [74], HIC of proteins is based on the same kind of interactions but with such a low strength that proteins are preserved in their native conformations. This is achieved by utilising mild eluents containing a high concentration of salts (in the absence of organic solvents) and a lower density of bonded ligands (typically 50-1000 mM) [75]. On the other hand, hydrophobic interaction is recognised as a non-specific interaction in IEC where denaturation is likely to occur once secondary interactions between hydrophobic patches of the protein and the stationary phase are stronger than electrostatic interactions involved in IEC [7]. Nevertheless, the existence of mixed-mode effects may provide a wider range of selectivity than that which can be achieved with a single chemistry [76].

The removal of non-specific hydrophobic interactions may be necessary in order to 1) obtain good mass recovery with preserved bioactivity, 2) gain predictable elution behaviour for solutes (which facilitates method optimisation), and 3) avoid slow adsorption-desorption kinetics that lead to significant band broadening [74]. Hydrophilicity of IEC stationary phases is also important from the viewpoint of multidimensional LC setup. IEC followed by RPLC is the most widely used 2D LC. For this combination, negligible mixed-mode interactions (i.e., IEC and HIC) are desired. Otherwise, the resultant 2D LC is not strictly orthogonal and the final overall peak capacity will be compromised [77].

*1.3.1.1 Polyacrylamide-based monoliths*

Soft gel materials such as crosslinked dextran, cellulose, polyacrylamide, agarose and polysaccharides have been historically known for low non-specific interactions with peptides and proteins, and are employed widely in gel electrophoresis and gel permeation chromatography [74]. However, these inert polymers are too soft to be used for HPLC.

Acrylamide (AAm) is a moderately hydrophilic monomer which is typically polymerised with a cross-linker to reinforce the required rigidity into the structure of polymer. In fact, co-polymerization of hydrophilic functional monomers and cross-linkers is a seemingly straightforward approach to obtain biocompatible materials. The most

common cross-linker is N,N′-methylenebisacrylamide (MBAA). This type of monoliths serves generally as a platform for sample preparation or affinity chromatography [72, 74]. For instance, poly(AAm-*co*-MBAA) monolith was prepared by co-polymerisation for potential use in the separation of biopolymers, immobilisation of proteins and solid-phase extraction [78]. Palm and Novotny prepared a porous polymeric monolith as a trypsin microreactor for fast peptide mapping by copolymerisation of AAm, MBAA and N-acryloxysuccinimide in an electrolyte buffer containing polyethylene glycol (PEG) as a molecular template [79]. The monolith featured high permeability and biocompatibility.

*1.3.1.2 Polymethacrylate-based monoliths*

Polyacrylate and polymethacrylate-based monoliths represent the largest and the most examined class of polymeric monoliths, due mainly their suitability for separation of biopolymers, such as proteins and polynucleotides as well as large particles, such as viruses [74, 80]. While there are instances of polymethacrylate-based monoliths for HIC [75, 81] and SEC [82, 83] of proteins, this type of monoliths have been mostly developed for RPLC and IEC applications. Recent advances in polymethacrylate-based monoliths for IEC of biomolecules are reviewed below with the emphasis on biocompatibility (hydrophilicity) of materials.

Co-polymerisation of hydrophilic functional monomers and cross-linkers is a seemingly straightforward approach to obtain biocompatible materials. Compared to silica-based monoliths, polymeric monoliths offer the advantage that by choosing the right functional monomer, monoliths for a variety of chromatographic purposes can be designed, such as for improved biocompatibility. Following their efforts to prepare polymeric monoliths with negligible non-specific interactions, Lee's group recently prepared CEX monolithic columns containing phosphoric acid functionality by co-polymerisation of phosphoric acid 2-hydroxyethyl methacrylate (PAHEMA) and bis[2-(methacryloyloxy)ethyl] phosphate (BMEP), as functional monomers, with polyethylene glycol diacrylate (PEGDA) and polyethylene glycol acrylate (PEGA) *via* photo-initiated polymerisation [84]. Monoliths with different extents of hydrophobicity were obtained. While poly(BMEP-*co*-PEGA) showed the lowest hydrophobicity in the series of columns prepared, the addition of 20% (v/v) acetonitrile to the eluents was still required in order to lessen hydrophobic interactions between natural peptides and the poly(PAHEMA-*co*-PEGDA) monolith. However, these materials showed less swelling and better permeability than the sulfonic acid-containing monoliths prepared previously by the same group [77, 85].

More promising results were obtained with homopolymerisation of MAEP where retention times of peptides and peak capacity varied only slightly with the addition of up to 20% (v/v) acetonitrile to the eluents, suggesting negligible hydrophobic interaction between peptides and the monolith [86]. Although using a single monomer makes the

optimisation of polymerisation conditions easier and improves the reproducibility of the synthesised monolith, careful selection of the parameters involved in polymerisation is still required in order to ensure acceptable rigidity and flow-through properties of the prepared materials. For example, it was shown that BMEP percentages lower than 26.8% (w/w) in the polymerisation mixture resulted in non-rigid materials, whereas non-porous materials were obtained for amounts higher than 31.8%. Also, an increase in UV exposure time from 2 to 5 min revealed no marked influence on the conversion of BMEP, while a further increase to 10 min increased the conversion, as indicated by a 33% increment in dynamic binding capacity (DBC) value to 72.7 mg lysozyme per mL of column volume [86].

In another study, poly(2-carboxyethyl acrylate-*co*-poly(ethylene glycol) diacrylate) was prepared by photo-initiated polymerisation for WCX chromatography of peptides and proteins [9]. While eluent pH has a negligible effect on the ionisation of strong ion-exchangers, it affects the extent of ionisation of weak ion-exchange functionalities, thus providing more opportunities to control selectivity and separation efficiency. Using the prepared column, baseline separation of a mixture of protein standards was obtained without the addition of organic solvents to the eluent. However, a further increase in the content of ethylether as a macropore-forming porogen caused an increase in the hydrophobicity of the monolith obtained. The authors also aimed to introduce more carboxylic acid groups on the surface of the monolith by increasing the ratio of functional monomer to cross-linker, while keeping the porogen

composition constant in the optimised recipe. Although a 50% increase in DBC was measured by this change, substantial hydrophobic interactions were again demonstrated by co-elution of proteins and significant tailing of the lysozyme peak. Interestingly, the opposite trends were observed in their earlier report [84] where an approximately tenfold decrease in DBC was measured by increasing the percentage of the functional monomer, BMEP, in the monomer mixture from 30 to 70%. This confirms again that the functionality obtained at the surface of monoliths synthesised by co-polymerisation is difficult to predict and careful characterisation of the materials is necessary [87].

*1.3.1.2.1 Post-polymerisation modification*

Post-polymerisation modification is another approach to obtaining functional monoliths for IEC. In contrast to the co-polymerisation method, the porous properties of a generic monolith can be optimised independently from the modification of surface chemistry, thereby enabling the preparation of numerous chemistries from the same support monolith [88]. Among others, glycidyl methacrylate (GMA)-based monoliths have been widely used for incorporating different functionalities through the epoxy group, which reacts readily with various reagents containing, for example, amine [89, 90] or thiol groups [91]. While there are several reports (see, eg. [60]) on the synthesis of WAX columns *via* reaction of surface epoxy groups with amines like diethylamide (DEA), less effort has been made to prepare the SAX ones. In one report, quaternary amine functionalities were incorporated into a

poly(GMA-*co*-DVB) monolith in a two-step reaction involving the ring-opening of the epoxy group with DEA followed by the alkylation of the resultant tertiary amine with diethyl sulfate [92]. Recently, a systematic study on the parameters affecting the modification reaction of poly(GMA-*co*-EDMA) monolith with DEA and triethylamine (TEA) was conducted by Bruchet *et al.* [93]. Their results indicated that while 96% of the epoxy groups were converted to tertiary amine functionality after an 8 h reaction in pure DEA at 65 °C, conversion efficiency did not exceed more than 68%, even at 85 °C for the reaction with pure TEA. Subsequently, a significant improvement in reaction efficiency was obtained by the addition of a protic solvent to the reaction. Over 90% transformation to quaternary amine was finally achieved using TEA dissolved in 50% (v/v) aqueous ethanol after 4 h reaction at 85°C. Increasing the reaction time from 4 to 8 h and the amine concentration in aqueous ethanol from 10 to 50% (v/v) showed no further enhancement in the reaction yield. The loading capacity of 10.9 ng/cm was also measured for the SAX capillary column obtained using the breakthrough curves of DNA in a salmon sperm solution (100 ng/μL).

Post-polymerisation modification also enables tailoring the hydrophilicity of the materials. For example, a fairly good transformation of surface chemistry from highly hydrophobic into hydrophilic in styrenic-based materials, such as poly(chloromethylstyrene)-*co*-divinylbenzene was successfully performed through a two-step modification process comprising of a reaction with ethylenediamine followed by γ-gluconolactone [61]. The modified column exhibited

comparable hydrophilicity to a poly(GMA-*co*-EDMA) bead after complete hydrolysis of its epoxy groups to diols. To achieve an increase in hydrophilicity, Ott *et al.* [63] modified the surface of their epoxy-based monolith with a hydrophilic poly(ethyleneglycol) diamine (2k Da) *via* a multi-step approach. The remaining epoxy groups of the generic monolith were first acid-hydrolysed to hydroxyl groups prior to the reaction with 3-glycidyloxypropyltrimethoxysilane. The silanisation reaction was conducted for 1 h at room temperature. The column was then filled with the polymer and incubated at 55 °C overnight in order to afford a hydrophilic coating.

Svec's group developed a UV-initiated photografting approach for the surface hydrophilisation of their classic poly(GMA-*co*-EDMA) monolith, which exhibits significant non-specific interactions with proteins even after a complete hydrolysis of residual epoxide groups to 2,3-dihydroxypropyl functionalities [94]. This undesired adsorption was largely avoided by photografting of a hydrophilic monomer, poly(ethylene glycol) methacrylate (PEGMA, 6 ethylene glycol units), onto the pore surface of poly(2,3-dihydroxypropyl methacrylate-*co*-ethylene dimethacrylate).

*1.3.1.2.2 Surface functionalisation with nanoparticles*

Introduced by Hilder *et al.* in 2004 [95], functionalisation of the pore surface with nanoparticles is the latest technique for tailoring the surface characteristics of monoliths. Nanoparticles can offer numerous

advantages; for example, their large surface-to-volume ratio can potentially enhance separation efficiency [96]. Very efficient separations were also reported with agglomerated latex ion-exchangers, owing to the existence of short diffusional paths, which leads to enhanced mass transfer [97]. This was the rationale behind Thayer *et al.* work who used a ProSwift™ SCX-1S (4.6 mm × 50 mm) monolith column for surface modification [98]. A dilute aqueous solution of pellicular AEX nanobeads (DNAPac PA200) was pumped through the column until break through was observed. The nanobead-coated monolith exhibited a further increase in monolith capacity and mass transfer, along with chromatographic behaviour typical of pellicular phases. The nanobead coating improved separation selectivity and helped control tailing and band broadening associated with hydrophobic interactions when compared to porous bead phases. In addition, the monolith showed separation of derivatized oligonucleotides from their unlabeled parents, and the ability to resolve several isobaric RNA linkage isomers, as well as phosphorothioate diastereoisomers in DNA and RNA.

By taking advantage of the well-known affinity of gold toward the amino and thiol functionalities, Svec's group has recently utilised gold nanoparticles (GNPs) for the modification of poly(GMA-*co*-EDMA) monoliths. In one study they modified the surface of a monolithic capillary column with cystamine followed by immobilisation of GNPs to incorporate a new chemistry for the selective isolation of peptides containing cysteine [99]. The GNPs were held firmly onto the surface of the monolith by stable multivalent linkages that prevented them from

being washed out from the column, even when the eluent contains competing thiol-containing compounds.

In an extension of this surface modification the dynamic nature of the bond between gold and thiol groups has been exploited to tailor the surface chemistry through the binding of a variety of "*exchangeable*" thiol-containing moieties, introducing the concept of monoliths with exchangeable chemistries [90]. Surface modification of the monolith was conducted by pumping a 2.5 mol/L cysteamine solution through the capillary column at a flow-rate of 1 μL/min for 30 min at room temperature, affording a monolith with 1.05 mmol/g thiol groups. Two approaches were examined for incorporation of GNPs: 1) *in situ* preparation *via* reduction of chloroauric acid using sodium citrate, which resulted in 15.37 atom % of gold with 40-50 nm in size, 2) modification *via* pumping a solution ($1.4 \times 10^{12}$ particles/mL) of commercially available preformed nanoparticles (15 nm) on to the thiol rich pore surface of the modified monolith. Although slower than the *in situ* formation of GNPs, this approach was simpler and provided a much higher content of GNPs. Capillary columns with reversed-phase and ion-exchange functionalities were then obtained by flushing the GNP-containing monoliths with 1-octadecanethiol and sodium-2-mercaptoethanesulfonate, respectively, and examined for the rapid separation of a standard protein mixture.

#### 1.3.1.3 Epoxy-based monoliths

It is well accepted that free-radical cross-linking (co)polymerisations inherently lead to heterogeneous polymers [53, 100, 101], given that the cross-linker has at least two vinyl groups. By assuming equal vinyl group reactivity, it is reasonable to expect the rate of consumption of the cross-linker is twice than that of the monovinyl monomer [53, 102]. Consequently, the cross-linker molecules are incorporated into the growing copolymer chains much more rapidly than the monomer molecules forming highly cross-linked nuclei in the early stages of the polymerisation reactions [103]. The high degree of cross-linking in the nuclei leads to a rapid phase separation of the polymer formed in poor porogenic solvents and a gradual coarsening of the monolith structure which results in some degree of structural heterogeneity [53, 104].

While free radical polymerisation utilising vinyl or (meth)acrylate monomers is the most commonly used method for the preparation of monoliths, some attempts have also been made to investigate other polymerisation systems, such as polycondensation. Unlike chain growth polymerisation methods, such as free radical polymerisation, polycondensation is a step growth polymerisation and features repeated activation of the chain end, thus allowing for homogenous growth of all polymer chains in the system no matter how long they are [66]. Typically in this approach, highly ordered 3D structures are created homogenously *via* phase separation polymerisation of epoxy monomers and amine

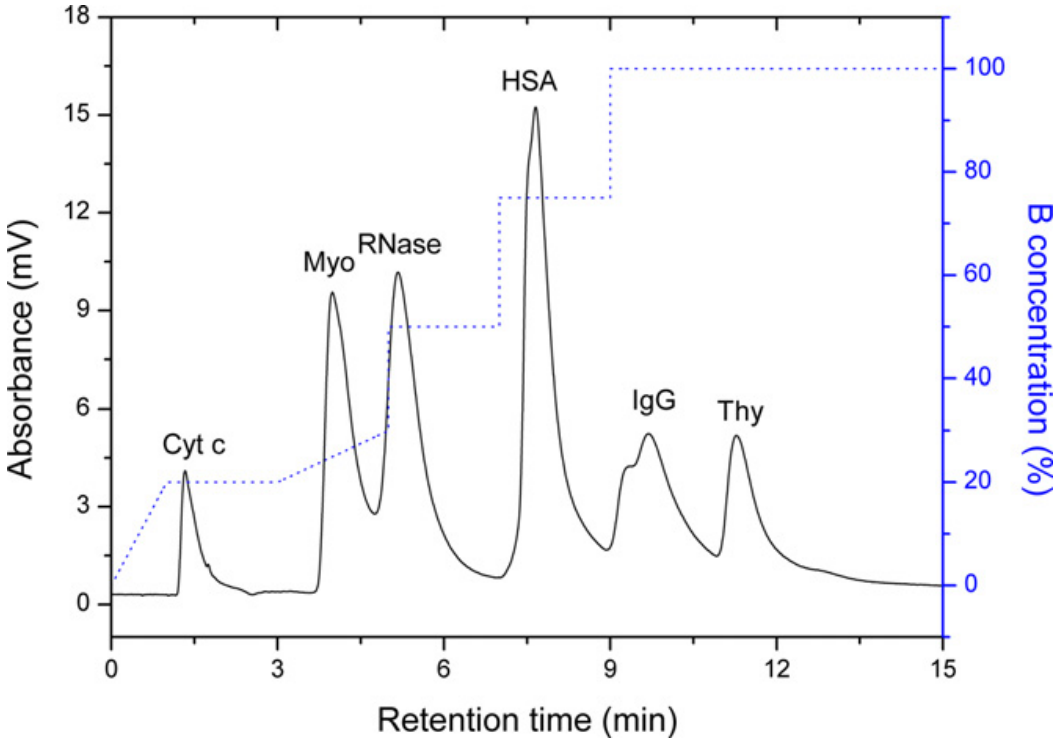


**Figure 1.3:** HIC separation of protein standards using a polyNIPAAm-grafted E-51 epoxy-based monolith (4.6 mm ×100 mm i.d.; reprinted from Ref. [105]).

curing agents in PEG as pore-forming solvent [104, 106]. Also, oxygen is not detrimental to these reactions, so careful de-aeration of the polymerisation solution is not necessary. The morphology of monoliths can be tailored by the mole ratio of epoxy to curing agent, the percentage and molecular weight (MW) of (polymeric) porogen and the polymerisation temperature. Of special interest is that monoliths derivedfrom this approach possess inherent hydrophilicity arising from the incorporation of heteroatoms into the main polymer chains [107, 108]. These materials also afford the possibility of modifications through surface hydroxyl and amino groups generated after curing, as well as residual epoxy groups. The applicability of surface modification of epoxy-based monoliths through hydroxyl groups was demonstrated by

Xin *et al.* [105]. The support monolith was prepared in a 100 mm × 4.6 mm i.d. stainless steel column by polycondensation of E-51 epoxy resin with 4,4'-methylene-bis-cyclohexylamine (NIPAAm) dissolved in a porogen system comprising DMF/PEG-200 (1/9 w/w). Polymerisation was performed at 80 °C for 12 h. The resultant monolith possessed hydrophobic properties stemming from aromatic moieties of epoxy resin as well as the hydrocarbon skeleton of the amine. Intended to be used for HIC of proteins (see **Figure 1.3**), a *"grafting from"* approach was then carried out in order to reinforce even further hydrophobicity into the monolith *via* surface-initiated atom transfer radical polymerisation (ATRP) of *N*-isopropylacrylamide.

The synthesis of epoxy-based monolithic capillary columns having weak ion-exchange functionality from polycondensation of tris(2,3-epoxypropyl)isocyanurate (TEPIC, 18%) and tris(2-aminoethyl)amine (2%) dissolved in PEG-200 (80%) has been reported recently and used for profiling of intact glycoprotein isoforms [109]. The polymerisation reaction was conducted at 80 °C for 12 h. The monolith exhibited relatively large through-pores of about 3-6 μm and a specific surface area of 4.1 $m^2/g$, which like other epoxy-based monoliths indicated the nonporous skeleton of materials in the dry state [66]. The ion-exchange functionality of the synthesised monolith originated from the residual primary amine groups present and the amine functionality introduced by the ring opening reaction of the residual epoxy groups. The post-modification reaction was conducted by pumping an aqueous solution of ammonia (50% v/v) through the capillary column at 60 °C for 48 h. The

ion-exchange capacity measured by frontal analysis of bovine serum albumin was only 1.3 mg/mL. The authors ascribed such a limited capacity to the low specific surface area of the material as well as the short spacer arm between the amine functionalities and the support monolith. The performance of the monolithic column prepared for resolving glycoprotein isoforms was also compared with a CE method. While CE exhibited superior resolution, more isoforms were detected in IEC.

While hydrophilicity of epoxy-based monoliths has made them suitable for separation of biomolecules with minimal non-specific interactions, the homogeneity of their structure, which has a root in their method of polymerisation, can be exploited for addressing the limitations associated with polymeric monoliths for the separation of small molecules. Such a limitation is raised from the structural heterogeneity of polymer monoliths prepared with conventional free-radical cross-linking polymerisations and is associated with the less cross-linked layer generated on the top of the first layer (highly cross-linked layer) possessing pore sizes of 2-4 nm in the swollen state [53]. While these pores are inaccessible for proteins with nanometres in size, small molecules permeate the gel porosity region and, depending on their size, have different penetration depths in the polymer gel structure, suggesting the mass transport to be diffusive rather than convective [53]. One immediate consequence of such phenomena is chromatographic dispersion of solutes in the gel structure, thereby reducing separation efficiency of small molecules [53, 110].

The suitability of epoxy-based monoliths for the separation of small molecules was demonstrated by Hosoya *et al.* utilising capillary columns prepared from the polycondensation of tris-(2,3-epoxypropyl) isocyanurate [104], or alternatively, 1,3-bis(N, N'-diglycidylaminomethyl) cyclohexane [111] as the epoxide-containing monomer with 4-[(4-aminocyclohexyl)methyl] cyclohexylamine (BACM) as the amine curing agent. Depending on the content of acetonitrile (ACN) in the aqueous mobile phase, columns were operated in both HILIC and RPLC modes, respectively for the separation of nucleic acid bases and nucleosides, and alkylbenzenes. These columns exhibited high permeability and up to 133,000 theoretical plates per metre (N/m) for alkylbenzenes.

### 1.3.2 Polymeric monolithic columns in proteomics research

Proteomics research aiming to investigate proteins released from gene expression in a cell, tissue or body fluids is of great importance, yet extraordinarily challenging due to the great dynamic range in the abundance of proteins [49].

Top-down and bottom-up are two common strategies applied in proteomics study. In the top-down strategy, proteins are separated by two-dimensional electrophoresis (2DE), followed by identification with tandem mass spectrometry (MS/MS). Although 2DE has great capacity for protein separation and is known as the most frequently used technique for protein quantification in clinical samples [112], it suffers from inherent limitations in the separation and detection of low

abundance proteins, membrane proteins, and proteins with extreme p*I* values and MW [49, 112]. Alternatively in recent years, more attention has been focused on the bottom-up proteomic strategy in which proteins are generally digested into peptides. Separation of peptides by one or 2D macro- or nano-LC is then followed by on-line MS/MS analysis and data processing [112]. This combination, when performed by employing capillary columns packed with sub-micrometre sized particles (< 2 μm), offers advantages to the analysis, such as high resolution and sensitivity as well as high peak capacity and throughput, but also with commensurate increase in the column back-pressure necessitating the employment of UHPLC technologies.

As an example, theoretical peak capacities ($C_p$) of up to 1,000 were reported by Shen *et al.* [113] using a 87 cm long capillary column (14.9–74.5 μm i.d.) packed with 3 μm $C_{18}$-bonded porous silica particles under a pressure of 18,000 psi. The column was successfully coupled to a hybrid quadrupole time-of-flight (Q-TOF) MS *via* a nano-electrospray ionisation (nano-ESI) interface for the analysis of proteolytic polypeptide mixtures. In order to further increase the peak capacity, Tao *et al.* [114] connected several short micro-columns in series by using zero dead-volume unions, and identified 1,692 proteins in a protein digest extracted from a rat brain, but through a long analysis time of 6.8 h.

Although typical bottom-up LC techniques with particulate columns appear to be well-suited for the current demands on separation efficiency, further improvements in the resolving power in a reasonable

analysis time with the current technology might appear as a real challenge in the near future. According to Giddings' theory [115], to achieve $C_P$s over 1,500 with a 200 cm column packed with 3 μm particles, the predicted separation time should be about 2,000 min, which is practically unreasonable to achieve. The packing of capillary columns is also not easy and requires a highly skilled worker because of the small particle sizes and small internal diameter of capillaries. Additional drawbacks include the need for retaining frits and specially designed pumps and accessories for delivering ultra-high pressures.

In the meantime, many efforts in column technology in recent years have also been devoted to developing monolith materials and this continues as an active area of research. By offering features, such as faster mass transfer (for large molecules, such as proteins), lower back-pressure, and easy preparation, employing monolith materials for routine applications has already come to play. Miniaturisation has also appeared as one area in which technologies based on particulate materials have started to fall behind their monolithic counterparts [72]. Along with the distinct advantages of the capillary column format, including the low consumption of both sample and solvents and a reduction in the peak broadening resulting from radial diffusion, an additional reduction in the size of capillary columns is particularly attractive for further improvement in the sensitivity of MS detection as sensitivity increases with the inverse square of the column diameter [116]. Such sensitivity improvements become more and more important for the separation and identification of complex samples, particularly in areas, such as

proteomics. While the current generation of commercial packed capillary columns generally has inner diameters in the range of 75 to 100 $\mu$m, packing smaller capillaries appears as a significant challenge [117].

*In situ* preparation of polymer-based monolithic stationary phases from liquid precursors provides a viable alternative to address this challenge as well. As a very good example, Karger and co-workers prepared a 20 μm i.d. poly(styrene-*co*-divinylbenzene) (PS-*co*-DVB) monolithic capillary columns to improve the detection sensitivity in LC-MS/MS analysis of peptides in a tryptic digest mixture [118]. Efficiencies (N/m) over 100,000 were achieved with optimised polymerisation and separation conditions. High mass sensitivity (~ 10 amol of peptides) in the MS and MS/MS modes using an ion trap MS was found with a factor of up to 20-fold improvement over a 75 μm column. As an extension of this work, large digested peptide fragments up to 10 kDa (e.g., from lysyl endopeptidase digestion) with or without modifications were well separated using 20 and 50 μm i.d. columns [119]. Importantly, the macroporous structure of the monolithic columns facilitated mass transport of large peptides with improved recovery relative to small pore size RP packings. High sequence coverage (>95%), including identification of phosphorylated and glycosylated particles, was achieved for β-casein using the 20 μm i.d. monolithic column. For peptides with greater ionization efficiency, detection limits as low as 400 zmol was obtained. Also their system demonstrated a typical peak capacity of ~ 200 for a 10 cm column.

Among all polymer monoliths, styrenic and methacrylate-based monoliths are more frequently used for proteomics applications. In one recent review Rozenbrand and van Bennekom summarised some recent applications of polymer monoliths, together with silica-based monoliths, in proteomics [52]. Along with PS-*co*-DVB monoliths which represent the most commonly used polymer monoliths for RP applications, methacrylate-based monoliths with RP chemistry can also be prepared, for example, by alkylation of the well-established poly(GMA-*co*-EDMA) monoliths [120], or alternatively by co-polymerisation of hydrophobic monomers , such as lauryl methacrylate (LMA) with a cross-linker. In one study, Moravcova *et al.* [121] prepared a very short (3 cm × 320 μm i.d.) poly(LMA-*co*-EDMA) capillary column for desalination, preconcentration, and separation of peptides from a bovine serum albumin (BSA) digest and an in-gel digest of *Hordeum vulgare*. Fractions were collected on MALDI target spots and analysed using TOF-MS. The sequence coverage for BSA increased from 17%, when no separation was performed, to 63%; and for *H. vulgare*, the 14 kDa spot revealed 16 proteins, approximately four times higher in comparison to the analysis without separation.

Polymer monoliths with chemistries other than RP have also been developed for proteomics applications, particularly in multidimensional (MD) separations. Given that the peak capacity of a MD system is theoretically the product of the peak capacity of each orthogonal dimension [115], combining two or even more orthogonal (multimodal) separation procedures will dramatically improve the overall separation

power and result in a much larger number of identified peptides [122]. In one report, a 150 μm i.d. capillary monolithic column with a SCX chemistry was prepared by co-polymerization of ethylene glycol methacrylate phosphate and bisacrylamide in a ternary porogenic solvent consisting of dimethylsulfoxide, dodecanol, and N,N'-dimethylformamide [123]. The column exhibited higher DBC, faster kinetic adsorption of peptides, and more than 10 times higher permeability than the column packed with commercially available SCX particles. The column then served as a trap column prior to an RP column in a nano-flow LC-MS/MS system for automated sample injection and on-line MD separation. Analysis of 19 μg of the tryptic digest of yeast proteins enabled identification of 1522 distinct proteins from 5608 unique peptides (total of 54,780 peptides) at a false positive rate of only 0.46%.

Zou and co-workers [112] developed a fully automated 2D system with integration of a RP-SCX biphasic trap column inserted prior to a packed $C_{18}$ column (12 cm × 75 μm i.d.). Their work was an extension of so called multidimensional protein identification technology, originally proposed by Yates and co-workers [124], based on packing particles with different chemistries in tandem in a single capillary, and is used widely in proteome analysis. A polymeric monolith with SCX chemistry was primarily prepared in a 7 cm long segment of the biphasic trap (14 cm × 200 μm i.d.) column by *in situ* co-polymerisation of ethylene glycol methacrylate phosphate and methylene bis-acrylamid, followed by packing the other 7 cm long segment with $C_{18}$ particles. Next, tryptic digests of the protein samples extracted from hepatocellular carcinoma

and normal liver tissues were loaded onto the RP segment of the biphasic trap column and labelled with different types of isotope dimethyl reagents in sequence. All the enriched peptides were then transferred to the SCX segment of the biphasic column, followed by on-line MD separation *via* stepwise salt eluting of the peptides to a 15 cm-long RP separation column using a binary gradient for the $\mu$LC-MS/MS analysis. Comparing to conventional manual isotope labelling and off-line fractionation technologies, this system was fully automated and time-saving. Integration of a phosphate SCX monolith into the biphasic trap column also allowed employing higher flow-rates for more throughputs. This system enabled quantification of over 1000 proteins through a 29 h proteome analysis, with the possibility of increasing to 1700 proteins once analysis time was extended to 63 h. After three replicate runs, 94 significantly up-regulated and 249 significantly down-regulated proteins were successfully observed.

Introduced by Alpert in 1990 [125], HILIC is recognised as a variant of normal-phase LC (NPLC) in which a column with hydrophilic chemistry is eluted with a mobile phase which is only 10 to 40% (v/v) aqueous [126]. HILIC has been successfully applied for the separation of a wide variety of polar solutes, including pharmaceuticals [127, 128], carbohydrates [129], peptides and proteins [122, 125, 126, 130, 131] as well as for the selective enrichment of glycopeptides and phosphopeptides in proteomics applications [132, 133]. In HILIC, an increase in retention is observed with increasing polarity or hydrophilicity of solutes, which is opposite to the trend observed in RPLC. As a result, HILIC has good

separation orthogonality to RPLC, enabling their integration into the MD separation of complex mixtures.

In one study, Gilar *et al.* [134] analysed a mixture of approximately 200 peptides using different stationary phases, including SEC, HILIC, SCX and RP at pH 2.6 and pH 10. HILIC was shown to have a separation power superior to both SCX and SEC. The orthogonality of the stationary phases was also determined by plotting the peptide retention times in two dimensions against each other. Although this study was not performed 2-dimensionally, it was still able to exhibit more orthogonality to RP for HILIC compared to SCX. This conclusion was further supported by another study where an off-line 2D HILIC-RP system was designed for separation of peptide mixtures [135]. A column with zwitterionic chemistry was chosen for the first dimension. Analysis of data revealed a dual-mode separation mechanism based on both hydrophilic partitioning of solutes within the aqueous sub-layer and electrostatic interactions with the stationary phase. These electrostatic interactions ensure that HILIC separation is more than merely the reverse of RP, while the presence of hydrophilic interactions caused similarly charged peptides to be eluted over a wider retention window. It was further noted that the orthogonality of HILIC with RP is dependent on the buffer pH, where a higher orthogonality was seen at pH 3, providing more flexibility in selectivity control.

HILIC is proving to be an attractive choice among the range of separation methods available for the proteomics researcher. Although the

combinations chosen so far for 2D LC–MS have been limited to HILIC–RP, the versatility of the polymeric monoliths is predicted to enable other combinations, such as SCX–HILIC and even MD approaches. On the other hand, the higher content of organic solvent utilised in HILIC compared to RP offers additional benefits, such as more compatibility of the mobile phase with ESI-MS and increased detection sensitivity, which may suggest HILIC to be an interesting candidate for the second dimension [131, 134].

## 1.4 Project aims

Developing monolithic columns, particularly based on polymeric monoliths, continue to be an active area of research in column technology due to the large potential of these materials, especially in bioseparations. However, in comparison to their silica-based counterparts, favourable features of polymeric monoliths, such as ease of preparation and more available monomers, reagents and methods enabling their preparation, also make them attractive to be explored for separation of small molecules.

Therefore, the general aim of this project has been to develop new polymeric monolithic columns for bioseparations with more emphasis on hydrophilicity of the materials, as one generally ignored criterion in previous studies. The suitability of some of the developed monoliths for separation of small molecules has also been considered. The specific aims of the project were:

- To explore the feasibility of resolving charge heterogeneity in mAbs using a pH gradient IEC approach and commercially available polymeric monolithic columns.
- To prepare new methacrylate-based polymer monoliths for IEC of proteins by focusing on hydrophilicity of the materials.
- To explore suitability of other polymerisation methods than free-radical polymerisation for preparing new polymeric monoliths to be used for separation of both small and large biomolecules.
- To evaluate the performance of the prepared columns for separation and characterisation of peptides under capillary HILIC mode and to investigate their applicability for proteomics studies.

# *Chapter 2*

# Experimental

Unless otherwise specified in particular chapters, this section summarises chemicals, instrumentation and procedures used throughout this research.

## 2.1 Chemicals and reagents

Unless specified otherwise, the chemicals used were of analytical reagent (AR) grade as follows.

**Table 2.1:** Chemicals used for buffer preparation

| Chemical | Formula | Supplier |
|---|---|---|
| Acetic acid | $CH_3COOH$ | Sigma-Aldrich |
| Formic acid | $HCOOH$ | Sigma-Aldrich |
| Trifluroacetic acid | $CF_3COOH$ | Sigma-Aldrich |
| Hydrochloric acid | $HCl$ | Sigma-Aldrich |
| Phosphoric acid | $H_3PO_4$ | Merck |
| Disodium hydrogen phosphate | $Na_2HPO_4.2H_2O$ | Sigma-Aldrich |
| Sodium dihydrogen phosphate | $NaH_2PO_4.H_2O$ | Sigma-Aldrich |
| Ammonium Acetate | $CH_3CO_2NH_4$ | Sigma-Aldrich |
| Sodium bicarbonate | $NaHCO_3$ | Sigma-Aldrich |
| Disodium carbonate | $Na_2CO_3$ | AnalaR |
| Ammonium formate | $HCOONH_4$ | Sigma-Aldrich |
| Tris(hydroxymethyl)aminomethane hydrochloride (Tris) | $NH_2C(CH_2OH)_3.HCl$ | Sigma-Aldrich |
| Sodium hydroxide (99%) | $NaOH$ | Sigma-Aldrich |
| Ethanolamine | $NH_2(CH_2)_2OH$ | Sigma-Aldrich |
| Diethanolamine | $NH(CH_2CH_2OH)_2$ | Sigma-Aldrich |
| Triethanolamine | $N(CH_2CH_2OH)_3$ | BDH Chemicals |
| Ammonium hydroxide (28% aqueous $NH_3$) | $NH_4OH$ | Fluka |
| Ammonium sulfate | $(NH_4)_2SO_4$ | Sigma-Aldrich |

**Table 2.2:** Chemicals used for monolith preparation and modifications

| Chemical | Formula | Supplier |
|---|---|---|
| (3-Glycidyloxypropyl)trimethoxysilane | $C_9H_{20}O_5Si$ | Sigma-Aldrich |
| 1-Decanol | $CH_3(CH_2)_9OH$ | Sigma-Aldrich |
| 1-Dodecanol | $CH_3(CH_2)_{11}OH$ | Sigma-Aldrich |
| 2,2′-Azobisisobutyronitrile (AIBN) | $(CH_3)_2C(CN)N=NC(CH_3)_2CN$ | MP Biomedicals |
| 2-Aminoethyl hydrogen sulfate (SEA) | $NH_2(CH_2)_2OSO_3H$ | Sigma-Aldrich |
| 2-Methoxyethanol | $CH_3O(CH_2)_2OH$ | Sigma-Aldrich |
| 3-(Trimethoxysilyl)propyl methacrylate (γ-MAPS) | $H_2C=C(CH_3)CO_2(CH_2)_3Si(OCH_3)_3$ | Sigma-Aldrich |
| Acetone | $CH_3COCH_3$ | Merck |
| Allylamine | $CH_2=CHCH_2NH_2$ | Sigma-Aldrich |
| Diethylamine | $NH(CH_2CH_3)_2$ | Sigma-Aldrich |
| Ethanol | $CH_3CH_2OH$ | Sigma-Aldrich |
| Ethylenediamine (EDA) | $NH_2(CH_2)_2NH_2$ | Sigma-Aldrich |
| Glycerol glycidyl ether (GE-100) | Mixture of $C_{12}H_{20}O_6$ and $C_9H_{16}O_4$ | Raschig GmbH |
| Glycidyl methacrylate (GMA) | $C_7H_{10}O_3$ | Sigma-Aldrich |
| Iminodiacetic acid (IDA) | $HN(CH_2COOH)_2$ | BDH Chemicals |
| Isopropanol | $(CH_3)_2CHOH$ | Sigma-Aldrich |
| Methanol | $CH_3OH$ | Sigma-Aldrich |
| N,N′-Methylenebisacrylamide (BIS) | $(CH_2=CHCONH)_2CH_2$ | Sigma-Aldrich |
| N-Isopropylacrylamide (NIPAm) | $H_2C=CHCONHCH(CH_3)_2$ | Sigma-Aldrich |
| O-Phosphorylethanolamine (PEA) | $NH_2(CH_2)_2OPO_3H_2$ | Sigma-Aldrich |
| Pentaerythritol triacrylate (PETA) | $(H_2C=CHCO_2CH_2)_3CCH_2OH$ | Sigma-Aldrich |
| Poly(ethylene glycol) (PEG) | $H(OCH_2CH_2)_nOH$ | Sigma-Aldrich |
| Tetrahydrofuran | $C_4H_8O$ | Sigma-Aldrich |
| Toluene | $C_6H_5CH_3$ | Sigma-Aldrich |

**Table 2.3:** Protein standards[1]

| Protein | MW (kDa) | Source | Experimental p*I*[2] |
|---|---|---|---|
| Trypsin inhibitor | 20.1 | Glycine max (soybean) | 4.6 |
| Ovalbumin | 42.8 | Chicken egg white | 4.9 |
| β-Lactoglobulin a & b | ~18.4 | Bovine milk | ~ 5.1 |
| Serum albumin | 66.0 | Bovine | 5.5 |
| Transferrin | 77.1 | Human | ~ 5.5 |
| Myoglobin | 17.0 | Equine heart | 7.2 |
| α-Chymotrypsinogen A | 25.6 | Bovine pancreas | 9.0 |
| Trypsinogen | 23.9 | Bovine pancreas | 9.3 |
| Ribonuclease A | 13.7 | Bovine pancreas | 9.4 |
| Cytochrome c | 11.7 | Equine heart | 10.0 |
| Trypsin | 23.8 | Bovine pancreas | 10.3 |
| Lysozyme | 14.3 | Chicken egg white | 11.2 |

[1] Supplied from Sigma-Aldrich.
[2] from Ahmed *et al.* [136].

**Table 2.4:** Nucleobases and nucleosides[1]

| Chemical | Formula | CAS Number |
|---|---|---|
| Adenine | $C_5H_5N_5$ | 73-24-5 |
| Adenosine | $C_{10}H_{13}N_5O_4$ | 58-61-7 |
| Cytidine | $C_9H_{13}N_3O_5$ | 65-46-3 |
| Cytosine | $C_4H_5N_3O$ | 71-30-7 |
| Deoxyguanosine | $C_{10}H_{13}N_5O_4$ | 3608-58-0 |
| Guanosine | $C_{10}H_{13}N_5O_5$ | 118-00-3 |
| Thymine | $C_5H_6N_2O_2$ | 65-71-4 |
| Uracil | $C_4H_4N_2O_2$ | 66-22-8 |
| Uridine | $C_9H_{12}N_2O_6$ | 58-96-8 |

[1] Supplied from Fluka.

**Table 2.5:** Benzoic acid derivatives[1]

| Chemical | Formula | p$K_{a1}$[2] |
|---|---|---|
| Benzoic acid (BA) | $C_6H_5COOH$ | 4.2 |
| 4-Propylbenzoic acid (4PBA) | $CH_3(CH_2)_2C_6H_4CO_2H$ | 4.4 |
| 4-Hydroxybenzoic acid (4HBA) | $HOC_6H_4CO_2H$ | 4.6 |
| 4-Aminobenzoic acid (PABA) | $H_2NC_6H_4CO_2H$ | 4.9 |
| 2,3-Dihydroxybenzoic acid (2,3DHBA) | $(HO)_2C_6H_4CO_2H$ | 3.0 |
| 2,4-Dihydroxybenzoic acid (2,3DHBA) | $(HO)_2C_6H_4CO_2H$ | 3.3 |
| 2,5-Dihydroxybenzoic acid (2,3DHBA) | $(HO)_2C_6H_4CO_2H$ | 3.0 |

[1] Supplied from Sigma-Aldrich.
[2] Obtained from [137].

## 2.2 Instruments

Conventional LC was performed using a Dionex DX-500 Liquid Chromatograph (Thermo Fisher Scientific, Lane Cove, Australia) consisting of a GP50 Gradient Pump, AD25 UV/Vis Absorbance Detector, AS50 Thermal Compartment and AS50 Autosampler. Detection was performed at 214 and 280 nm. Flow-rate was 1 mL/min, the injection volume was 10 μL and the column compartment temperature was set at 30 °C. Instrument control and data acquisition were performed using Dionex Chromeleon software, version 6.80 SR5.

Capillary LC separations were performed on a Dionex UltiMate™ 3000 HPLC System equipped with a DGP-3600M gradient pump, including a membrane degasser unit, a FLM-3300 column compartment including a capillary flow-splitter (split ratio 100:1), a VWD-3400 UV detector equipped with a 45 nL flow cell and a WPS-3000 autosampler

fitted with a 100 nL sample loop. Chromeleon® software (Ver. 6.80) was used for system control and data processing (data collection rate 2.5 Hz).

Electrospray ionization time of flight (ESI-TOF) mass spectrometry was performed on a micrOTOF-Q mass spectrometer (Bruker Daltonics, Melbourne, Australia) equipped with an Agilent G1385A microflow nebuliser (Agilent technologies, Melbourne, Australia). Argon was used as a nebulising gas and nitrogen as a dry gas. The instrument was tuned and calibrated using an Agilent ES Tuning Mix (catalogue no. G2431A) in enhanced quadratic mode. All system control and data acquisitions were conducted with Bruker Daltonics software. The deconvolution of ESI mass spectra was performed using a maximum entropy algorithm (Bruker Daltonics).

iCE was performed using an iCE280 analyser (Toronto, ON, Canada) with operational software from Convergent Bioscience, equipped with an Alcott 719 AL autosampler.

Pore size distribution profiles of the dried monoliths were determined using a Micromeritics Autopore IV 9500 mercury intrusion porosimeter (Norcross, GA, USA). BET specific surface area measurements were performed on a Micromeritics TriStar II 3020 based on nitrogen adsorption-desorption isotherms.

Scanning electron microscopy (SEM) images of the capillary monolithic columns were captured using a Hitachi SU-70 field emission scanning electron microscope (Tokyo, Japan), after coating the samples (~

5mm length capillary columns) with a conducting platinum layer (~ 4 nm thickness). SEM experiments for normal bore columns were performed using a FEI Quanta 600 MLA environmental scanning electron microscope (Hillsboro, OR, USA).

### 2.2.1 Other instruments

pH was measured using a pH meter model labCHEM-CP from TPS (Springwood, QLD, Australia). Water was purified *via* a Milli-Q water purification system (Millipore, Bedford, MA) and filtered through a 0.2 μm nylon filter prior to use. A vacuum oven (max. -100 kPa) model V30D from SEM (Magill, SA, Australia) was used. Syringe pump model PHD 2000 was from Harvard Apparatus (Holliston, MA, USA). Vortex mixer was model VM1 from Ratek Instruments (Boronia, VIC, Australia). The thermostated water bath used was model 8102 from PolyScience (PA, USA) and the GC oven was Hewlett Packard model 5890 (Agilent Technologies, CA, USA).

## 2.3 General procedures

### 2.3.1. Surface modification of fused-silica capillaries

The inner surface of the polyamide-coated fused-silica capillaries (purchased from Polymicro Technologies, Phoenix, AZ, USA) was first activated following procedures described previously [94, 104] with some modifications. Briefly, a length of capillary (3 m) was rinsed sequentially with acetone and water, then flushed with 0.2 M sodium hydroxide solution until the outlet flow exhibited an alkaline pH and flow was

continued at 30 μL/h for 60 min using a syringe pump, followed by flushing with water until a neutral pH of the outlet flow was detected. The capillary was then rinsed with 0.2 M hydrochloric acid solution in the same manner, followed by acetone and then the capillary was dried with compressed nitrogen for 1 h. Depending on the type of monolith to be prepared later in the capillary, different silanisation reagents were employed on the next step. For epoxy-based monolith, a 50% (v/v) solution of 3-glycidyloxypropyltrimethoxysilane in acetone was pumped through the capillary at 30 μL/h for 60 min. The capillary was then sealed at both ends with rubber septa and kept at 80 °C in a GC oven overnight. For methacrylate-based monoliths, a 20% (v/v) solution of 3-(trimethoxysilyl)propyl methacrylate (γ-MAPS) in 95% ethanol with apparent pH adjusted to 5 using acetic acid was pumped through the capillary at a flow-rate of 0.25 μL/min at room temperature for 90 min. Finally, the capillaries were flushed with acetone and then dried again with nitrogen. In order to allow the condensation reaction to complete, the activated capillaries were then sealed at both ends and stored for at least 24 h before use [138].

### 2.3.2 Surface modification of glass-lined tubing (GLTs)

The surface of the glass-lined tubing (GLT, 1/4" o.d. × 4 mm i.d. × 5 cm; SGE, Melbourne, Australia) was vinylised according to the procedure reported elsewhere [139] with some modifications. To activate the surface, the GLT was placed into a slightly bigger test tube, filled with 1 M sodium hydroxide solution and heated in a GC oven at 100 ˚C for 1 h. The solution was then discarded and the GLT was washed extensively

with water until neutral pH was attained. The procedure was repeated with 1.2 M hydrochloric acid, followed by washing with acetone and drying in a vacuum oven. The dried GLT was then immersed in the test tube filled with a solution of γ-MAPS in acetone (30 %wt.). The test tube was sealed and left in the dark at room temperature overnight. After vinylisation the GLT was rinsed with acetone and dried in a vacuum oven.

### 2.3.3 Column permeability measurement

The flow resistance of a column is characterised by the column permeability, *K*, which is calculated using Darcy's equation:

$$K = \frac{FL\eta}{\Delta P \pi r^2}$$

where $F$ is the volumetric flow-rate, $L$ is the column length, $\eta$ is the eluent viscosity, $\Delta P$ is the column back pressure , and $r$ is the column inner radius [140].

### 2.3.4 Dynamic binding capacity (DBC) measurements

The protein binding capacity of an IEX monolith was determined using frontal analysis. The column was first equilibrated with a solution of 10 mM phosphate buffer at pH 6 (eluent A), and then loaded with a solution of lysozyme (1 mg/mL) in eluent A and UV absorbance at 214 nm was measured. DBC was calculated at 50% of the final absorbance value of the breakthrough curve and expressed in mg/mL of column

volume [94]. The volume of connecting tubing was corrected by replacing the column with a zero dead-volume union.

### 2.3.5 Enzymatic digestion of proteins

Cytochrome c was dissolved in 50 mM ammonium acetate containing 20% (v/v) ACN to a concentration of 1 mg/mL. Trypsin was then added at a substrate-to-enzyme ratio of 50:1 (w/w) and the solution was incubated at 37 ˚C for 24 h. The proteolysis was terminated by the addition of formic acid to a final concentration of 0.1% (v/v). The mixture was further diluted to 0.5 mg/mL in 50% (v/v) methanol in water before injection.

# *Chapter 3*

# Charge Heterogeneity Profiling of Monoclonal Antibodies Using Low Ionic Strength Ion-exchange Chromatography and Well-controlled pH Gradients on Monolithic Columns

## 3.1 Introduction

The advances in biotechnology in the last quarter of the 20th century have led to the development of new technologies for the production of complex biomolecules which could potentially be used in human health care in the areas of diagnostics and prevention, and treatment of diseases. Qualities, such as high (target) selectivity, the ability to initiate immune recognition of the target, and long circulation half-lives, have made the development of humanized monoclonal antibodies (mAbs) the fastest growing segment of therapeutic drugs [42, 141]. In the production of mAbs the final product often exhibits a number of variations from the expected or desired structure. These alterations may result from either known or novel types of post-translational modifications or from spontaneous, non-enzymatic protein degradation which bring about charge and size heterogeneity. Common modifications of the primary sequence include N-glycosylation, methionine oxidation,

proteolytic fragmentation, and deamidation [142]. It has been shown that charge variants of therapeutic proteins can have significantly different bioactivity. For example, Harris *et al.* [143] showed that deamidated variants of recombinant human mAbs had reduced potency in a bioactivity assay. As protein charge heterogeneity is an important factor in quality assessment of protein therapeutics, regulatory authorities, such as the International Conference on Harmonisation (ICH) have set criteria for monitoring and characterising the degree and profile of variations to ensure lot-to-lot consistency and product stability [144].

Considering the large size of antibodies and the minor structural diversity between the variants, the existence of these variants imposes a significant challenge for their separation. Ion-exchange chromatography IEC is a non-denaturing technique used widely to separate and isolate protein charge variants for subsequent characterisation. However, when operating under a salt gradient approach (classical mode), IEC has been shown to exhibit limited selectivity when complex proteins with the same number of effective charges are to be separated [145] and lack of robustness when targeted mAbs are to be analysed [21].

cIEF is another separation technique used frequently to assess charge heterogeneity of proteins in which a complex mixture of ampholytes (polyionic organic electrolytes) is used to establish a pH gradient in a capillary with the aid of an electric field. The electric field causes protein isoforms to focus along the capillary according to their isoelectric point where they have zero net charge and are then mobilised

toward an on-column detector located at one end of the capillary. Due to the distortion of the pH gradient, which affects reproducibility in migration time and peak area, the mobilisation step often requires optimisation [146]. The introduction of imaged iCE has overcome this issue by eliminating the need for the mobilisation step through single point detection of the entire imaged capillary. While cIEF is perhaps the most powerful of the known separation technologies for charge variants, the difficulty of collecting fractions when compared to IEC has confined the method to be suitable for monitoring of variants but not for their preparative separation or isolation (peak identification) [42, 145]. Also, some authors believe that while the separations are consistent between the two methods, cIEF is not as precise as IEC and therefore cannot be considered as a suitable replacement [17]. To the contrary however, some have concluded that CE techniques could be superior to IEC in terms of both separation speed and obtainable resolution and therefore could constitute a routine tool for assessing charge heterogeneity of proteins [146, 147].

Developed by Sluyterman *et al.* [27-31] in the late 1970s, CF (internal pH gradient) is recognised as the chromatographic analogy to IEF [17] mitigating many of the shortcomings of classical IEC and combining some unique features of both methods. CF has been demonstrated to be useful for separating protein isoforms due to its high resolving power and ability to retain the native state of protein [21, 23]. However, there are some limitations to this technique, such as the cost of polyampholite buffers employed, the necessity of column regeneration

after each separation, and the inflexibility in controlling the slope of the generated pH gradient [21, 35, 38].

Alternatively, pH gradient approach can be conducted externally by mixing prior to the column two eluting buffers of different pHs consisting of common buffer species. As the slope and profile of the pH gradient can be easily controlled by changing the elution parameters with less dependence on the buffer composition and column chemistry, this manner of introducing a pH gradient should allow for more convenient method development and optimisation [35, 38]. The externally-induced pH gradient approach was applied for the separation of deamidated variants of a mAb [142], resolving C-terminal lysine isoforms after treating with carboxypeptidase B [21] and also for the analysis of charge variants of full-length mAbs [17].

Currently, particle-packed columns represent the most common stationary phases for HPLC. Despite immense popularity, their application for rapid and efficient separation of macromolecules is not as convenient as for small molecules. This is mostly because of slow diffusional mass transfer of large solutes and also the large void volume existing between the packed particles [148]. In the meantime, biocompatibility of stationary phase has become a new challenge when analysing biomolecules (including peptide and proteins). As defined by Li *et al.* [74], a biocompatible stationary phase material should be able to resist nonspecific adsorption of biomolecules and preserve the bioactivity of the target biomolecules. These challenges are well met by employing

monolithic media. Mass transfer in monolithic sorbents is mostly dominated by convection, rather than diffusion, and is therefore fast, even for large biomolecules. On the other hand, the expected biocompatibility of the most frequently used polymers in making porous monoliths, i.e., poly(meth)acrylate and polyacrylamide, make these stationary phases highly suit for use in protein separation applications. Advances in polymer monoliths for IEC of biomolecules have been reviewed recently and the importance of reducing non-specific interactions between analyte and stationary phase has been noted [69]. While IEC of proteins using monolithic columns is frequently seen in the literature [77, 85, 95], very little effort has been directed toward employing this technique for separation of large proteins, such as mAbs.

Based on recent efforts to resolve charge variants of mAbs with the aid of ion-exchange (IEX) monolithic columns [149], the maximum achievable resolution for mAb isoforms was pursued in this work using CEX columns in combination with simple, yet efficient, buffer systems. Unlike previous reports [16, 17, 35, 145], IEC was performed employing shallow pH profiles over a limited pH range (typically 1 pH unit) generated by single component buffer systems at very low ionic strength. The suitability of the proposed buffer system in direct coupling of IEC and MS was also demonstrated. Due to their size and complexity, mAbs are typically characterised by two or more orthogonal separation methods [17]. Therefore, the performance of the developed method was also assessed by comparing the results with those obtained by iCE. It was

hoped that similar charge heterogeneity profiles could be achieved for mAbs analysed under two different separation mechanisms.

## 3.2 Experimental

The general experimental details, including chemicals and instrumentation, are presented in Chapter 2. Specific experimental conditions are given in each of the figure captions.

### 3.2.1 Chemicals and reagents

Pharmalyte pH 3-10, sucrose and urea (for iCE experiments) and methanol (LC-MS grade) were all obtained from Sigma-Aldrich. Methyl cellulose (1%) and the Chemical Test Kit were from Convergent Bioscience (Toronto, ON, Canada). The p*I* markers, including p*I*s 5.13, 6.14, 7.2 and 9.5, were also obtained from Convergent Bioscience. Samples of three different mAb formulations, which are referred to as mAb1, mAb2 and mAb3, were prepared by recombinant DNA technology at Pfizer Inc (St. Louis, MO, USA).

### 3.2.2 Chromatography

The monolithic IEX columns used were ProSwift™ SCX-1S and ProSwift™ WCX-1S (4.6 × 50 mm) and the packed column was a ProPac WCX-10, 4 × 250 mm, all from Dionex (Thermo Fisher Scientific, Lane Cove, Australia). The monolithic columns are methacrylate-based with sulfonic acid and carboxylic acid functionalities for SCX and WCX,

respectively. The ProPac WCX is a tentacle type ion-exchanger bearing carboxylate groups.

All chromatograms were transferred to ASCII files and redrawn using Origin 8.1 (Northampton, MA, USA).

Unless otherwise stated, mobile phases were generally prepared by dissolving appropriate amounts of the buffer components in water prior to splitting into two aliquots denoted as eluent A and B. The pH of each portion was then adjusted with concentrated sodium hydroxide or hydrochloric acid. The elution was performed by a linearly ascending pH gradient from 0 to 100% eluent B followed by isocratic elution for 3 to 5 min before returning the eluent composition to the starting condition (100% eluent A). The gradient volumes were 10 and 30 mL for monolithic and packed columns, corresponding to about 14 and 10 column volumes, respectively. For each elution, the column was pre-equilibrated with at least three column volumes of eluent A prior to sample introduction. Prior to integration, each sample chromatogram was subtracted from the relevant blank injection prepared from eluent A. Fractions of the column effluent were collected every 1 min and the pH was measured offline.

MAb samples were analysed as received without buffer exchange or any other sample pretreatment process. After dilution in eluent A to a concentration of approximately 0.2 mg/mL, samples were stored at 5 ˚C until analysed.

### 3.2.3 Liquid chromatography-mass spectrometry (LC-MS)

CEX chromatography was carried out using a ProSwift™WCX-1S (4.6 × 50 mm) column under pH gradient mode. 5 mM ammonium hydroxide (AMH) buffer containing 20% (v/v) methanol was used at pH 9.5 as eluent A and at pH 10.5 as eluent B. pH of eluents was adjusted before mixing with methanol. Elution was performed by running a linear gradient of eluent A to eluent B in 20 min at a flow-rate of 0.4 mL/min, which was split (1:100) before introducing into the MS.

Coupled with the CEX chromatography, ESI-TOF-MS was performed in a positive ion mode with *m*/*z* range of 500-10000 and a capillary voltage of 4500V (-500 V end plate offset). Drying gas flow of 5 L/min at 300 ˚C was used with a 20.3 psi nebuliser gas pressure.

### 3.2.4 iCE

For iCE experiments a transparent capillary column (50 mm, 100 μm i.d.) was used with its inner surface coated with fluorocarbon to minimise electroosmotic flow. The test solutions were prepared using various amounts of p*I* markers, pharmalyte, 1% methyl cellulose, 5 M urea, 20% sucrose, and mAb samples. Throughout the analysis, the capillary was kept at ambient temperature while the autosampler was set at 8 or 15 ˚C, depending on the mAb sample analysed. The injection volume was 35 μL and the analysis was performed by applying a sample transfer time of 100 s, prefocusing at 1500 V for 1 min, followed by focusing for 5 min at 3 kV. Detection was performed at 280 nm.

## 3.3 Results and Discussion

With the aim of improving the resolution, a series of new buffer systems based on both organic and inorganic buffer species was designed and applied using monolithic columns. To obtain sufficient binding of the proteins to the cation-exchanger, the lowest pH of the gradient was chosen to be at least 1 pH unit below the electrophoretic p*I* values of mAbs, that is 8.8 for mAb1, 8.5 for mAb2 and 8.4 for mAb3.

### 3.3.1. Triethylamine-diethylamine (TEA-DEA) buffer system

The first buffer system that was successful in eluting two of the mAbs of interest was prepared by mixing equimolar amounts of TEA (p$K_a$ 7.76) and DEA (p$K_a$ 8.88) resulting in a system buffering the pH range of approximately 7.6 to 10. **Figure 3.1** shows the separation achieved for mAb1 and mAb2 on a ProSwift SCX-1S column using this buffer system in the pH range of 7.6-10 with each buffer component at a concentration of 12.5 mM. A somewhat linear pH profile for this system over the studied pH range was achieved (**Figure 3.1**). No elution was observed for mAb3. Acidic isoforms (p*I* lower than the main component) are observed for mAb1, while basic isoforms are more pronounced for mAb2. Indications of additional isoforms are also present but as faint shoulders of the main peaks. The effect of flattening the pH gradient profile on chromatographic resolution was of special interest in this study. As the pH gradient slope was reduced there was more time for differential

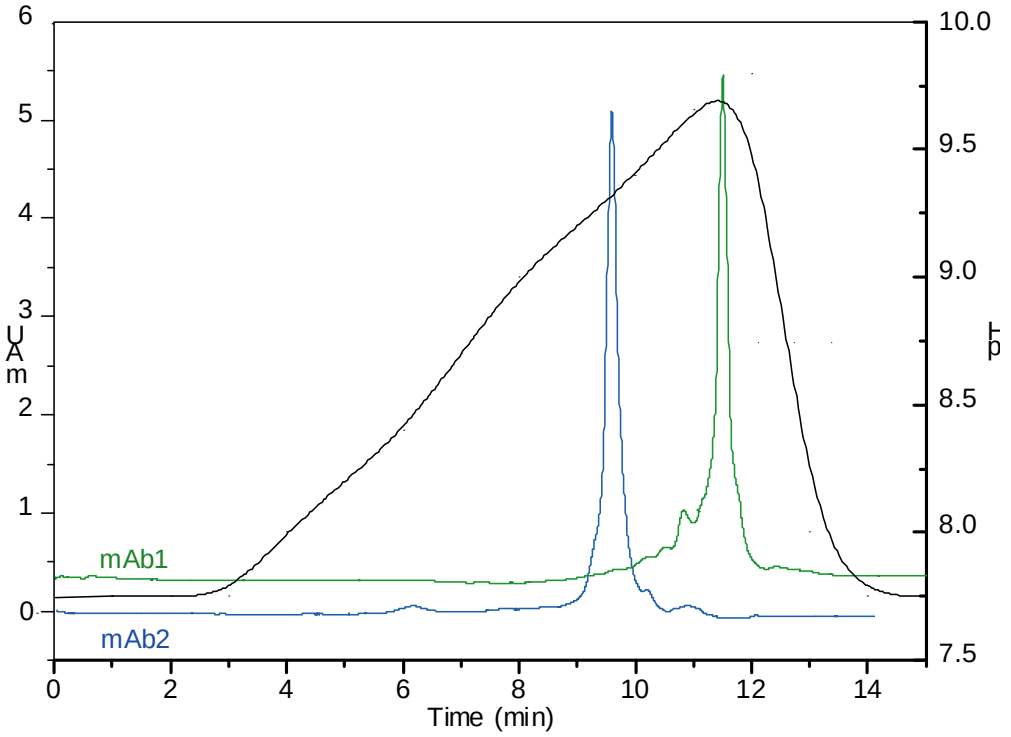


**Figure 3.1:** pH gradient separation obtained for mAb1 and mAb2. The mobile phase composition was 12.5 mM DEA and 12.5 mM TEA at pH 7.8 (eluent A) and pH 10 (eluent B). Gradient: 0-100 % B in 10 min, 100% B for 3 min. Column: ProSwift SCX-1S (4.6 × 50 mm); Detection: UV at 280 nm; Flow-rate: 1 mL/min; Column compartment temperature: 30 ˚C. Dashed line represents the pH profile obtained.

movement of the isoforms through the column, which could lead to better resolution [145].

In CF, it is possible to generate shallow gradient slopes by limiting the pH range of the gradient or reducing the concentration of the mobile phase buffer components [29, 31, 150]. Data presented later in this work show that these two strategies for obtaining higher resolution are also applicable to the external pH gradient approach.

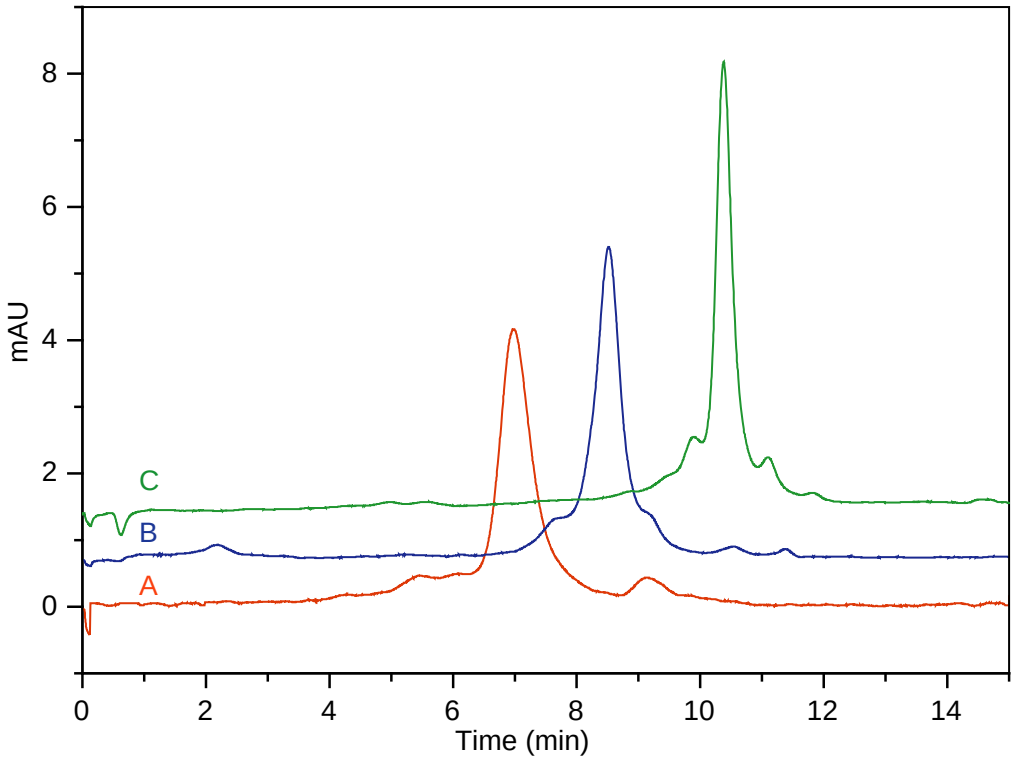


**Figure 3.2:** The effect of eluent concentration (DEA) on the elution profile of mAb2. (A) 20 mM, pH 9-10; (B) 10 mM, pH 9-10; (C) 5 mM, pH 9.2-10.2. Other conditions as in Figure 3.1.

### 3.3.2 DEA buffer system

As seen in **Figure 3.1**, elution of mAbs in the TEA-DEA buffer system occurred around the end of the pH range applied. The pH of eluent A was therefore increased from 7.5 to 9. A simultaneous reduction in gradient slope was achieved as the gradient time remained unchanged at 10 min. In addition, because of its negligible buffering capacity in the new pH range (pH 9-10), TEA was removed from the buffer system.

The effect of buffer concentration within the range 20 to 5 mM on separation efficiency of mAb2 isoforms is shown in **Figure 3.2**. A decrease

in buffer concentration at the same gradient slope resulted in an increase in resolution of variants from the main peak. For elution at 5 mM, a further increase in working pH range from 9-10 to 9.2-10.2 was required. These findings are in agreement with Farnan and Moreno [17], who they achieved higher resolution for mAb isoforms by a 4-fold decrease in the concentration of the buffer.

The impact of column chemistry on separation efficiency was also evaluated. A trivial impact of column chemistry on the selectivity is recognisable for both mAb1 (**Figure 3.3a**) and mAb2 (**Figure 3.3b**). In addition, there are more prominent fluctuations in the pH profile and a longer titration time for the weak cation-exchanger (see pH profiles). As the working pH range is high enough to ensure full ionisation of the carboxylic group of the weak cation-exchanger (p$K_a$ ~ 5), the reason for differences in the pH profile might be due to the different chemistries of the stationary phases [149].

### 3.3.3 Ammonium hydroxide (AMH) buffer system

Although suitable for resolving the isoforms of given mAbs, the low volatility of DEA could potentially limit its application for MS detection. In order to address this issue, we explored the use of AMH, which is a volatile buffer species with p$K_a$ 9.25. For this buffer, acceptable

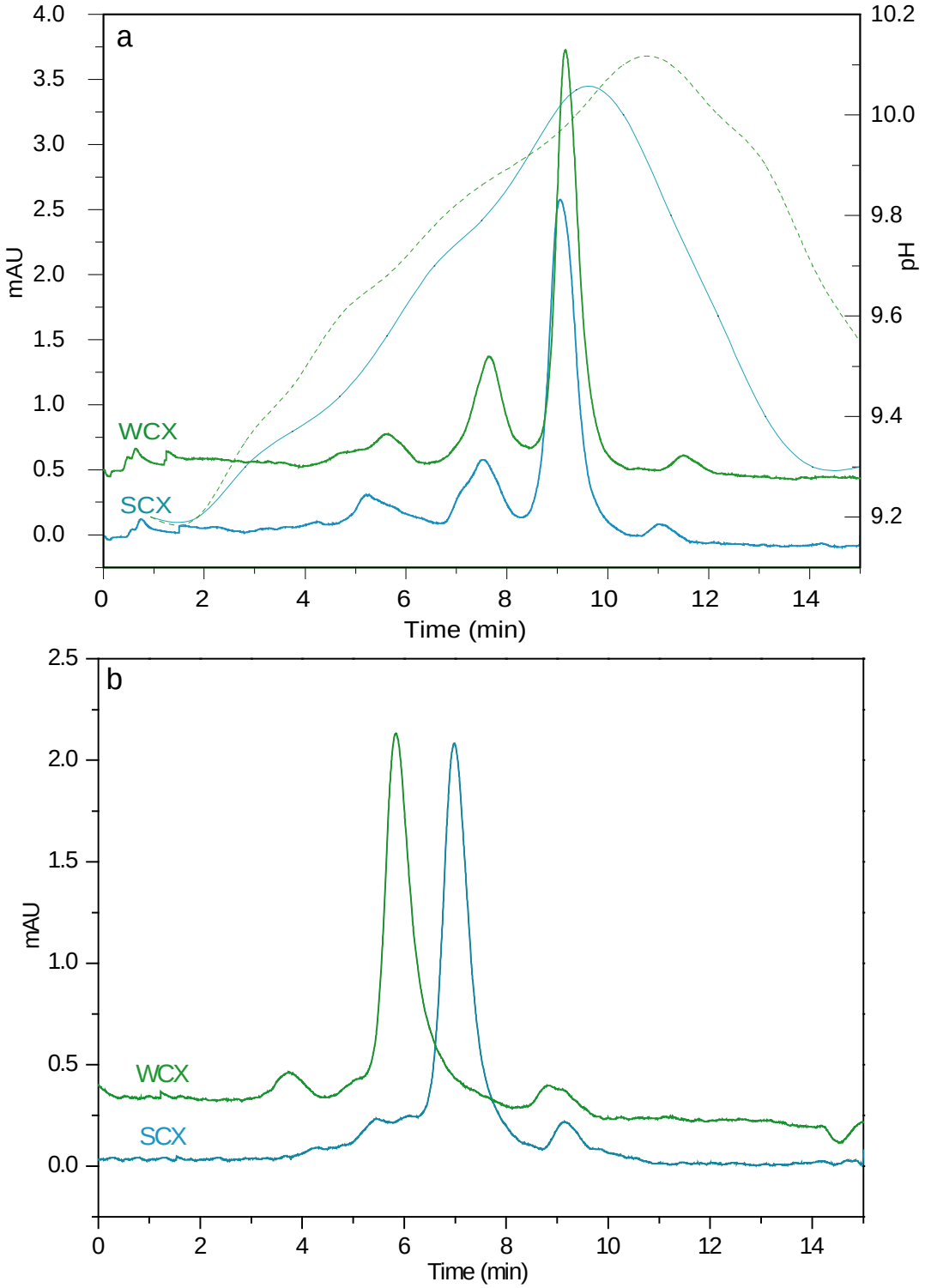


**Figure 3.3:** Comparison of separation of variants for mAb1 (a) and mAb2 (b) on ProSwift WCX-1S and ProSwift SCX-1S columns. Eluent: 5 mM DEA, pH 9.2-10.2. Other conditions as in Figure 3.1.

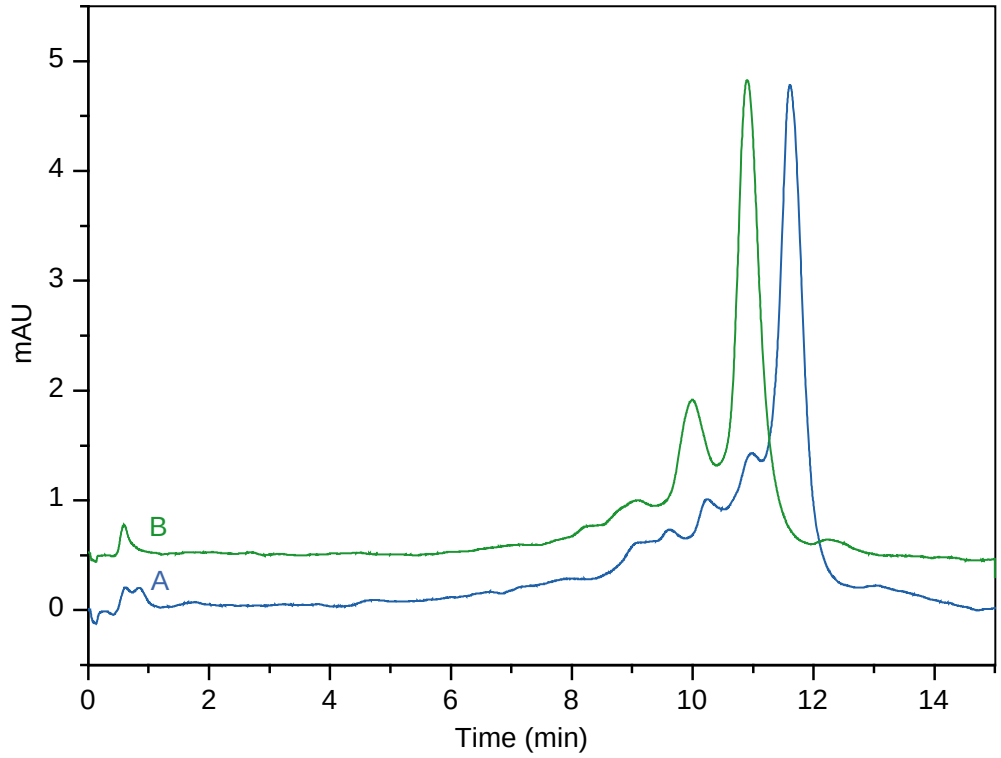


**Figure 3.4:** Interrelationship between eluent concentration and pH range on separation efficiency of mAb1. The gradient slope was 0.1 pH units/min. Eluent: 5 mM AMH, pH 9.2-10.2 (A); 2.5 mM AMH, pH 9.5-10.5 (B). Other conditions as in Figure 3.1.

chromatographic resolution of protein isoforms was obtained even at buffer concentrations lower than 5 mM (**Figure 3.4**). This demonstrates that focusing effect of the buffer system increases by decreasing its concentration. Similar to the earlier results, obtained with the EDA-TEA buffer, the optimum pH range had to be adjusted when the eluent concentration was decreased to promote maximum separation efficiency.

**Figure 3.5** displays the effect of eluent pH range and gradient slope on resolving mAb1 isoforms. By maintaining the gradient slope at 0.1 pH units/min, it was found that although the fine structure of the

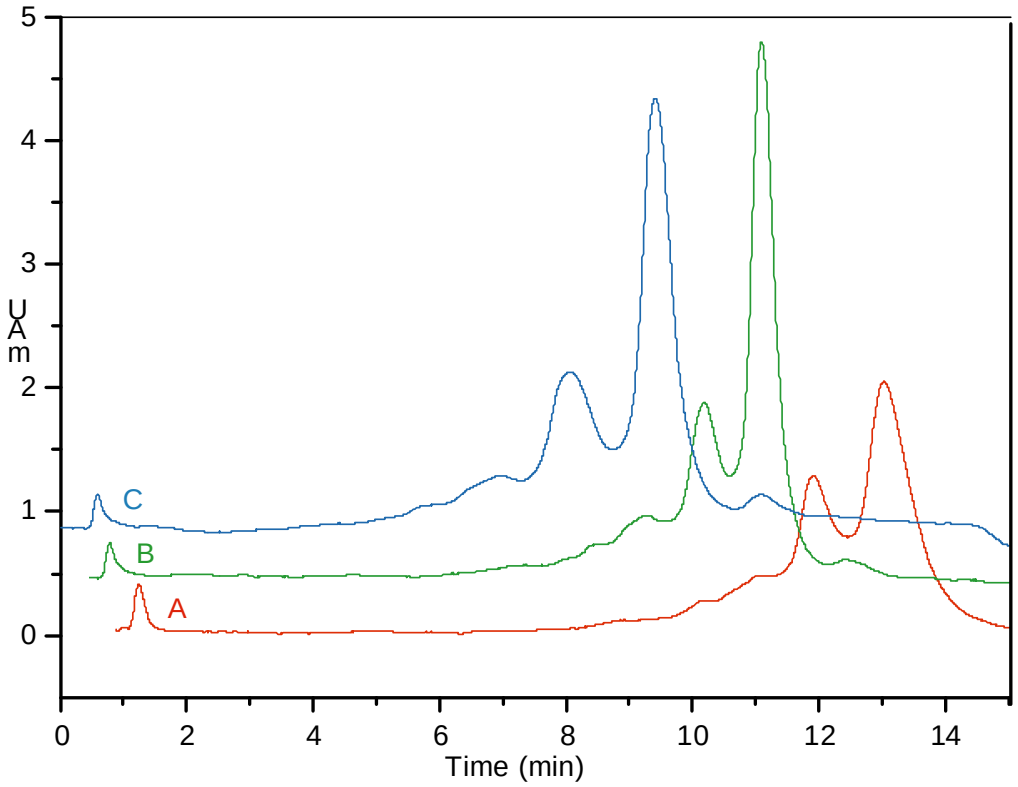


**Figure 3.5:** Influence of operational pH range and gradient slope on resolution of mAb1 variants. Eluent: 2.5 mM AMH. pH range and gradient slope: 9.3-10.3 and 0.1 (A); 9.5-10.5 and 0.1 (B); 9.7-10.5 and 0.08 pH units/min (C). Other conditions as in Figure 3.1.

acidic region remains unaltered (**Figure 3.5**, traces A and B), basic variants previously hidden within the threshold of the major peak were clearly resolved when the pH range was raised 0.2 pH units further from 9.3-10.3 to 9.5-10.5. This step-wise optimisation approach illustrates the possibilities offered when using a pH gradient over a narrow pH range, in that it enables not only formation of a controlled pH profile, but also permits the fine tuning of pH within the range defined by the applied buffer system to obtain the maximum separation efficiency.

Interestingly, it was found that low ionic strength eluents generated a significantly high back-pressure with the ProPac WCX-10 column (pressure upper limit = 120 bar). When 5 mM AMH pH 9.5 at 0.5 mL/min was used, the initial back-pressure of 94 bar was monitored and found to be unstable and to increase gradually. This behaviour is most likely due to the osmotic pressure generated from the difference between the water content of the very dilute eluent and the IEX sorbent.

Unlike the packed column, the high permeability of the monolithic ion-exchangers resulting from their porous properties allowed fast generation of pH gradients at moderate and stable back-pressure (< 70 bar) even at very low buffer concentrations, as well as minimizing column titration times (typically less than 5 min). These merits offer a rapid analysis time that is applicable for high-throughput process development. While quite successful in resolving charge heterogeneity of mAb1 and mAb2, the simplified buffer systems failed to elute mAb3 unless the eluent ionic strength was increased through addition of a salt.

Rozhkova [21] has previously reported the suitability of conducting pH gradient separation of mAb variants by adding NaCl into eluents. Accordingly, 2.5 mM AMH eluent, pH 9-10 containing different concentrations of NaCl ranging from 20 to 40 mM were used for eluting mAb3. The results indicated partial resolution of the main component from part of the acidic species (**Figure 3.6**). Basic variants, however, remained hidden presumably under the wide shoulder of the major peak.

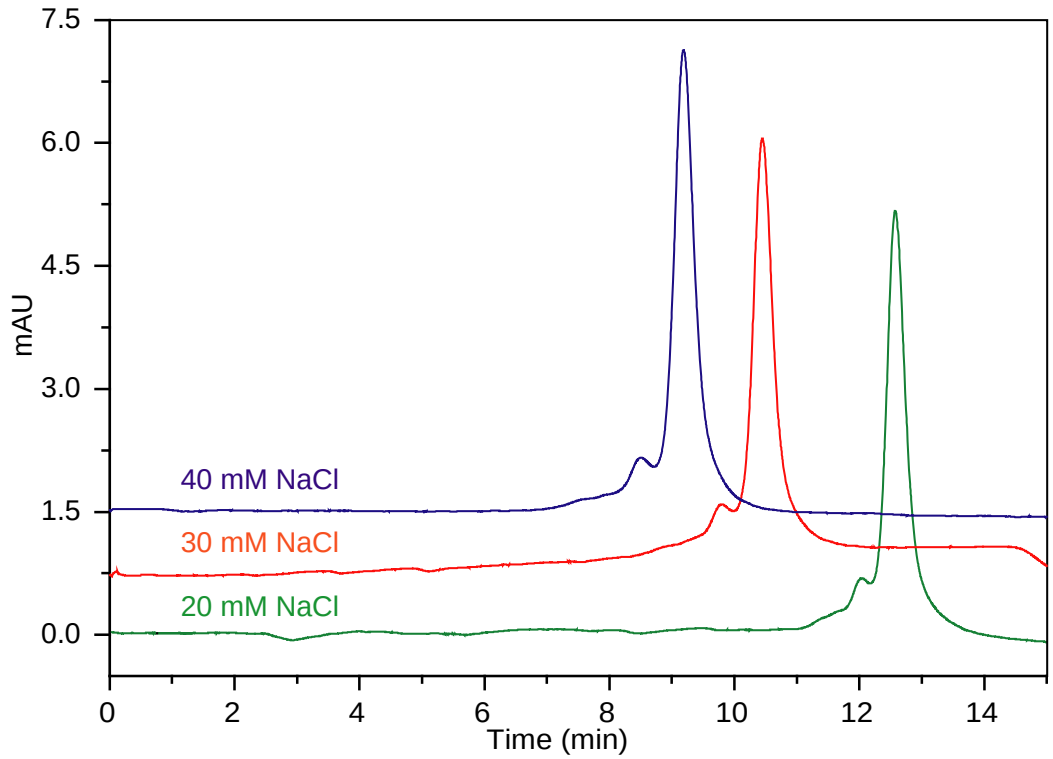


**Figure 3.6:** Effect of NaCl concentration on pH gradient elution of mAb3. Eluent: 2.5 mM AMH containing the indicated level of NaCl, pH 9-10. Other conditions as in Figure 3.1.

One possible explanation for this strong retention might be due to the differences in modification site, kind of modification, and/or degree of modification occurring in the protein [42], all of which influence the strength of interactions between the protein molecule and the ion-exchanger. These modifications vary from those that change the number of charge residues on the surface of the protein to those being less connected to the charge, such as change in antibody conformation. Deamidation, for example, is one possible modification which is likely to have an effect on retention of a protein by affecting the number of positively charged groups over the surface of a protein and hence the

binding of the protein to a cation-exchanger [142]. It is also just as likely that the behavior of mAb3 is caused by a clustering of charge on a particular surface of the mAb. Further investigation is required to confidently determine the characteristics of the mAb variants.

### 3.3.4 Retention Mechanism

**Figure 3.1** clearly indicates mAbs are retained at pH values above their p*I* values, where the proteins carrying the same charge as the stationary phase. While no retention is normally expected, a similar phenomenon was noted for other buffer systems developed here when the initial pH of the eluent was shifted even further toward a more basic pH. This can be explained using the augmented electrostatic interaction model developed by Tsonev and Hirsh [145], which suggests that although a protein accumulates an increasing density of charges with the same sign as the ion-exchanger when titrated using a pH gradient, small localised patches of the opposite charge will preferentially orient protein molecules toward the stationary phase. This allows the protein to remain adsorbed to the stationary phase even when the net charge on the protein is the same as that of the stationary phase. Extending the repulsive electrostatic forces through further increases in pH finally dominates the electrostatic attractions, leading to elution of the protein at a specific pH, termed the $pI_{app}$, that is the pH at which the protein is eluted from the column. The relationship between p*I* and $pI_{app}$ for a protein can be interpreted using the equations derived by Sluyterman and Elgersma [30] and has been verified experimentally [27-31, 35]. Accordingly, the difference between p*I* and $pI_{app}$ is directly proportional to the

dimensionless Donnan potential and to the rate of change of the protein charge with pH (*dZ*/*dpH*). While the Donnan potential is affected principally by the concentration of charged groups in the ion-exchanger, the ionic strength, and pH of an eluent, *dZ*/*dpH* is the protein-dependent contributor to the apparent p*I* shift.

### 3.3.5 Effects of eluent concentration and pH on resolution

The overriding consideration in this work was to maximise achievable resolution for mAb isoforms. pH and ionic strength are two major characteristics of the eluent that govern the elution and separation of proteins in pH gradient IEC. Here, advantage was taken of the general expressions proposed by Sluyterman and Elgersma [30] for the pH gradient approach to explain the interplay between these two parameters and their effects on separation efficiency.

Peak width and peak separation are the two determinants of resolution. The width of a protein band in terms of pH unit can be written as:

$$(\Delta pH)^2 \approx D\,(dpH/dV)/\varphi\,(dZ/dpH) \quad (1)$$

where $D$ denotes the diffusion coefficient of a protein, $dpH/dV$ the pH gradient slope and $\varphi$ the Donnan potential [30]. This equation implies that an increase in peak focusing is consistent with the lower ionic strength (buffer concentration) used, which increases the absolute value of $\phi$.

Evidence of this inference can be seen in a comparison of trace A and B in **Figure 3.2**, in which the resolution gained for the main isoforms of mAb2 can be related to the focusing effect obtained by decreasing the ionic strength. In fact, superior ability of pH gradient IEC over that of conventional salt gradient IEC at fixed pH to focus eluent bands is well known [35]. The absence of a focusing effect in fixed pH, salt gradient-based IEC can be partly related to the lack of the Donnan potential, as a result of high salt concentration involved. Comparison of Trace C to Traces A and B in **Figure 3.2** indicates that while employing the same pH range is likely to maintain the $dZ/dpH$ (traces A and B), the positive effect of this kinetic factor on peak width can be highlighted by shifting up the pH range further (trace C), which along with more decrease in ionic strength leads to an increase in resolution to an even a greater extent. The dominating effect of $dZ/dpH$ on peak focusing can also be seen by comparing traces A and B in **Figure 3.5,** where there is likely no significant difference between the Donnan potentials due to the constant eluent concentration (2.5 mM). Counter to expectations the peaks became broader when another determinant of peak width in Eq.1, i.e., the pH gradient slope ($dpH/dV$), decreased further from 0.1 (trace B) to 0.08 pH unit/mL (trace C), while keeping the other conditions unchanged. This was probably due to the domination of the diffusion coefficient of protein ($D$). This therefore suggests that the rate of titrating the ion-exchanger with pH has become lower than the rate at which proteins attain charge equilibrium, which could compromise the peak focusing gains from shallower gradients.

The contribution of the other determinant of resolution, i.e. peak separation, appears to be the main factor in the resolution gains observed for isoforms in **Figure 3.4**, where even the peak focussing for the main isoforms seems to be compromised, despite the expected focussing effects as the eluent concentration decreased and the pH range shifted up further. In fact, almost all of the post-translational modifications and degradations can change surface charge properties of an antibody either directly by changing the number of charged groups or indirectly by introducing conformational alterations [42]. According to the electrostatic model developed by Tsonev and Hirsh [145], there is a relationship between the magnitude of a shift in p*I* and the relative charge distribution in a given protein. This in turn implies that isoforms can be resolved based on their $pI_{app}$ when titrated by a gradient of pH, relating the resolution achieved in **Figure 3.4** to a greater separation of the peaks. Similar arguments based on the distribution of charges on the surface of a protein have also been used to explain the trends observed in resolution for *CF* of β-lactoglobulin A and B [29], and haemoglobin variants [29, 34].

### 3.3.6 Loading capacity

The loading capacity of the proposed approach for the separation of mAb charge variants was also assessed. While some minor loss of purity occurred when a sample load of about 118 μg mAb1 was injected onto the column, the overall separation pattern and the fine structure of the acidic elution region remained unchanged (**Figure 3.7**). By considering the low ionic strength of the buffer system employed, this

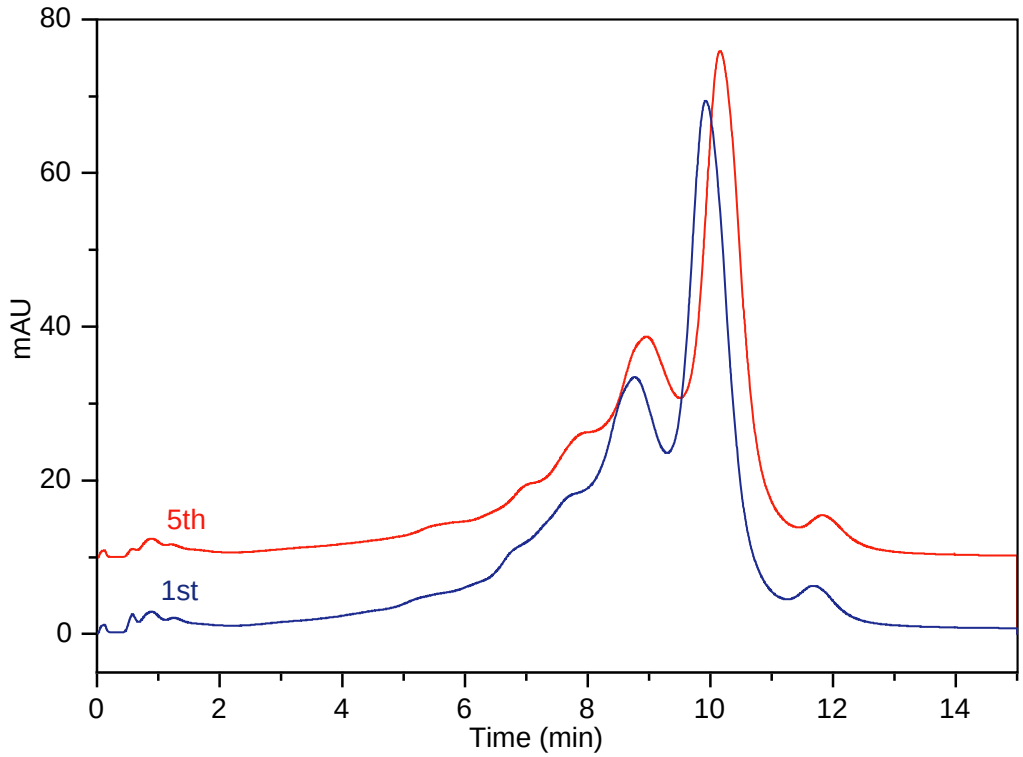


**Figure 3.7:** Overlay of typical elution profiles for the first and the fifth injection of mAb1 in evaluating the loading capacity of ProSwift SCX-1S column. Eluent: 2.5 mM AMH, pH 9.5-10.5. Sample load: 118 µg of stock solution of mAb1 directly injected without dilution. Other conditions as in Figure 3.1.

infers a significant advantage of this approach for scale-up, enabling it to be used along with classical IEC for preparative purposes.

### 3.3.7 Profiling charge heterogeneity of mAbs by iCE

To assess the resolving power offered by the developed procedure, analysis of the given mAbs by iCE was also included in the study. The difference in separation mechanism of each technique may offer the orthogonal and complementary information required to obtain an unambiguous assignment of protein variants. The obtained profiles (**Figure 3.8**) demonstrate clearly the distribution of isoforms within

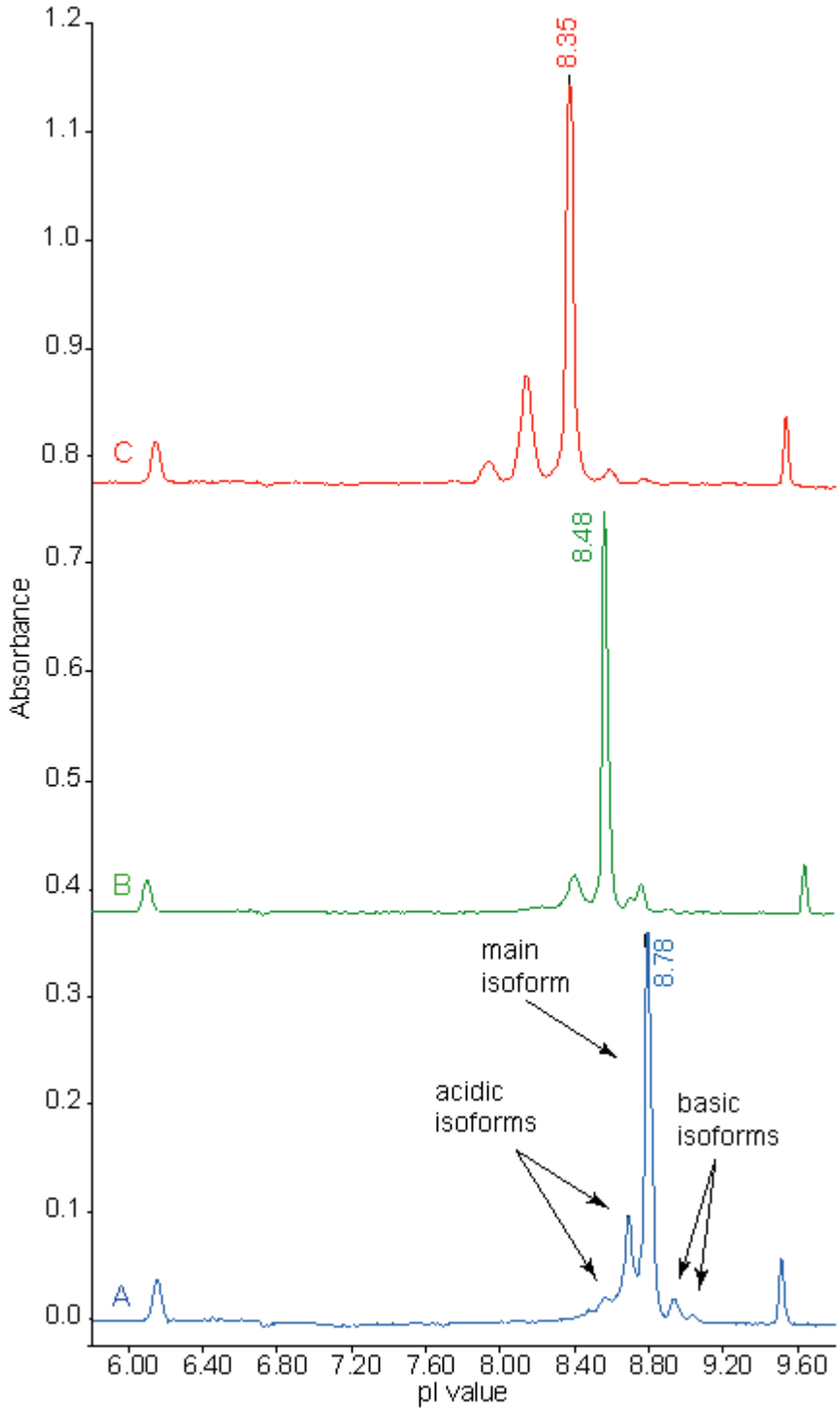


**Figure 3.8:** iCE profiles for mAb1 (A), mAb2 (B) and mAb3 (C) (analysis conditions are described in Experimental section).

acidic, main and basic species of the mAbs. A comparison between iCE profiles and IEX chromatograms reveals some interesting similarities in separation efficiency. For example, there is a striking similarity between the two methods in resolving mAb1 acidic isoforms, although iCE offers more resolution in the basic region (compare **Figure 3.5** (B) and **Figure 3.8** (A). However, the resolution between the main isoform and variants using IEC appears to be superior to that obtained using iCE when the DEA buffer system was employed, (see **Figure 3.3a**). As demonstrated in **Figure 3.8** (B) and **Figure 3.3b**, some similarities in resolving isoforms between pH gradient IEC and iCE can also be seen for mAb2. As an indication of peak purity, the peak area percent for the sum of the acidic species, the major peak and the sum of the basic species were also compared in both separation methods (**Table 3.1**).

It was not possible to achieve equivalent separation efficiency for all of the different antibodies analysed by IEC under identical separation conditions. The DEA buffer system for mAb1 and the AMH buffer system for mAb2 indicate closer overlap between iCE and IEC peak area percent data. For mAb3, while increasing the ionic strength of the buffer system through the addition of an inert salt provided better separation efficiency than that obtained in previous work [149], this strategy still appears inadequate in providing purities comparable to iCE.

Further comparison between the obtained profiles highlights another interesting correlation between the two techniques. The difference between the p$I_{app}$ of the first isoform (~10) and the last one

**Table 3.1:** Reproducibility comparison of CEX chromatography and iCE.

| Characteristic | CEX | | | | | | iCE | | |
|---|---|---|---|---|---|---|---|---|---|
| | DEA[a] | | | AMH[b] | | | | | |
| | **mAb1** | **mAb2** | **mAb3** | **mAb1** | **mAb2** | **mAb3** | **mAb1** | **mAb2** | **mAb3** |
| **Acidic species %** | 31.3 (5.2) | 13.3 (1.3) | - | 38.5 (1.7) | 16.6 (1.2) | 15.9 (1.5) | 29.4 (0.4) | 19.5 (0.4) | 16.6 (1.8) |
| **Main component %** | 64.5 (5.1) | 77.4 (2.7) | - | 58.2 (1.5) | 74.3 (1.4) | 84.1 (2.3) | 63.8 (0.3) | 69.5 (0.2) | 78.0 (0.5) |
| **Basic species %** | 4.2 (0.8) | 9.4 (2.8) | - | 3.3 (0.9) | 9.1 (2.2) | - | 6.8 (1.6) | 11.0 (0.5) | 5.4 (1.5) |
| **Retention of main peak by CEX (min)** | 9.0 (2.2) | 6.9 (2.5) | - | 10.8 (1.8) | 9.8 (3.1) | 9.1 (1.7) | - | - | - |
| **p*I* of main peak by iCE** | - | - | - | - | - | - | 8.78 (0.02) | 8.48 (0.03) | 8.35 (0.01) |

RSDs % of the measurements are given in parentheses (n = 5 for CEX and 3 for iCE).

[a] 5 mM DEA, pH 9.2-10.2.

[b] 2.5 mM AMH, pH 9.5-10.5.

(~10.4) in the IEC profile of mAb1, for example, is about 0.4 pH units (see pH profile in **Figure 3.3a**), which correlates well to the p*I* range (approximately 0.5 p*I* units) over which the separation was achieved in the corresponding iCE profiles. This observation also lends more support to the comparability of the separation efficiency of the two approaches, despite the differences in separation mechanism.

### 3.3.8 LC-MS analysis

Unlike RPLC, IEC is not easily hyphenated with MS due to the high content of salt involved **[151]**.Therefore, the integrated MS-based strategies are traditionally performed in multi-dimensional approaches relying on the separation efficiency of CEX chromatography for protein fractionation in the first dimension and MS compatibility of RPLC in the second dimension. The feasibility of the direct coupling of the developed low ionic strength pH gradient with MS was probed employing the AMH buffer system with a ProSwift WCX-1S column and mAb1 as an example. Methanol (20% v/v) was added to both eluents in order to enhance the electrospray efficiency. **Figure 3.9** shows the averaged mass spectrum of the intact mAb1 after pH gradient elution. The averaged mass spectrum was acquired in the range from 12 to 22 min from the corresponding base peak chromatogram (**Figure 3.10**) and featured multiply charged ions (ammonium adducts) from 24+ to 30+. Further magnification of the spectrum (see insets) revealed more charge states which can be attributed to the existence of different species (isoforms).

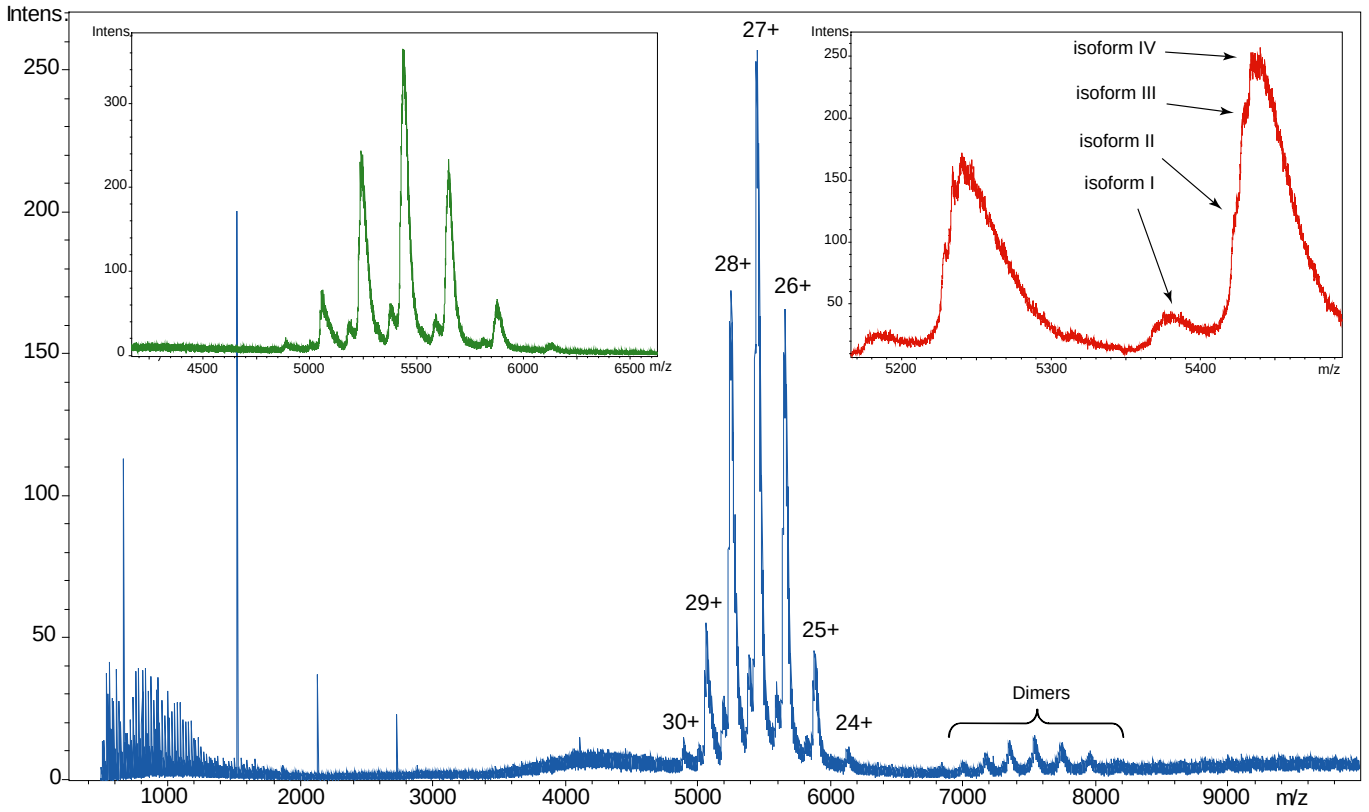


**Figure 3.9:** ESI mass spectrum of intact mAb1 with insets showing the expanded view of charge states of the antibody.

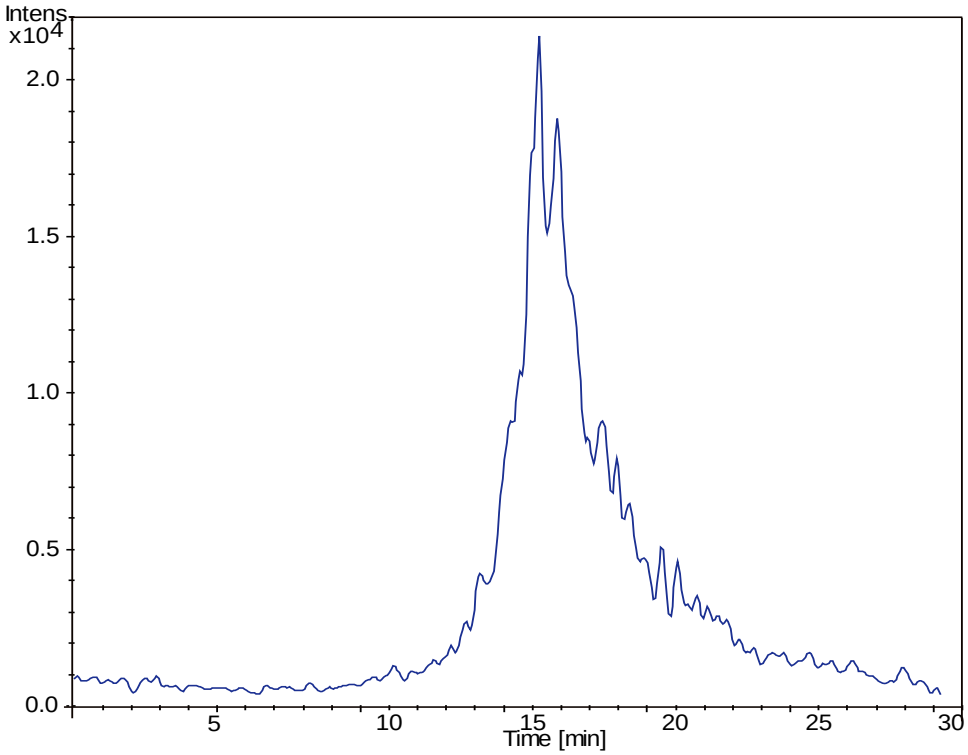


**Figure 3.10:** (smoothed) base peak chromatogram of intact mAb1 eluted by running a pH gradient (5 mM AMH, pH 9.5 to 10.5) over a ProSwift WCX-1S column. Gradient: 0-100 % B in 20 min, 100% B for 5 min. Column: ProSwift WCX-1S (4.6 × 50 mm); Flow-rate: 0.4 mL/min (splitted (1:100) before introducing into MS).

To gain more insight into the possible modifications, deconvolution of the intact mass spectrum was performed using a maximum entropy algorithm (**Figure 3.11**). Based on the deconvoluted results, four different isomers were proposed, however, the resolution provided by the TOF instrument did not allow further unambiguous identification of the previously described modifications. Nevertheless, the results suggested that this approach was viable for the study of the existence of different isoforms of mAbs, especially in combination with

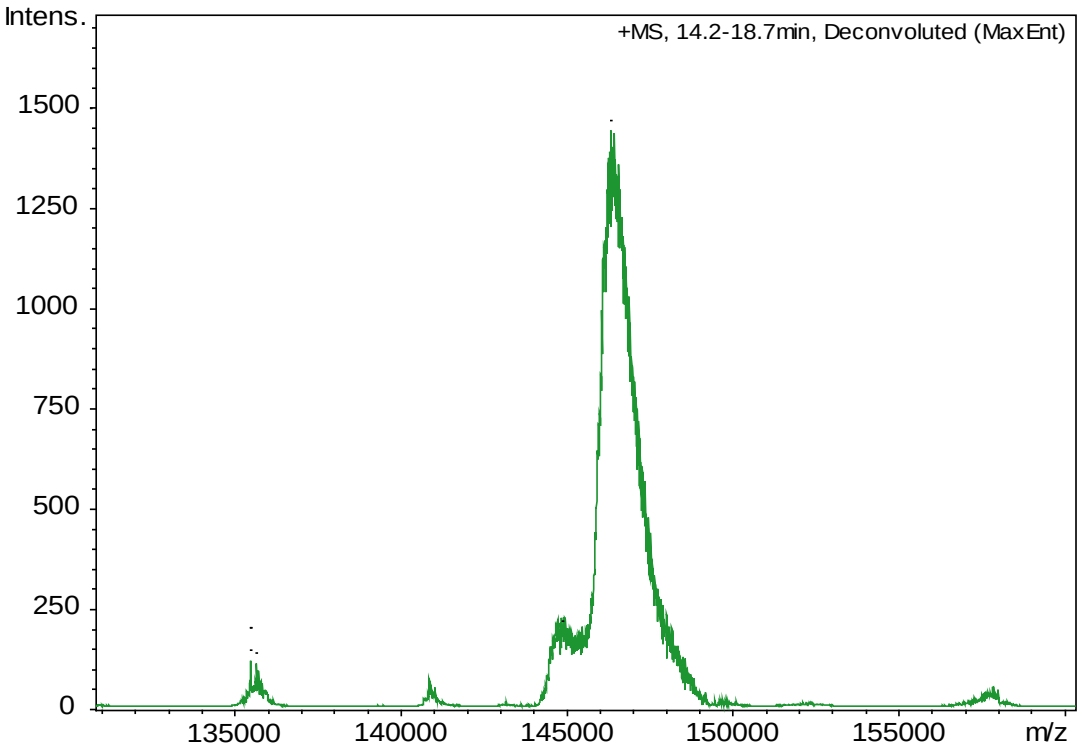


**Figure 3.11:** Deconvoluted ESI mass spectrum of intact mAb1 (ammonium adducts) obtained by performing the maximum entropy algorithm.

MS instrument with higher resolving power, which can be the focus of future studies.

## 3.4 Conclusion

The application of a shallow pH gradient generated by simple component buffer systems within a narrow pH range in combination with (CEX) monolithic columns provided remarkable results for the separation of mAbs. The separation of basic and acidic isoforms with qualities comparable to iCE was achieved at very low ionic strength, suggesting the prevailing effect of the eluent concentration on separation efficiency. The expressions developed by Sluyterman and Elgersma were

used for interpreting the obtained results, with the dominant factors being the Donnan potential, which is directly proportional to the ionic strength, and the rate of protein charge alteration with pH, principally through their effects on both peak width and peak separation. Resolution improvement through peak separation was hypothesised to occur *via* increasing the electrophoretic p*I* of variants to a different extent determined by the relative charge distribution on the protein surface. This potentially confers more separation capability in pH gradient IEC than for a conventional salt gradient IEC at a fixed pH. By keeping in mind the observed trends of increasing p*I*, this concept might potentially be used for other mAbs by choosing a suitable buffer component that has a buffering capacity that can cover the protein p$I_{app}$.

While packed columns may not be used conveniently with the developed dilute buffer systems due to the high back-pressure involved, the possibility of high-throughput analysis and fast re-equilibration time can be considered as additional advantages of the proposed approach when using monolithic columns.

Employing volatile buffer species at very low concentration also enables direct interfacing of ion-exchange separation to MS through electrospray ionization interface. The possibility of rapid verification of sequence composition of mAbs *via* accurate mass measurement and identification of post-translational modifications is expected when using MS detection with high resolving power.

As inferred from the results, despite the elution occurring at pH values where both strong and weak CEX columns are expected to be fully ionised, there are differences in the pH profiles, which most likely result from the type of ion-exchanger. Further studies of the pH gradient elution of mAbs might therefore benefit from the inclusion of other IEX chemistries. It is expected that more improvements in separation efficiency should be achieved through designing monolithic sorbents with lower buffering properties, higher biocompatibility, and permeability (for employing higher flow-rates), which can be the focus of future investigations.

# *Chapter 4*

# Methacrylate-based Polymeric Monoliths for Cation-Exchange Chromatography of Proteins

## 4.1 Introduction

IEC is an important separation mode for analysing biomolecules including peptides, proteins, oligonucleotides, and viruses due to its high capacity and ability to perform separations under non-denaturing conditions [9, 86, 152]. Compared to other chromatographic modes, such as RPLC and affinity chromatography, IEC is conducted at near physiological conditions that are not prone to cause protein denaturation and thus enable structural maintenance of proteins and preservation of their bioactivity [69, 152]. Also, in comparison to hydrophobic interaction chromatography, a lower salt concentration is used in IEC, thereby avoiding precipitation of biomolecules due to a high salt content [9].

High capacity and high resolving power have enabled IEC to be used successfully for many applications, such as purification of proteins and removal of viruses [9]. One important application of IEC is in 2D LC of extremely complex peptide mixtures, such as in "shotgun" proteomics [153]. In fact, due to the orthogonality of the separation mechanisms of IEC to RPLC, using IEC (particularly with a SCX column) as the first dimension is the most widely used 2D LC combinations [77]. For such combinations, however, one important criterion is the hydrophilicity of

the IEX column, which prevents non-specific (hydrophobic) interactions of peptides. Otherwise, the resultant 2D LC setup is not fully orthogonal and the final overall peak capacity is compromised [77]. In the worse case, some very hydrophobic peptides will not be eluted from the IEX column [77]. Currently, the Polysulfoethyl A stationary phase, which is a silica-based particle-packed column developed by Alpert in the late 1980s [154], is the most widely used column for SCX chromatography of peptides and proteins [77]. However, this column has been found to exhibit some hydrophobicity, and 15-25% ACN is required to suppress hydrophobic interactions to improve peak shapes and resolution [77, 154].

Since their emergence in the late 1980s, polymeric monoliths have received considerable interest due to favourable features, such as ease of preparation, enhanced mass transfer as a result of high permeability, and chemical and mechanical stability. Polymeric monoliths are typically used to separate biomolecules due to their pH stability, high loading capacity and biocompatibility [86]. Considering the suitability of IEC approach for the separation of biomolecules, monolithic IEX stationary phases would therefore appear to be highly desirable for bioseparation.

There are several approaches to introduce IEX functionalities into monolithic stationary phases. The most straightforward is copolymerisation of an ionisable monomer with a cross-linker [94]. Recently, attempts have been made by Lee's group for preparing IEX polymeric monoliths exhibiting minimal non-specific interactions for separation of peptides and proteins [9, 77, 85, 86, 152, 155]. Monoliths

with improved biocompatibility were synthesised by co-polymerisation of PEG-acrylate and PEG-diacrylate cross-linkers with a variety of IEX-containing monomers possessing different extents of hydrophobicity. For example, while monoliths prepared by co-polymerisation of 2-acrylamido-2-methyl-1-propanesulfonic acid (AMPS) and poly(ethylene glycol) diacrylate required 40% ACN to suppress any hydrophobic interactions, negligible hydrophobicity was observed when AMPS was replaced by vinylsulfonic acid, containing a lower hydrocarbon content [74, 77].

Although it is a simple and single-step approach, co-polymerisation suffers from some limitations, such as difficulty in finding a suitable porogen system that can dissolve ionisable monomers and that also forms a good monolith with the desired mechanical stability and pore structures, as well as distribution of some of the IEX functionalities throughout the polymer matrix. Such functionalities buried within the monolith scaffold are not accessible for large molecules, such as proteins and therefore do not make any significant contribution in the DBC of the stationary phase. Instead, as a result of the exchange of counter-ions and change in solvation, they can cause swelling and shrinking of the polymer matrix, depending on the pH and the salt content of eluents [94, 156].

Alternatively, post-polymerisation modification can be used to generate IEX functionalities on the pore surface of monoliths. In contrast to the single step co-polymerisation, this approach allows independent optimisation of porous properties of the monolith scaffold and surface

chemistry. For example, epoxy groups of GMA-based monoliths were reacted with ionisable compounds, such as ethelenediamine (EDA) [157], DEA [60, 92, 93], TEA [158], poly(ethylene imine) [159], iminodiacetic acid [160], and sodium sulfate [160-162] to afford IEX functionalities.

While EDMA is the most widely used cross-linker for synthesising methacrylate-based monoliths, some studies have shown significant non-specific interactions with proteins in monoliths prepared with EDMA [74, 94, 163]. This undesirable adsorption can be addressed by replacing EDMA with more hydrophilic cross-linkers, such as poly(ethylene glycol) diacrylate [163], or alternatively, by grafting hydrophilic monomers, such as poly(ethylene glycol) methacrylate onto the pore surface of the generic monolith in order to mask the hydrophobicity induced by the polymer matrix [94, 164].

Here, the development of a new methacrylate-based polymeric monolith prepared by co-polymerisation of GMA as a reactive monomer with pentaerythritol triacrylate (PETA) as a cross-linker is reported. CEX functionalities were then incorporated onto the pore surface of the monolith *via* aminolysis of GMA with amine reagents containing CEX groups. It was hoped that by utilising PETA as a hydrophilic cross-linker efficient separation of proteins with minimal non-specific interactions would be achieved.

## 4.2 Experimental

The general experimental details, including chemicals and instrumentation, are presented in Chapter 2. Specific experimental conditions are given in each of the figure captions.

### 4.2.1 Chemicals and reagents

All chemicals were used as received except the GMA that was freed from inhibitors by passage through a Pasteur pipette packed partially with basic alumina oxide, and 2,2′-azobisisobutyronitrile (AIBN) that was recrystallised from methanol.

### 4.2.2 Polymer monolith preparation

The polymer precursor was prepared in 4-mL glass vials by mixing monomer, cross-linker, initiator (AIBN, 1% wt. with respect to monomers), and porogens (see **Table 4.1** for recipes). The mixture was vortex-mixed and de-oxygenated with a nitrogen stream for ~ 5 min. A surface-modified capillary (100 μm i.d.) was then filled with the mixture using a glass syringe and both ends were sealed with rubber septa. Some recipes were also tried in an analytical column format by filling a modified GLT (1/4″ o.d. × 4 mm i.d. × 5 cm) with the mixture, followed by sealing both ends with plugged end-fittings. The polymerisation reaction was conducted in a thermostated water bath at different temperatures (55-65 ˚C) for 24 h. For polymerisation under pressure, the end-fitting on the bottom-end of the column was plugged, while the other end-fitting was connected to the nitrogen line through PEEK tubing. A PEEK spacer

**Table 4.1:** Recipes and characteristics of monoliths synthesised in this study.

| Monolith | Monomer | Cross-linker | Porogen[1] | | Co-porogen | | Porosimetry data | | | BET surface area ($m^2/g$) |
|---|---|---|---|---|---|---|---|---|---|---|
| | GMA, wt% | PETA, wt% | I, wt% | II, wt% | 1-decanol | 1-dodecanol | MPD[2] (nm) | $D_p$[3] (nm) | $V_p$[4] (mL/g) | |
| **M1** | 30 | 10 | 50 | - | 10 | - | 1058 | 963 | 1.3 | N.D. |
| **M2** | 30 | 10 | 50 | - | - | 10 | 1064 | 962 | 1.3 | N.D. |
| **M3** | 30 | 10 | - | 54 | 6 | - | 726 | 666 | 1.0 | N.D. |
| **M4** | 25 | 15 | - | 54 | 6 | - | 585 | 548 | 1.0 | 5.2 |
| **M5** | 30 | 15 | - | 49.5 | 5.5 | - | 612 | 551 | 0.9 | 3.9 |
| **M6** | 35 | 10 | - | 49.5 | 5.5 | - | 818 | 798 | 0.7 | 3.2 |
| **M7** | 35 | 15 | - | 45 | 5 | - | 746 | 798 | 1.0 | 3.9 |
| **M8** | 40 | 10 | - | 45 | 5 | - | 1004 | 961 | 0.8 | 2.6 |
| **M9** | 40 | 10 | - | 45 | 5 | - | 1076 | 965 | 0.8 | 2.6 |
| **M10** | 40 | 10 | - | 35 | 15 | - | 1035 | 960 | 0.8 | 3.2 |

Polymerisation temperature: M1-M2 (65 ˚C), M3-M8 (55 ˚C), M9-M10 (60 ˚C)

[1] Porogen: 20 wt% PEG-10k in 2-methoxyethanol (I) or in methanol (II).

[2] Median pore diameter.

[3] Pore size at the peak of the pore distribution curve.

[4] Pore volume.

(1/4″ o.d. × 4 mm i.d. × 3 mm) was placed between the GLT and the end-fitting and carefully filled with the polymerisation mixture as well. The set-up was then connected to the nitrogen line and immersed into the water bath in upright position. A pressure of ~ 5 bar was then applied to the set-up and maintained during polymerisation. Upon completion of the reaction the set-up was removed from the water bath and cooled down to room temperature before disconnecting from the nitrogen line.

### 4.2.3 Post-polymerisation modifications

1 M solutions of two amine reagents containing sulfonic acid and phosphoric acid functionalities, namely 2-aminoethyl hydrogen sulfate (SEA) and o-phosphorylethanolamine (PEA) were prepared in 1 M carbonate buffer at different pH values by adding sodium hydroxide solution (5 M). About 450 μL of each solution was pumped through each column for 24 h at 75 °C. Acid hydrolysis of unreacted epoxides was then accomplished by pumping a 0.5 M sulfuric acid solution through the column at 30 μL/h for 4 h at 75 °C. The entire reaction scheme is shown in **Figure 4.1**.

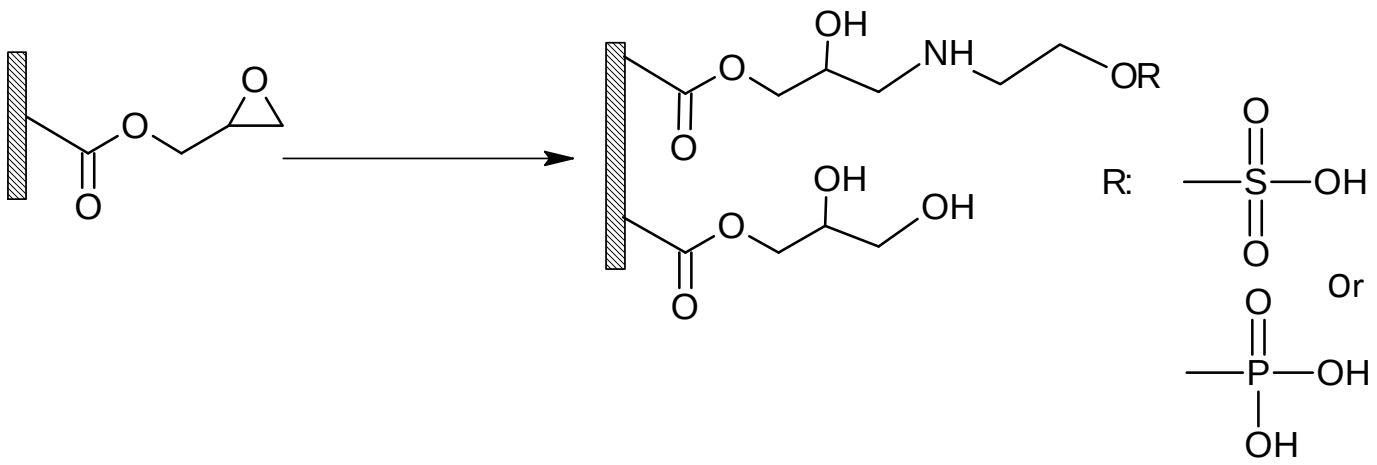


**Figure 4.1:** Reaction scheme for post-polymerisation modification of poly(GMA-co-PETA) monolith. Reaction conditions: (1) 1 M R-$NH_2$ (SEA or PEA) in 1 M carbonate buffer (pH 10.5), for 24 h at 75 °C; (2) 0.5 M $H_2SO_4$, for 4 h at 75 °C.

## 4.3 Results and discussion

### 4.3.1 Polymer monolith preparation

The preparation of a novel (meth)acrylate-based monolith with superior hydrophilicity than the classic poly(GMA-*co*-EDMA) was the aim of this work. PETA is an acrylate-based cross-linker, which makes it more hydrophilic than methacrylate-based analogies like EDMA. Together with three acrylate units, the hydrophilicity of this cross-linker is also strengthened with the presence of a hydroxyl group on the other end of the molecule. Therefore, monoliths synthesised using PETA as cross-linker are believed to be highly hydrophilic/hydrated [165-170], which would minimise the hydrophobic interaction of proteins with the monolith matrix.

The porosity and flow-through characteristics of a polymeric monolith can be controlled by tuning key variables, including the composition of pore-forming solvents (porogen and co-porogen), the content of cross-linker and polymerisation temperature. Along with temperature, the choice of pore-forming solvents is another means for controlling the porous properties of monoliths without changing the chemical composition of the final polymer. The porogenic solvents control the porosity of the monolith through solvation of the polymer chains in the reaction medium during the early stages of polymerisation [50]. The composition of pore-forming solvents was initially adopted from a recipe developed by Irgum's group [171]. They used PEG with a

wide range of MW as the porogen for preparing polymeric monoliths suitable for protein separations. Because of its unique characteristics, such as biocompatibility, PEG was hypothesised to establish wide pores with a protein-friendly surface, which is desirable for bioseparations. The suitability of PEGs as a porogen has also been demonstrated by polymeric monoliths prepared *via* a polymerisation mechanism other than free-radical initiation, such as epoxy-based monoliths that are prepared by polycondensation [104-106]. Like the original recipe, PEG with MW of 10,000 (PEG-10k) dissolved in 2-methoxyethanol (20 wt%) was initially used as porogen together with either 1-decanol or 1-dodecanol as co-porogen.

As seen in **Table 4.1**, monoliths with very similar porous properties were achieved (M1 and M2). Although monoliths with wider pores (Median Pore Diameter (MPD) = 1.6 and 1.7 μm) were reported for the original recipe in which a different monomer composition was used and the polymerisation was performed *via* UV-initiation, the porous properties of those monoliths also showed negligible difference [171], suggesting similar solvating properties for 1-decanol and 1-dodecanol as co-porogen. Both monoliths showed pore characteristics highly suitable for the separation of large biomolecules, such as proteins (MPDs ~ 1 μm and pore volumes > 1.0), but since 1-dodecanol is solid at room temperature, 1-decanol was ultimately preferred over 1-dodecanol for further studies. The porogen system also became solid at room temperature and required warming up (< 45 ˚C) before use. However, due to the volatility of 2-methoxyethanol, heating would cause a change

in the composition of the porogen. Further, a mass reduction was observed when purging the polymerisation mixture with nitrogen. 2-methoxyethanol was replaced with methanol in the porogen system. However, this modification resulted in a significant reduction in the porous properties of the monoliths, suggesting that methanol was a better solvent than 2-methoxyethanol for the monolith (see **Table 4.1**). Systematic optimisation of the polymerisation mixture was therefore conducted by manipulating other variables, including temperature and monomer composition.

As expected, a further reduction in the average pore size was also observed with increasing the percentage of cross-linker in the monomer composition (see M3 and M4 in **Table 4.1**), which is known as a result of an earlier formation of highly cross-linked globules with a reduced propensity to join together [50]. Conversely, an increase in pore size was observed by keeping all variables constant but increasing the percentage of GMA in the monomer composition (see M5 and M6 in **Table 4.1**). MPDs larger than 1.0 μm reappeared with further increase in the GMA content up to 40%. A higher content of GMA was also beneficial considering the higher ion-exchange capacity that would be incorporated on the pore surface of monoliths during post-polymerisation modifications. On the other hand, the surface area of the monoliths in the dry state remained basically unaltered by these changes to less than 5 $m^2/g$ (see **Table 4.1**), which is not unusual for a polymeric monolith with such a large pore size. The last three monoliths in **Table 4.1** demonstrated very similar porous properties, despite some differences in the ratio of

porogen to co-porogen and polymerisation temperature. While porous characteristics of monoliths are generally sensitive to even minor changes in the variables, this result may suggest more reproducibility for the prepared monolith. Monolith M9 (**Table 4.1**), which showed slightly larger MPD, was ultimately chosen for further studies.

Direct visual images of the poly(GMA-*co*-PETA) monoliths were provided by SEM micrographs. **Figure 4.2** shows SEM images for monolith M9 as an example. A typical "cauliflower" morphology of methacrylate-based monoliths is seen with obvious flow-through pores across the structure. Also, the monolith is uniform and firmly attached to the capillary wall. Very similar morphologies were observed for other monoliths as well.

*4.3.1.1 Monolith preparation in conventional dimension*

The majority of contributions focused on developing monolithic materials for chromatography have been devoted to micro-bore dimensions (mostly in fused-silica capillaries), primarily because of the difficulty in keeping the monolith in contact with the inner wall of a mould with a conventional dimension during the chromatography as a result of inherent shrinkage of polymers. Due to the larger surface-to-volume ratio in capillaries than conventional dimensions (2-5 mm i.d.), such shrinkage does not normally cause detachment of monoliths in the capillary format [139].

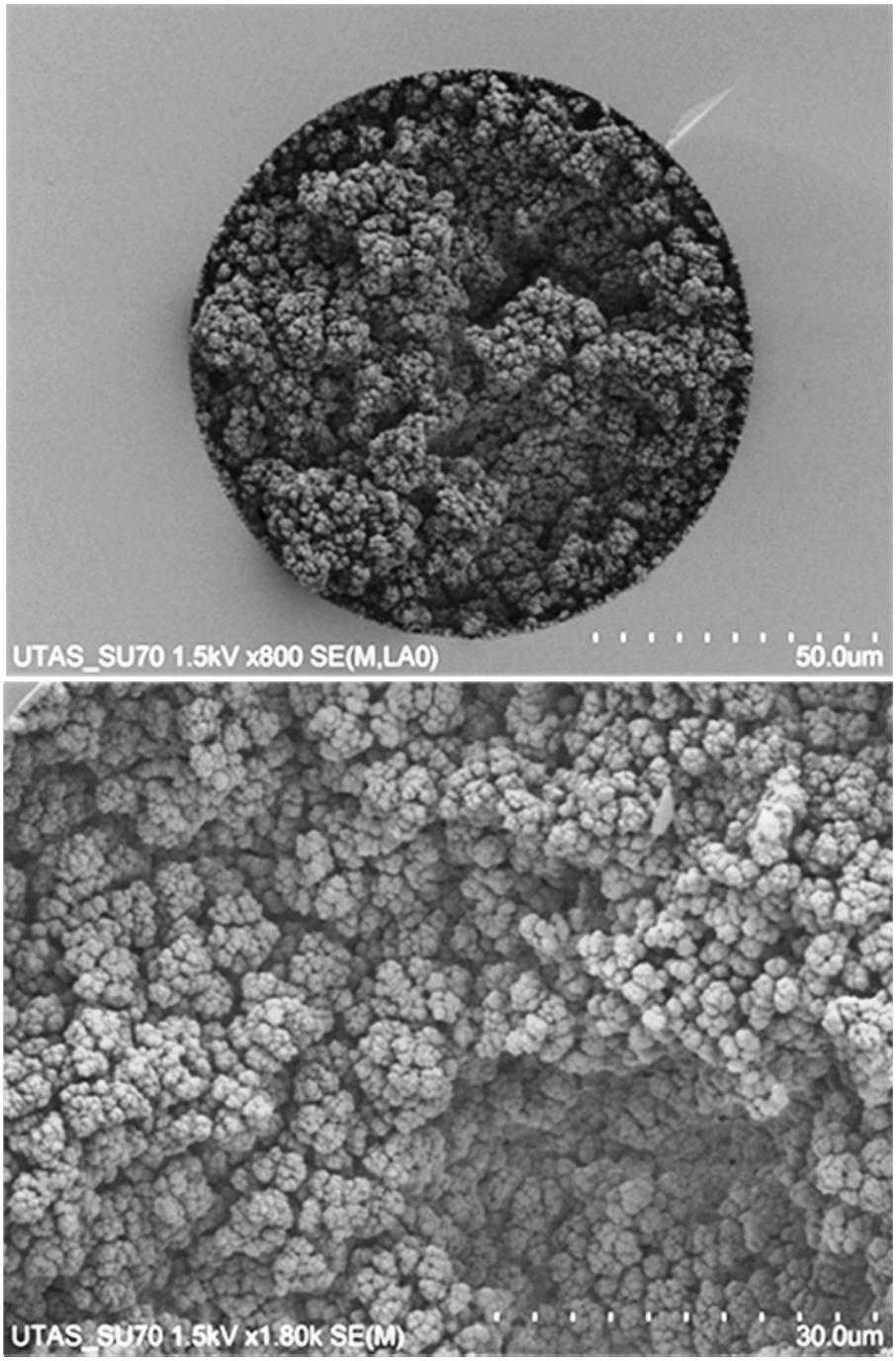


**Figure 4.2:** SEM images of monolith M9.

On the other hand, the application of capillary columns requires equipment capable of precisely delivering very low flow-rates, injecting small volumes, having minimal extra-column void and detector cell volumes. While many laboratories are still equipped with conventional analytical chromatographs that are unable to operate with micro-bore columns, it is desirable to develop monolithic columns with conventional analytical dimensions.

Several attempts were made to prepare poly(GMA-*co*-PETA) monoliths in stainless steel GLTs. Unlike fused-silica capillaries, vinylisation of the inner wall of the conventional bore tubes does not seem necessary provided that the polymer can swell enough in the mobile phase during operation to ensure good contact of the monolith with the column wall. As an example, Svec and Fréchet in one of the early reports on polymer monoliths prepared their classic poly(GMA-*co*-EDMA) monolith directly within a stainless steel tube of 50 × 8 mm i.d. dimension [172]. Nevertheless, in the present study, vinylisation on the inner wall of GLTs was conducted prior to polymerisation to permit covalent attachment of the monolith. Although washing of the column post-polymerisation was performed with tetrahydrofuran (THF), which is less polar than ACN and methanol, to ensure swelling of the monolith, a gradual decrease in the column back-pressure was observed. Further inspection by SEM showed partial detachment of the monolith from the column wall.

Allington *et al.* [173] suggested polymerisation under pressure in order to compensate for shrinkage during polymerisation. Pressure can be applied to the column using a piston or a gas filling the space above the polymerisation mixture. The latter approach was adopted by Smirnov *et al*. and successfully performed for making a poly(divinylbenzene-*co*-ethylvinylbenzene-*co*-2-hydroxyethyl methacrylate) monolith inside vinylised glass columns (150 × 3 mm i.d.) [139].

Since the volume of the reaction mixture decreased during the polymerisation, a pre-column was also connected to the upper end of the column and polymerisation was performed under constant pressure of nitrogen (3 bar). Unfortunately, this approach also did not result in a firm attachment of our monolith to the wall even under pressures as high as 10 bar (see **Figure 4.3**).

This approach was not pursued and further studies were limited to the capillary format. However, other approaches might be considered for future studies, such as using tubes with smaller internal diameter (2 mm) to limit the extent of shrinkage, or modification of the polymerisation recipe by increasing the content of cross-linker in order to get more cross-linked structure, which affords less swelling propensity [86, 174, 175]. Further, post-polymerisation compression of the monolith inside the tube could be considered as another alternative [58]. However, this is not a straightforward approach and requires experience, and special fittings and accessories (see Chapter 6 for a suggestion). This strategy has been successfully commercialised by Dionex

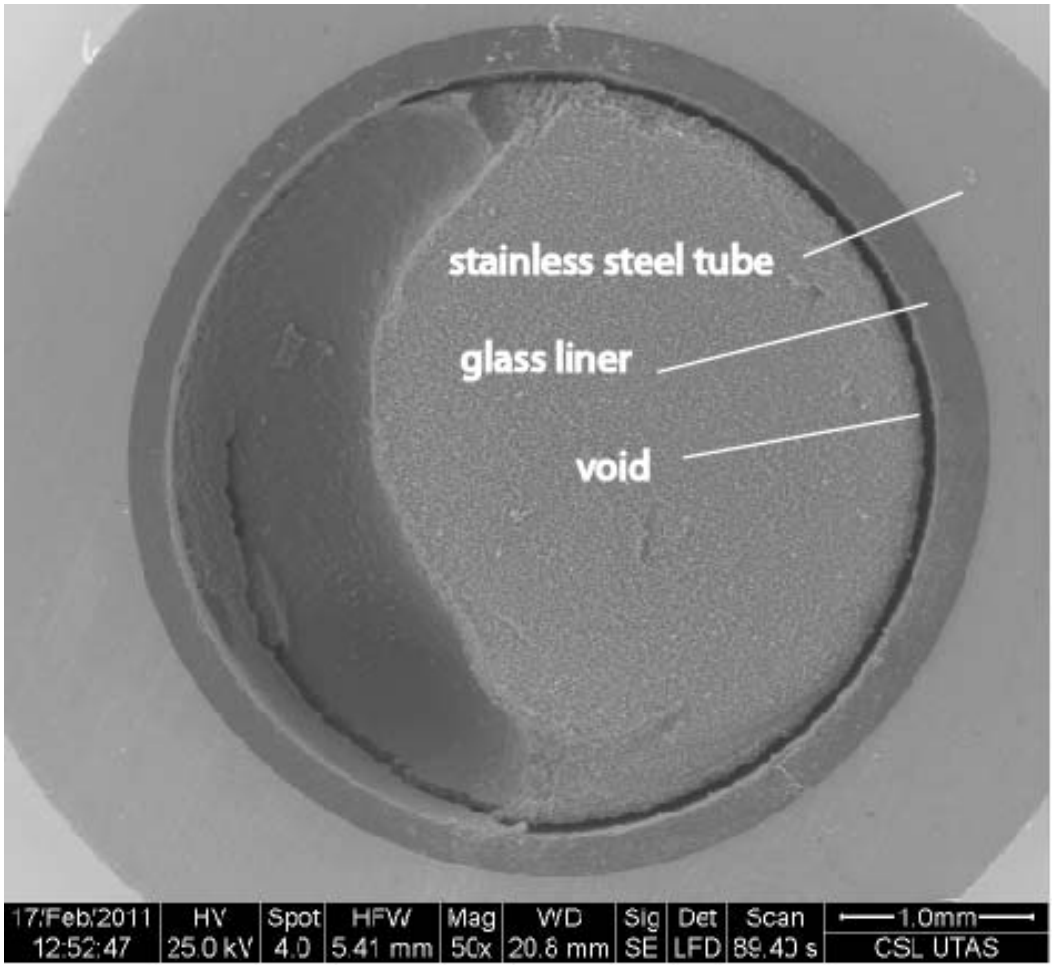


**Figure 4.3:** SEM image of poly(GMA-co-PETA) monolith polymerised in a GLT.

(Thermo Fisher Scientific Inc.) for making polymeric monolithic columns inside PEEK and stainless steel tubes (2.1 and 4.6 mm i.d.).

### 4.3.2 Stability of poly(GMA-*co*-PETA) monoliths

Relationships between column pressure and eluent flow-rate were measured using different solvents, including water and methanol to evaluate the mechanical stability of the synthesised monolith. A linear dependence of flow-rate on column back-pressure was observed (**Figure**

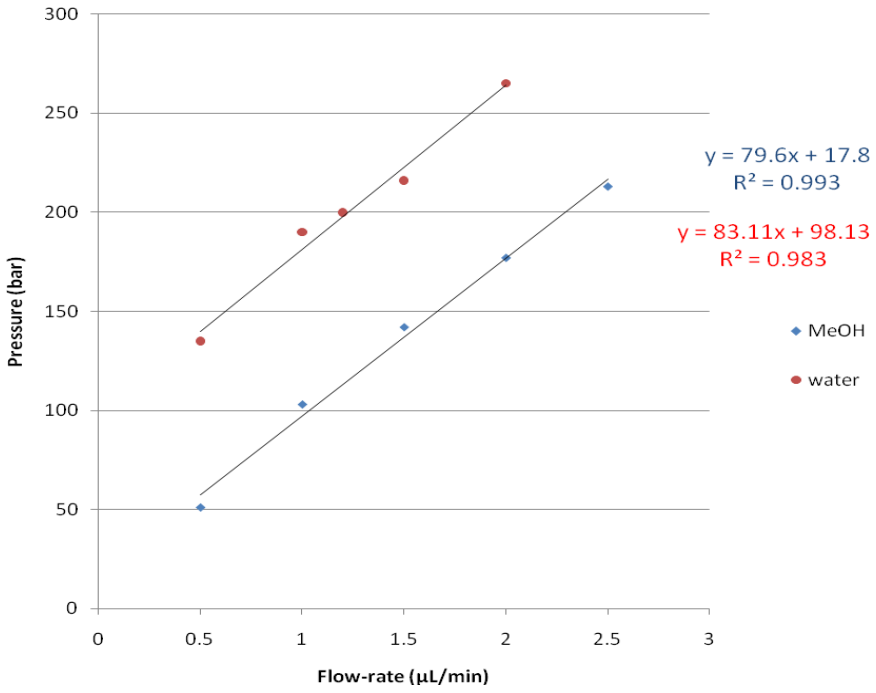


**Figure 4.4:** Relationship between column back-pressure and volumetric flow-rate for a poly(GMA-*co*-PETA) monolithic column (21 cm × 100 µm i.d.) using water or methanol as eluent.

**4.4**), indicating the absence of monolith compression at least up to 1050 bar/m. Interestingly, the plots also appear to be parallel, which can suggest the absence of swelling or shrinking of the monolith in solvents with different polarities. It is worth mentioning that, due to the non-calibrated pressure transducer on the pump, a positive back-pressure was recorded at zero flow-rate, which resulted in deviation of lines from the origin.

Further study on the swelling or shrinking of a monolith can be performed by measuring permeability in different solvents. Upon swelling, the monolith through-pores decrease in size, leading to lower

permeability, and *vice versa*. The permeability values calculated using Darcy's law were $38.6 \times 10^{-15}$ m$^2$ and $35.1 \times 10^{-15}$ m$^2$ in water and methanol, respectively. These results indicate again the non-significant swelling or shrinkage of the monolith in the studied eluents.

### 4.3.3 Post-polymerisation modifications

Monoliths containing reactive functionalities, such as epoxide groups, are benefited from a wide variety of chemistries that can be incorporated into the monolith pores *via* post-polymerisation modification reactions, mostly with reagents containing amine or thiol groups. These reactions can be easily performed with liquid reagents simply by saturating the monolith with the neat reagent, followed by reaction at elevated temperature.

Monoliths with anion-exchange functionalities were prepared by this approach using, for example, ethylenediamine (EDA) [157] and DEA [60, 92, 93]. On the other hand, the incorporation of CEX functionalities requires using sodium salts of reagents. Because of the SN2 mechanism involved, the use of aprotic solvents, such as THF or ACN is preferred to prevent the unwanted hydrolysis of epoxides. However, the use of such solvents is hindered by the very limited solubility of the solid forms of the reagents. Therefore, a reaction in aqueous medium appears to be the only possibility.

*4.3.3.1 Effect of pH on modification reaction*

The pH of the aqueous reaction medium is the most important variable that needs to be optimised. While basic pH is required in order to keep the amine functionality of the modification reagent active in its neutral form, higher pH can cause domination of the competitive hydrolysis reaction of epoxide and also increase the likelihood of hydrolysis of siloxane bonds that covalently attach the monolith to the capillary wall. Therefore, the optimum pH of the modification was initially investigated with the aim of obtaining the highest possible IEX capacity.

To evaluate the dependence of reaction yield on the pH of the modification reaction, DBC was measured for columns treated with two different reagents at three different pH values. DBC is an important characteristic of IEX columns, which determines column resolution and loadability [152]. Therefore, it is reasonable to conclude that the reaction yield (and IEX capacity) would be higher for the column that exhibited higher DBC. Since the columns were designed for IEC of large biomolecules, and to be consistent with the literature, lysozyme was chosen to measure the DBC [9, 86, 152]. modification reaction. The highest DBC values, expressed in mg/mL of polymer volume, were measured at pH 10.5. Accordingly, a DBC of 5.4 mg/mL was measured for the SEA column, which is better than the DBC of the Dionex ProPac SCX column.

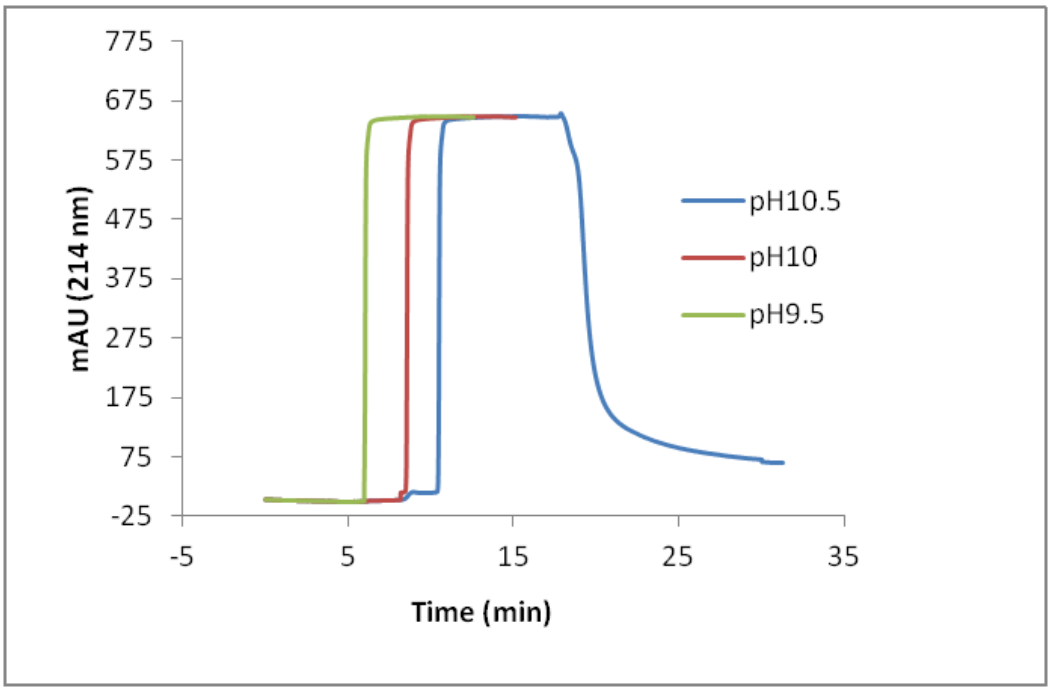


**Figure 4.5** shows typical results obtained for the columns modified with SEA. Sharp breakthrough curves represent excellent mass transfer kinetics of the columns, which is an inherent characteristic of monolithic materials. As expected, DBC was increased by increasing the pH of **Figure 4.5:** Breakthrough curves for lysozyme on poly(GMA-*co*-PETA) monolith modified with SEA at different pH values. Conditions: 7 cm × 100 µm i.d. column; Eluent A: 10 mM phosphate at pH 6.0, Eluent B: 1 M NaCl in A; Flow-rate: 2 µL/min; Injection: 1.0 mg/mL lysozyme (5 µL); UV detection at 214 nm.

The PEA column had a DBC of 15.1 mg/mL, which is lower than the value of 19.3 mg/mL reported by Dionex for the ProSwift WCX-1S monolithic column [94].

### 4.3.4 IEC of proteins: effect of eluent pH on selectivity

Eluent pH has a prominent effect on the separation efficiency of proteins as it determines the extent of ionisation of both ion-exchanger

and solutes [152]. While pH has a negligible effect on the ionisation of strong ion-exchange sorbents, weak ion-exchangers possess charged functional groups only over a narrower pH range. Since pH can affect the ionisation of a weak ion-exchanger significantly, these type of sorbents provide more opportunity for controlling the selectivity during method optimisation [9].

**Figures 4.6** and **4.7** show the effect of eluent pH on the separation efficiency and selectivity of a test mixture consisting of five basic proteins using columns modified with SEA and PEA, respectively. While separation efficiency in terms of resolution and peak shape changed markedly in both cases as a result of pH changes, the retention times of all solutes except trypsinogen showed only small changes. The best separation efficiency for the SEA column was achieved at pH 6.0 as a result of more protonation of the proteins, which leads to narrower peaks (as a result of longer retentions in the gradient elution). This is in agreement with previous reports on increasing the peak capacity of CEX columns in the separation of proteins by decreasing the pH [9, 86, 152]. Trypsinogen showed somewhat unusual behaviour; a single peak at pH 6.0 was split into two peaks at higher pH values with a dramatic change in selectivity at pH 8.0. This is probably caused by a partial change in protein conformation at some pH values.

The PEA column demonstrated the highest separation efficiency at pH 7.0. While peaks appeared to be sharper with this column, more resolution between cytochrome c and lysozyme was achieved with the

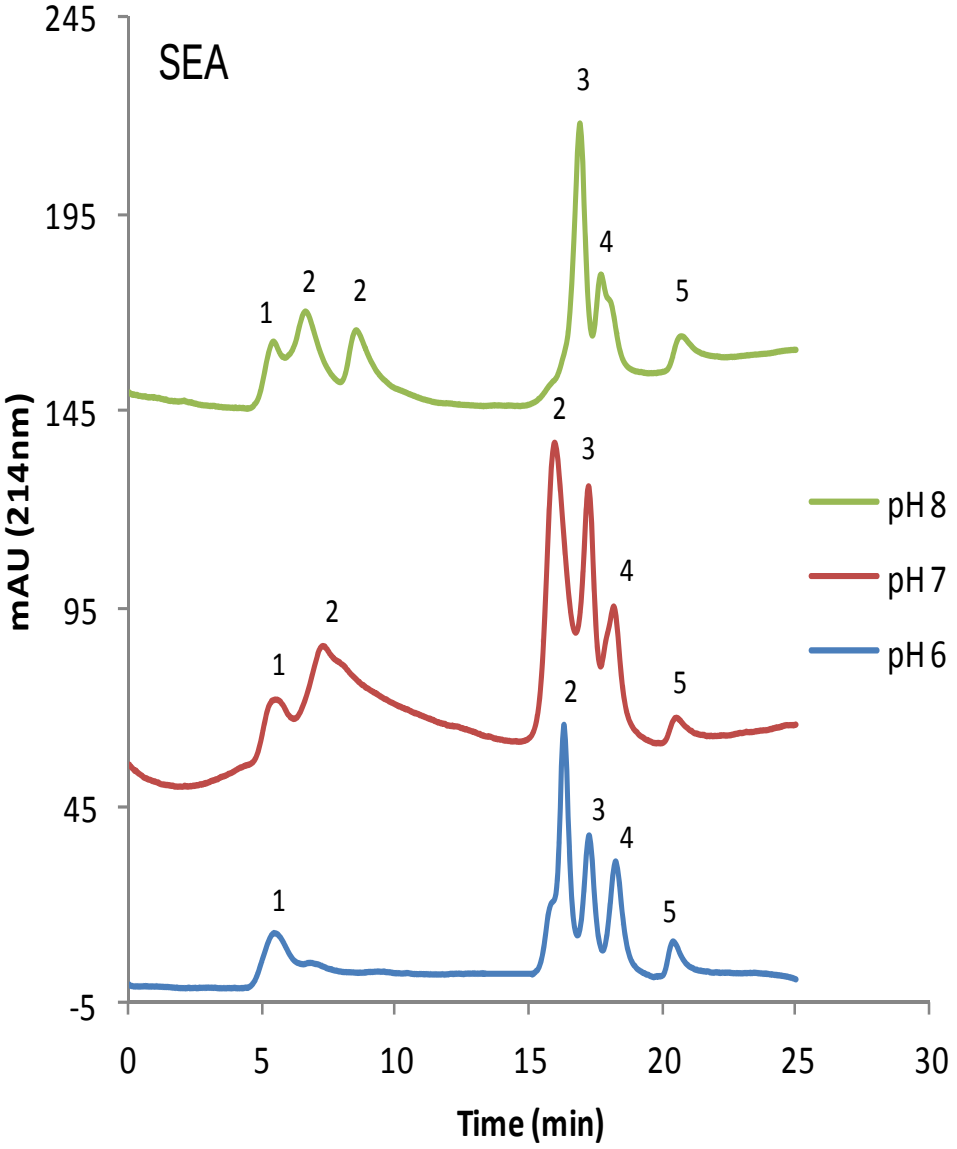


**Figure 4.6:** Effect of eluent pH on the separation of standard proteins using SEA column. Column: 15 cm × 100 µm i.d.; Eluent A: 10 mM phosphate (with indicated pH), B: 1 M NaCl in A; Elution: 1% A for 5 min then linear gradient to 99% B in 10 min, 99% B for 5 min; Flow-rate 1 µL/min; Inj. vol. 100 nL; UV detection at 214 nm. Peak identifications: (1) albumin (7.1 µg/mL), (2) trypsinogen (36 µg/mL), (3) $\alpha$-chymotrypsinogen A (36 µg/mL), (4) cytochrome c (14.2 µg/mL) and (5) lysozyme (36 µg/mL).

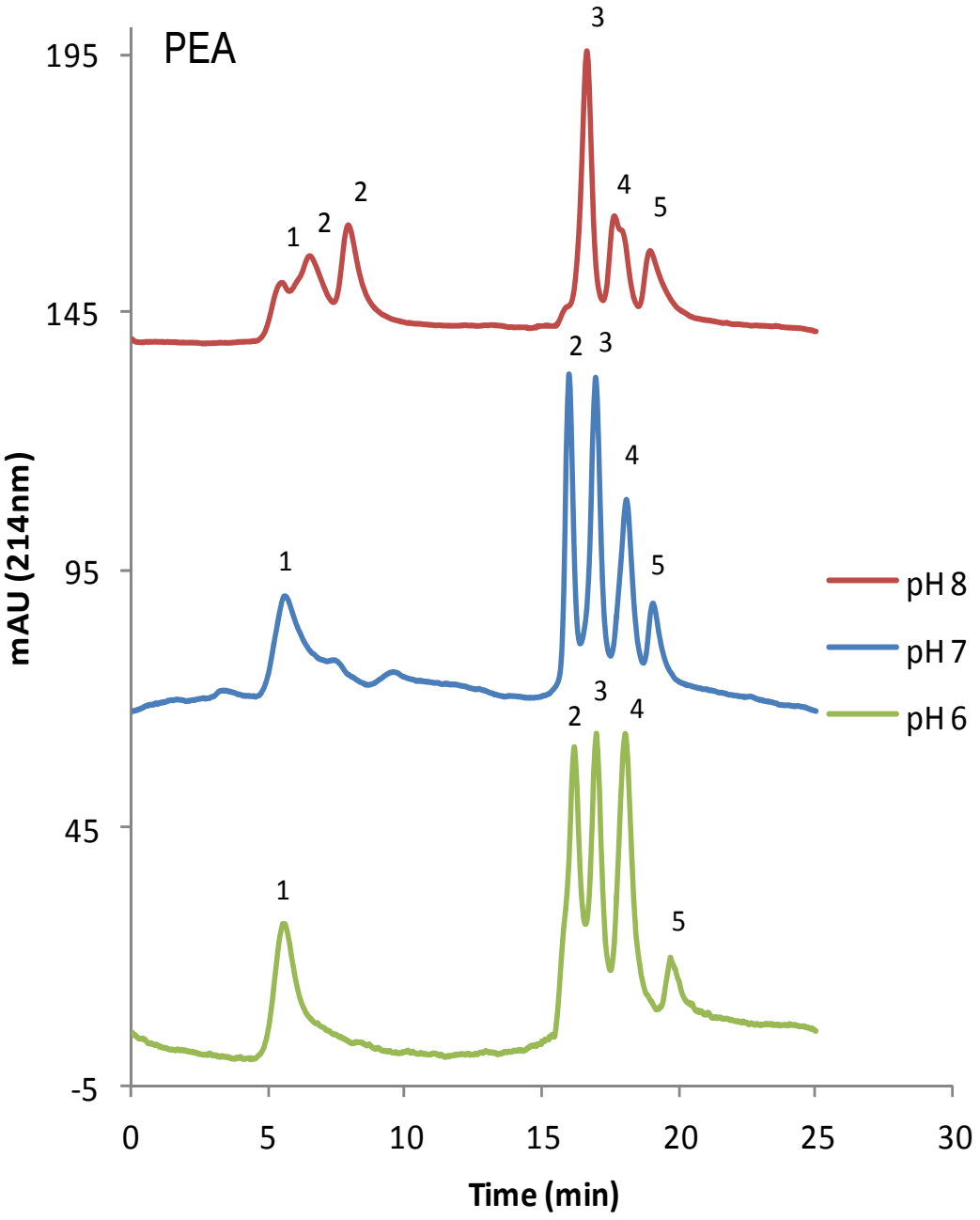


**Figure 4.7:** Effect of eluent pH on the separation of standard proteins using PEA column. Conditions and peak identifications as in Figure 4.6.

SEA column. Interestingly, at pH 8.0 both columns showed comparable efficiency in terms of peak shape and selectivity for the studied proteins.

### 4.3.5 Hydrophobic interactions

Hydrophobic interactions between biomolecules and stationary the phase are undesirable in IEC and developing a monolith with minimal hydrophobic interaction was a major goal in this study. Hydrophobic interactions can contribute greatly to the mechanism of separation when using a high concentration of salt in the eluent [9, 86, 152]. The possible contribution of hydrophobic interactions on retention times of proteins was studied using the PEA column and upon an approach suggested in the literature [9, 86, 94, 152]. Accordingly, the retention factors of the proteins were recorded in eluents containing various concentrations of sodium chloride under isocratic conditions.

As shown in **Figure 4.8**, a linear dependence between logarithm of retention factor and logarithm of salt concentration in the eluent suggested that the separation was mainly governed by an IEX mechanism, with a non-significant contribution of hydrophobic interactions [9, 86, 94, 152].

**Figure 4.9** demonstrates a typical isocratic separation of four proteins when using 0.85 M sodium chloride in 10 mM phosphate buffer at pH 7.0 as eluent. The column also exhibited separation efficiency of approximately 55,000 plates/m for the separation of lysozyme, which is

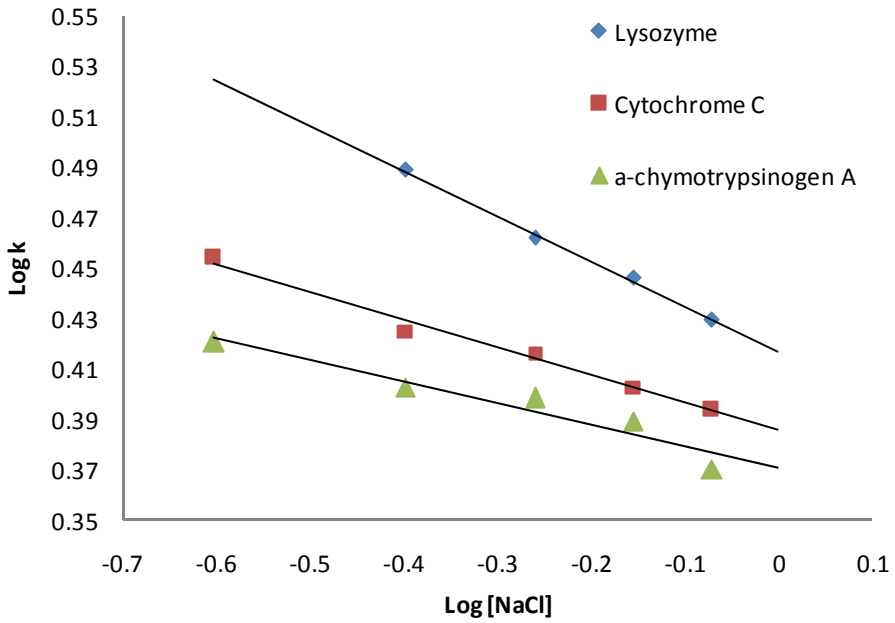


**Figure 4.8:** Relationship between retention factor (k) and salt concentration in isocratic separation of selected proteins. Conditions: 14 cm × 100 μm i.d. PEA column; Eluent: 10 mM phosphate buffer pH 7.0 containing various concentrations of NaCl; Flow-rate: 1.0 μL/min; other conditions as in Figure 4.6.

superior to the efficiency of a WCX column (75 μm i.d.) developed by Lee's group (40,000 plates/m) [9], but still lower than another WCX column that developed by the same group *via* co-polymerisation of a single phosphate-containing dimethacrylate monomer (71,000 plates/m) [86]. However, it is worth mentioning that they took advantage of on-column detection, which provides a higher efficiency as a result of narrower peaks.

## 4.4 Conclusions

New polymer monoliths were prepared by thermally-initiated co-polymerisation of GMA as a reacting monomer and PETA as a hydrophilic cross-linker. The monolith recipe and polymerisation

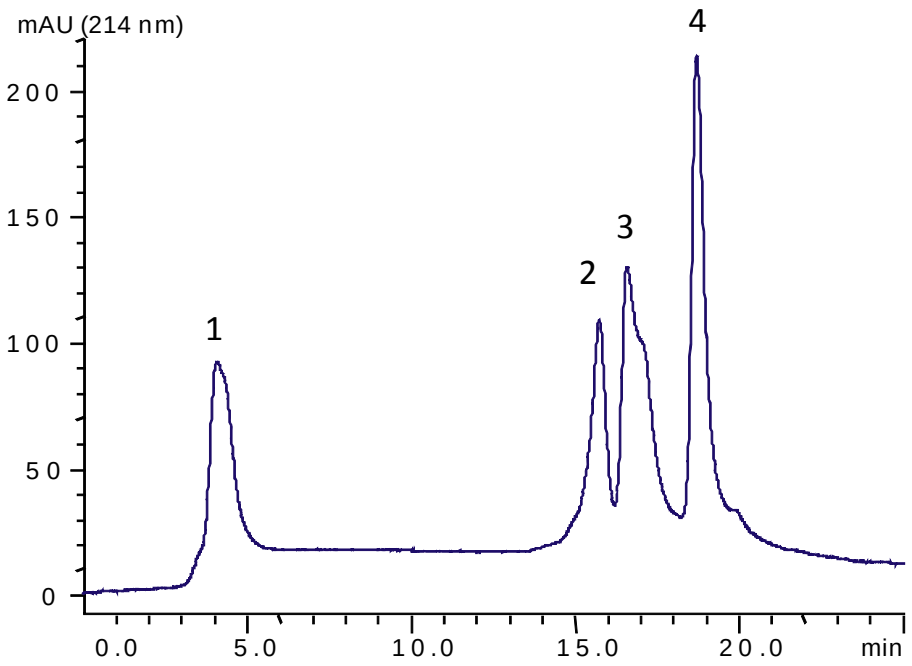


**Figure 4.9:** Representative chromatogram for isocratic separation of proteins using the PEA column. Conditions: Eluent, 0.85 M sodium chloride in 10 mM phosphate buffer at pH 7.0. Peaks are: Albumin (1), $\alpha$-chymotrypsinogen A (2), cytochrome c (3) and lysozyme (4). Other conditions as in Figure 4.6.

conditions were optimised to obtain a monolith with characteristics suitable for separation of biomacromolecules. While shrinking of the material prevented making monoliths with conventional dimensions, the monoliths were prepared successfully in 100 µm i.d. capillaries, demonstrating homogeneity and good mechanical stability. The post-polymerisation modification of the monolith was performed *via* optimised reaction conditions in order to incorporate CEX functionalities using amine reagents containing phosphoric acid (WCX) or sulfonic acid (SCX) groups. DBC values of up to 15.1 mg/mL were measured using lysozyme as a standard probe, which is better or comparable to some of the commercially available columns. Compared to a previously developed monolith intended for the same purpose, the resulting

monoliths also demonstrated higher separation efficiency (approximately 55,000 plates/m) in an isocratic separation of sample proteins.

# *Chapter 5*

# Epoxy-based Monoliths for Capillary Liquid Chromatography of Small and Large Molecules

## 5.1 Introduction

Favourable characteristics, such as the relatively high permeability leading to enhanced mass transfer, the simplicity of fabrication and general biocompatibility have made polymer monoliths well-suited for the separation of biomolecules, from small peptides and oligonucleotides to large intact proteins and plasmid DNA. However, the application of polymer monoliths for the efficient separation of small molecules has still remained a challenge. It has been hypothesised that this may be due to their monomodal pore size distribution and the absence of mesopores [176, 177], or alternatively due to the significant gel porosity in the monolith scaffold in the swollen state, which arise from the inherent heterogeneity associated with the free-radical cross-linking copolymerisation synthesis [53, 178]. Moreover, organic polymer monoliths may suffer from high swelling propensity in organic solvents, leading to poor mechanical stability and reduced separation performance [54, 175, 177]. This deficiency might be more prominent in the HILIC mode, which involves higher contents of organic solvents in the mobile phase than the reversed-phase mode.

Attempts have been made to address these limitations by tailoring the porous properties of polymer monoliths in order to make them more suitable for the separation of small molecules through, for example, low-density monolith preparations [55], incomplete polymerisation [174], increasing the degree of cross-linking [175], post-polymerisation hyper-cross-linking [179] and high-temperature separations [180]. Nevertheless, there are still some limitations or difficulties associated with these approaches. For example, incomplete polymerisation could lead to a decrease in mechanical stability and affect swelling propensity of the polymer in organic solvents [181]. Hyper-cross-linking is a multistep process which also causes a decrease in the column permeability [140]. Similarly, incorporation of carbon nanotubes into the polymer monoliths, in order to enhance the separation efficiency of small molecules, led to a 3.8 fold increase in column back-pressure, which resulted in applicable flow-rates lower than 0.25 μL/min [182]. An excellent review was published recently by Nischang *et al.* which summarises recent advances in polymer monoliths for the separation of small molecules and describes in detail the challenges involved [54]. At the same time, inorganic (silica) monoliths have proven to be well-suited for the separation of small molecules, but they also suffer from some drawbacks. These include poor phase stability under extreme pH ranges, and a relatively complicated synthetic process which is sensitive to small changes in conditions, as well as radial inhomogeneity [54, 175, 177, 181, 183].

A recent approach to the preparation of porous polymer monoliths is polycondensation [66], with which 3D skeletal structures can typically

be created *via* polymerisation-induced phase separation of epoxy resin monomers and amine curing agents in, for example, PEG as pore-forming solvent at constant temperature [106, 108, 176]. Unlike in free radical polymerisation, oxygen does not interfere in these reactions, so careful de-aeration of the polymerisation solution is not necessary. The chief advantage of these materials is their inherent hydrophilicity originating from the incorporation of heteroatoms (N and O) in their polymeric scaffolds. This characteristic can be exploited for designing biocompatible monoliths which are suitable for separation of biomolecules [74]. A wide range of chemistries can also be incorporated on the surface of the monolith *via* post-polymerisation modification through residual epoxide, hydroxyl and amine groups generated after curing. Xin *et al.* used surface-initiated atom transfer radical polymerisation approach for grafting a hydrophobic monomer, N-isopropylacrylamide, onto the surface of E-51 epoxy-based monolith *via* residual hydroxyl groups [105]. The chromatographic performance of this material was demonstrated using HIC of human serum proteins. More recently, weak-anion exchange WAX chromatography of glycoprotein isoforms was reported using epoxy-based monoliths [109]. Residual epoxides were treated with ammonia solution to maximise the content of amino groups on the surface.

The suitability of epoxy-based monoliths for the separation of small molecules was demonstrated by Hosoya *et al.* utilising capillary columns prepared from the polycondensation of tris-(2,3-epoxypropyl) isocyanurate [176], or alternatively, 1,3-bis(N, N'-

diglycidylaminomethyl)cyclohexane [111] as the epoxide-containing monomer with 4-[(4-aminocyclohexyl)methyl] cyclohexylamine (BACM) as the amine curing agent. Depending on the content of ACN in the aqueous mobile phase, columns were operated in both HILIC and RPLC modes and were claimed to exhibit high permeability and up to 133,000 theoretical plates per metre (N/m) for alkylbenzenes.

In this chapter this approach is extended and the synthesis of a new epoxy-based monolith is outlined and its suitability for separation of both small molecule probes (including nucleic acid bases and nucleotides as well as some benzoic acid derivatives) and tryptic peptides, as examples of medium-molecular weight solutes, is demonstrated in the HILIC mode. Post-polymerisation modification of monoliths was also performed, enabling separation of protein standards under both IEX and HIC modes. With this the aim is to demonstrate the versatility that is offered by this approach, resulting in monolithic materials suitable for the separation of both small and large molecules.

## 5.2 Experimental

The general experimental details, including chemicals and instrumentation are presented in Chapter 2. Specific experimental conditions are given in each of the figure captions.

### 5.2.1 Sample preparation

For HILIC analyses, solutes were dissolved in ACN/water or ACN/0.1 M HCl at a concentration of 0.5-5 mg/mL. Further dilutions

were made in mobile phases. Stock solutions of proteins were prepared in water (10 mg/mL), followed by further dilution to about 0.2 mg/mL in eluent A (in the IEX mode) or eluent B (in the HIC mode). In the IEX mode, eluent (A) was 10 mM phosphate buffer pH 6 and eluent (B) was 1 M sodium chloride in (A). In the HIC mode, eluent (A) was 3 M ammonium sulfate in (B), which was 100 mM phosphate buffer pH 7.

### 5.2.2 Mass spectrometry

ESI-MS analysis was performed in the positive ion mode with a *m*/*z* range of 100-2000. For MS/MS experiments, the two most abundant precursor ions were subjected to collision-induced dissociation at low energy. Active exclusion was enabled on the instrument for two tandem mass spectra with an exclusion time interval of 1 min.

The peptide identifications were performed using the on-line version of Mascot MS/MS ions search (Matrix Science Ltd., London, UK) and the public database SwissProt. In data analysis, only one missed cleavage was allowed with the mass tolerances of ± 0.5 Da for both precursor and fragment ions. The deamination (N-term C), Gln →Pyro-Glu (N-term Q) and methionine oxidation were chosen as variable modifications.

### 5.2.3 Polymer monolith preparation

Each polymerisation mixture was prepared in a 4-mL glass vial by mixing epoxy monomer (GE-100) and porogen(s). The mixture was vortex-mixed without de-aeration. Depending on the porogen used, some

mixtures solidified upon the addition of porogen, so pre-heating (60 ˚C) of the mixture was required, followed by mixing again until formation of a homogenous, transparent liquid occurred. Amine curing agent was added subsequently followed by vortex-mixing. The vial was kept stationary and warm (T < 60 ˚C) for 1-2 min to remove air bubbles. The modified capillary was then quickly filled with this mixture using a warm glass syringe before haziness reappeared. The polycondensation polymerisation was conducted at different temperatures (70-120 ˚C) for at least 20 h. The monolithic column chosen for LC applications in this work (M4 in **Table 5.1**) was prepared by polymerising a mixture consisting of 0.7 g GE-100, 0.5 g PEG-1000 (melted at 60 ˚C), 1.3 g 1-decanol and 80 μL EDA at 80 ˚C in a thermostated water bath for 22 h. **Figure 5.1** shows schematically the polycondensation reaction performed. Both ends of the capillary were then cut and the column was connected to the HPLC system and put inside the column compartment with the temperature pre-set at 50 ˚C in order to melt the solidified porogen inside the monolith pores. The column was then washed sequentially with water and methanol (~ 100 column volumes each). The excess of the polymerisation mixture remaining in the glass vial was also polymerised under the same conditions (this is referred to as the bulk monolith). After completion of the reaction, the vial containing the bulk monolith was crushed carefully, the polymer cut into small pieces, Soxhlet extracted with methanol overnight to remove any soluble compounds, and vacuum dried (for at least 24 h) prior to characterisation experiments.

**Table 5.1:** Chemical composition and physical properties of monoliths

| Monolith | Recipe | | | | | | Physical properties | | | | |
|---|---|---|---|---|---|---|---|---|---|---|---|
| | **GE-100 (g)** | **EDA (μL)** | **PEG-k (g)** | **PEG-10k[1] (g)** | **1-decanol (g)** | **1-dodecanol (g)** | **MPD[2] (nm)** | **$D_p$[3] (nm)** | **Pore vol. (mL/g)** | **Porosity (%)** | **Surface area ($m^2$/g)** |
| **M1** | 0.7 | 80 | - | 1.8 | - | - | 1191 | 1160 | 0.76 | 47 | 1.6 |
| **M2** | 0.7 | 80 | - | 1.5 | 0.3 | - | 1048 | 1058 | 0.73 | 49 | 0.9 |
| **M3** | 0.7 | 80 | 0.5 | - | - | 1.3 | 1764 | 1672 | 1.6 | 65 | 2.2 |
| **M4** | 0.7 | 80 | 0.5 | - | 1.3 | - | 716 | 659 | 1.22 | 62 | 3.6 |
| **M5** | 0.7 | 80 | - | 1.8 | - | - | 590 | 657 | 0.67 | 45 | 1.8 |
| **M6** | 0.9 | 102 | - | 1.2 | - | 0.3 | 1008 | 964 | 0.56 | 42 | 1.5 |

The mole ratio of epoxide to amine groups was 2:1 in all experiments; the weight ratio of monomers to porogen(s) is 3:7, except in 6 which was 4:6; Polymerisation temperature is 80 °C, except in 6 which was 90 °C.

[1] 20 %wt. solution in isopropanol (M2), methanol (M5) or 2-methoxyethanol (M1 and M6).

[2] Median pore diameter.

[3] Pore size at the peak of pore distribution curve.

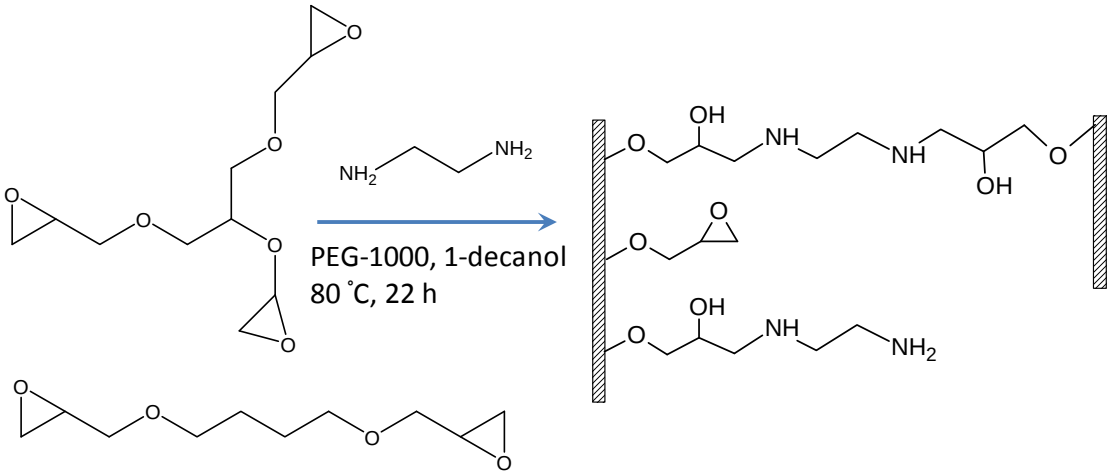


**Figure 5.1:** Schematic polycondensation procedure for preparing epoxy-based monolith (M4). See text for more details.

### 5.2.4 Post-polymerisation modifications

Acid hydrolysis of the residual epoxide groups was performed by passing a 0.5 M sulfuric acid solution through the column at 30 µL/h for 4 h at 75 ˚C. Alternatively, neat EDA was pumped into the column at room temperature for 2 h then the column was sealed at both ends and submerged into a thermostated water bath for 5 h at 65 ˚C. After completion of the reactions, both columns were flushed with water until the outflow was neutral. The resultant columns contained mixed diol-amino and amino chemistries, respectively (see **Figure 5.2a**).

An IEX column was prepared following the procedure described in Chapter 4 for the poly(GMA-*co*-PETA) monolith. Briefly, a 1 M solution of SEA in 1 M carbonate buffer was prepared and the pH was adjusted to 10.5 by adding sodium hydroxide solution (5 M). About 450 µL of this solution was pumped through the column for 24 h at 75 ˚C. Acid hydrolysis of unreacted epoxides was then accomplished, as described above for the diol-amino column (see **Figure 5.2b**).

The HIC column was prepared by grafting a co-polymerised hydrogel N-isopropylacrylamide (NIPAm) and methylenebisacrylamide (BIS) on the pore surface of the epoxy monolith, using a procedure previously reported by Peters *et al.* [184] with some modifications. **Figure 5.2c** schematically demonstrates the modification reactions. In the first step a vinylisation reaction between residual epoxides and allylamine was carried out. The column was washed with water and a 50 wt% aqueous solution of allylamine was pumped through the column for 2 h at 60 μL/h. Then the column was sealed at both ends and kept at 60 ˚C in a water bath for 16 h, followed by extensive flushing with water until the outflow was neutral. In the next step, a polymerisation mixture consisting of NIPAm (9.9 wt%), BIS (0.1 wt%) and AIBN (1 wt% with respect to monomers) was prepared in toluene, then centrifuged for 10 min at 3000 rpm to remove solid particles and deoxygenated with nitrogen for 10 min. The column was flushed with THF and toluene and the grafting solution was pumped through at 60 μL/h for 2 h. The capillary was sealed at both ends and placed in a water bath at 60 ˚C for 15 h. Finally, the column was sequentially flushed with THF and water (4 h each) at 30 μL/min.

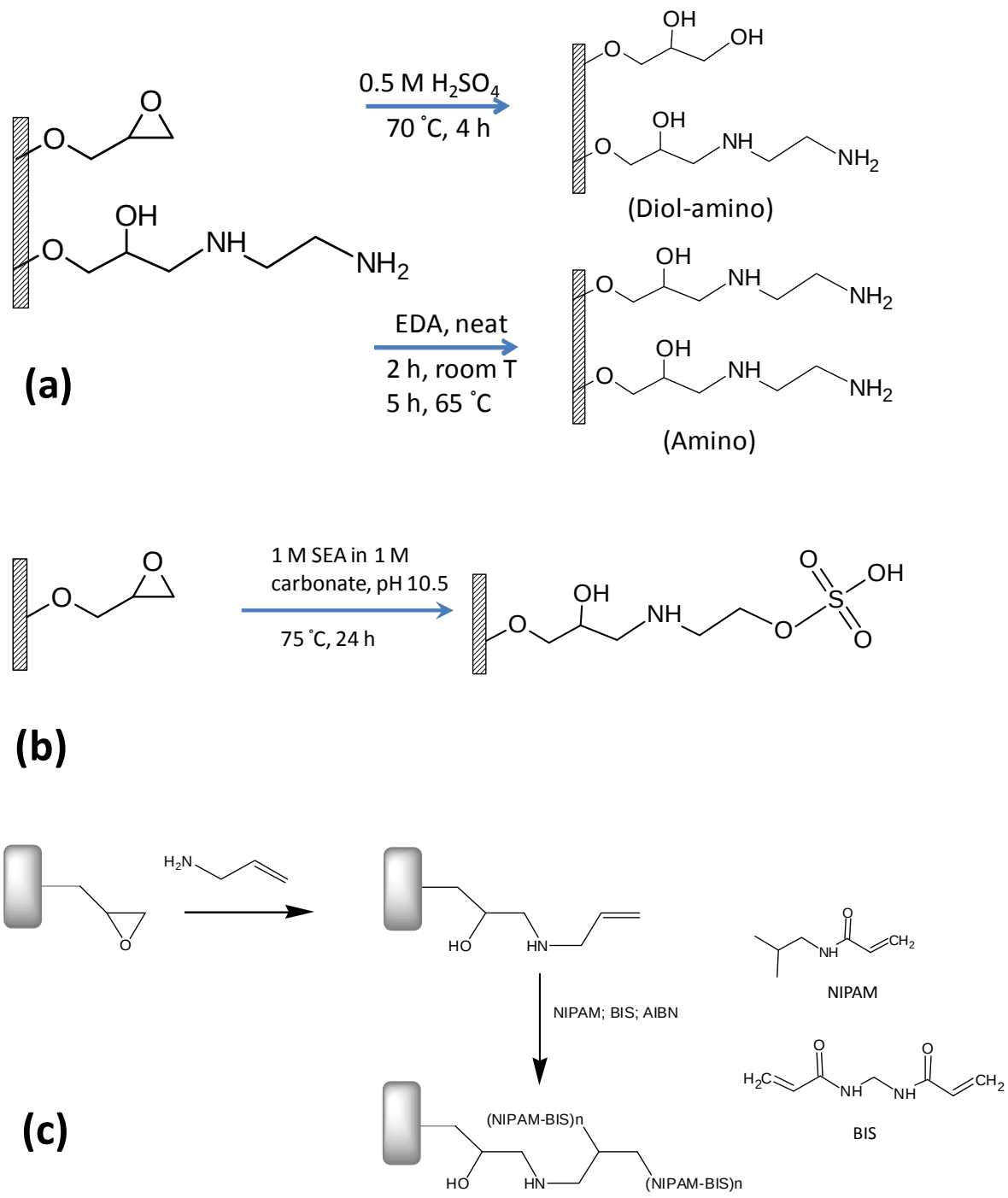


**Figure 5.2:** Post-polymerisation modifications of the monolith M4 *via* residual epoxide groups. (a) acid hydrolysis and aminolysis, (b) IEX functionalisation and (c) HIC chemistry.

## 5.3. Results and discussion

### 5.3.1 Monolith preparation

The aim of this work was to design a monolith that could be suitable for both the separation of small molecules as well as larger biomolecules. Therefore, monomers (epoxy resin and amine) were chosen such that the final monolith should exhibit good biocompatibility [74]. GE-100 was chosen as the epoxide-containing monomer, and is a mixture of di- and trifunctional epoxides based on glycidyl glycerol (**Figure 5.1**), possessing enough hydrophilicity for this purpose. Although there are only a few reports of epoxy-based monoliths used for separations in the literature, BACM has been used most as the amine curing agent [105, 111, 176]. However, EDA was preferred here since the cyclohexyl moieties in BACM are likely to induce some degree of unwanted hydrophobicity to the monolith structure.

PEG is a unique polymer. While its hydrophilic head group comprising hydroxyl groups provides good water solubility at low temperature, its polyoxyethylene chain allows solubility in most organic solvents [185]. PEGs with different MW have been used successfully as the primary choice for designing epoxy-based monoliths [106, 108, 109, 111, 176].

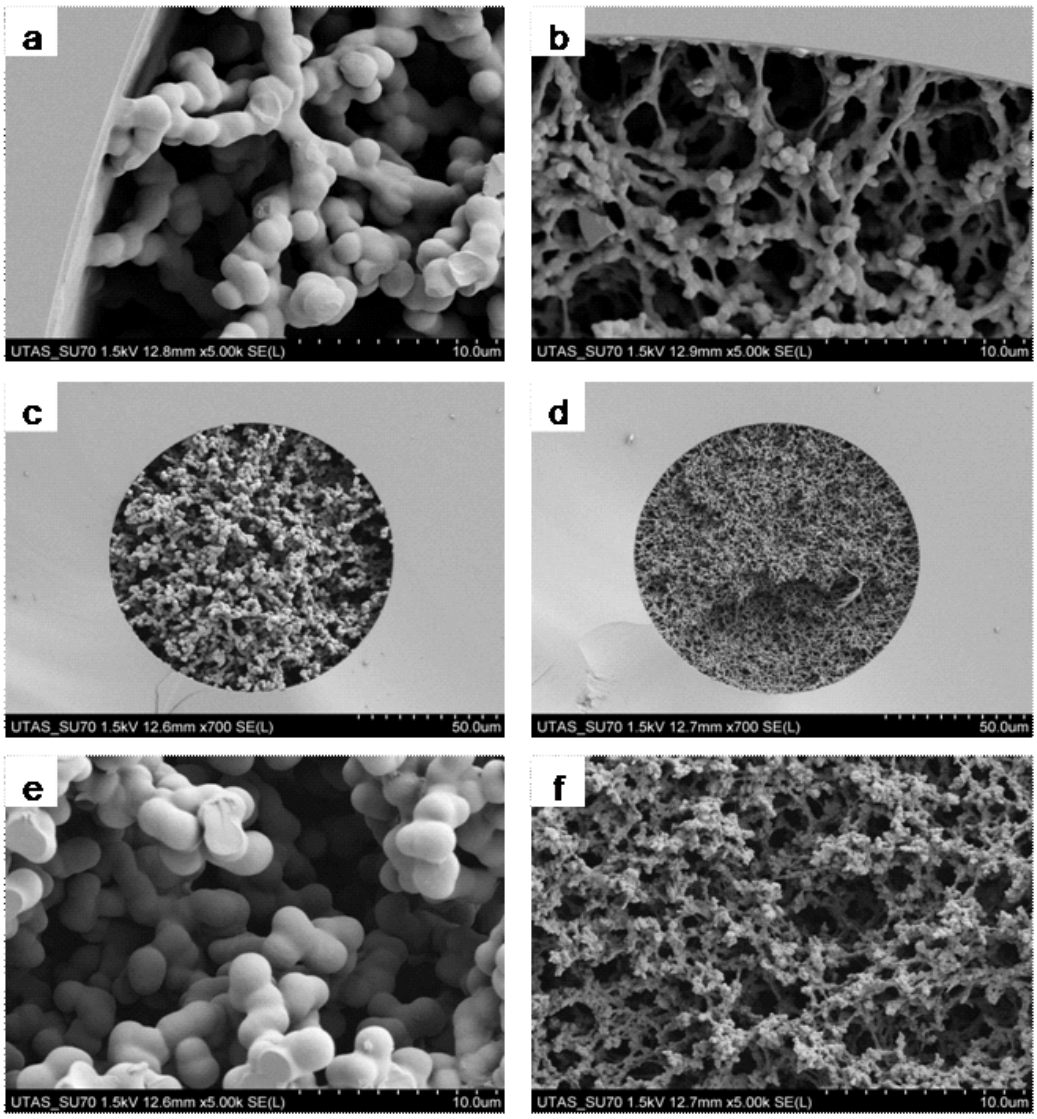


**Figure 5.3:** Scanning electron micrographs of some of the monoliths (Table 5.1); (a) M1 (magnification 5000x), (b) M5 (5000x), (c) M3, (d) M4, (e) M3 (5000x), (f) M4 (5000x).

The polymerisation conditions leading to monoliths with 3D scaffolds were obtained by trial and error. Mass conversions better than 90% were obtained by comparing the weight of the dry polymer monolith to that of the monomers in the recipe. Primarily, the mole ratio of epoxide functionality in GE-100 to the amine group in EDA was varied from 5:1 to 1:5, while PEGs with MW of 200, 400, 800, 1000, and 10,000 (10k) were used as porogen. For PEG-10k, a 20 wt% solution in 2-methoxyethanol [185], methanol or isopropanol was employed. Transparent soft gels were achieved at mole ratios higher than 3:1, even at temperatures as high as 120 °C, whereas non-homogenous, amber coloured solids were obtained for the ratio of 1:3. Phase separations leading to white, solid monoliths appeared at mole ratios of 2:1 and 1.5:1, with more homogeneity in the colour for the former.

The morphology of the polymer was also significantly affected by the MW of PEG. By keeping the weight ratio of porogen to monomers constant at 7:3, transparent, glassy gels with PEG-200 and 400 turned into translucent, and then semi-hard materials by further increasing the MW to 10k. Despite the homogenous morphology and 3D structure (**Figure 5.3**); the monolith prepared using a PEG-10k solution in methanol as the porogen showed significant shrinkage during polymerisation. Substituting methanol with isopropanol resulted in a structure with a thicker skeleton, yet less shrinkage. Porosimetry data showed an almost 2-fold increase in median pore diameter with this change (**Table 5.1**). A

very similar morphology was also obtained with PEG-10k in 2-methoxyethanol.

Further investigation revealed the necessity of using a macropore-forming solvent as co-porogen to obtain sufficient permeability in monoliths prepared with PEG-1000 as the porogen. In fact, a uniform and solid structure with adequate permeability was never obtained when PEGs smaller than 1000 were used as porogens, even in the presence of appreciable amounts of co-porogens. As is common with methacrylate-based monoliths, long-chain alcohols, 1-decanol and 1-dodecanol, was used as co-porogen with weight ratios up to 28% with respect to the porogen (PEG-1000). As seen in **Figure 5.3**, fused globules of about 1.8 μm thickness were obtained with 1-dodecanol, whereas 1-decanol resulted in a homogenous, sponge-like structure. These differences are also reflected in porosimetry data (**Table 5.1**) where monoliths with 1-dodecanol as co-porogen exhibited median pore diameters almost 2.5 times larger than the monolith formed with 1-decanol, yet with only 33% difference in pore volume.

It is worth noting that the measured porosities were lower than expected from the content of porogen in the monolith recipe (70%), which could be due to the shrinkage of monoliths in the dry state, with seemingly more shrinkage for monoliths prepared using PEG-10k solutions as the porogen.

Based on the characterisation results, monolith M4 in **Table 5.1** was chosen for surface modification and chromatographic evaluation. As seen in Figure 5.3, this monolith also demonstrates the smallest domain size, i.e., the combined average size of the macropores and microglobules. Previous studies showed that the efficiency of monolithic stationary phases increases by decreasing the domain size [55, 186]. Pore size distribution profiles indicated that the majority of the total pore volume (1.2 mL/g) in this monolith, 58%, corresponded to the pores in the range of 500-2000 nm and 23% in the range of 2000-4600 nm, thus resulting in a column with high permeability. Pores smaller than 500 nm (150-500 nm) represented only 19% of the total pore volume, with an absence of mesopores (2-50 nm), which is expected from the nonporous skeleton of epoxy-based monoliths in the dry state [66]. This monolith also exhibited slightly higher surface area (**Table 5.1**) than the other monoliths, possibly due to its sponge-like morphology.

Column pressure drops were measured for the diol-amino modified column using ACN and water to evaluate the permeability and mechanical stability of the synthesised monolith. A linear dependence of flow-rate on column back-pressure (**Figure 5.4**) indicated that the monolith was not compressed, at least up to 260 bar (~ 3.9 mm/s of water). The permeability of the column was then measured as reported elsewhere using Darcy's equation [140]. Permeability values of $6.6 \times 10^{-14}$ and $5 \times 10^{-14}$ $m^2$ were obtained respectively, using either ACN or water as eluent. These results suggest swelling of the monolith in aqueous media, which also reflects the desired hydrophilicity of monolith structure.

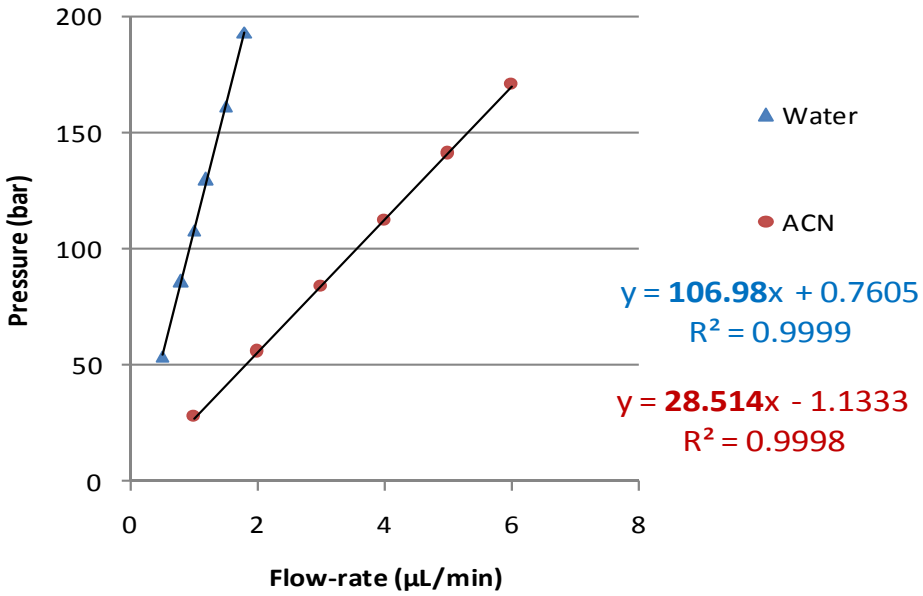


**Figure 5.4:** Correlation between column back-pressure and flow-rate in the diol-amino column (18.5 cm × 100 µm i.d.) using ACN and water as eluent.

### 5.3.2 Separation of small molecules

*5.3.2.1 Nucleobases and nucleosides*

Acid hydrolysis of residual epoxide groups increased the hydrophilicity of the monolith surface. Together with residual amino groups, the mixed diol-amino chemistry obtained can provide a suitable environment for separation under the HILIC mode. A group of nucleobases and nucleosides, including thymine, uracil, uridine, cytosine, adenosine, adenine, cytidine, deoxyguanosine and guanosine was chosen to evaluate the separation performance of the column for some polar and closely related neutral compounds that are known to be difficult to retain in RPLC [187, 188]. **Figure 5.5** shows a typical separation obtained with up to 12% water in ACN. Although not all solutes were baseline resolved,

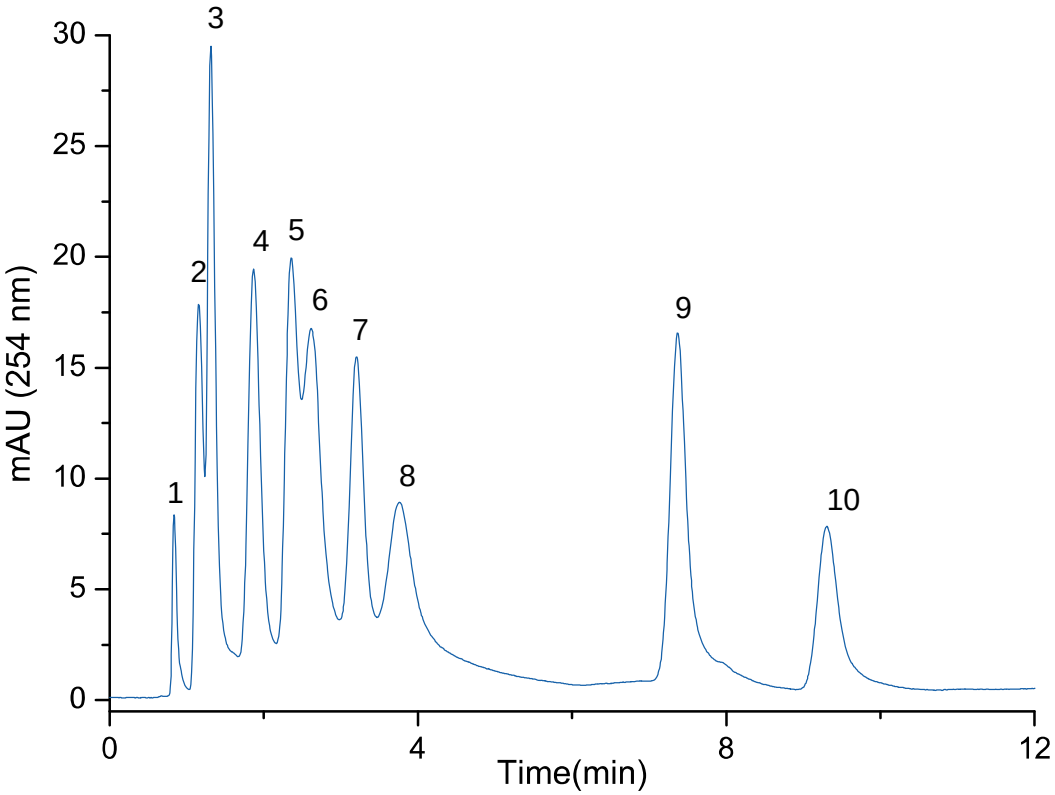


**Figure 5.5:** Separation of nucleobases and nucleosides on the diol-amino column (18.5 cm × 100 μm i.d.). Conditions: eluent A, ACN; B, water; elution, 7% B (0-4min), 12% B (4.1-15min); flow-rate, 4 μL/min; injection vol., 100 nL; UV detection at 254 nm. Peaks are toluene (void volume marker, 1), thymine (2), uracil (3), uridine (4), cytosine (5), adenosine (6), adenine (7), cytidine (8), deoxyguanosine (9) and guanosine (10).

the separation was completed in 10 min with the high permeability of the column enabling a flow-rate of 4 μL/min to be used.

A separation efficiency of 11,600 plates/m was recorded for the last eluting solute (guanosine) through an isocratic elution (10% ACN), which is about 30% higher than the efficiency reported previously for an epoxy-based monolith using the same eluent [176]. As expected for separations in the HILIC mode, the retention times for all solutes increased with increasing ACN concentration, which led to slightly higher resolutions

between some pairs, but also with commensurate increases in peak widths.

*5.3.2.2 Benzoic acids*

Columns with mixed-mode behaviour have become increasingly popular in the separation of highly polar molecules, including ions that are weakly or not retained in RPLC [126, 188-190]. Unlike RPLC, where the means of controlling the separation selectivity are rather limited, mixed-mode chemistries provide more flexibility in method development using variations in the eluent pH, ionic strength, or organic solvent concentration and thus permit application to a wider range of analytes [188, 191]. Owing to the presence of primary and secondary amine functionality on the surface, the monolith prepared here is also expected to offer the possibility of weak electrostatic interaction with charged analytes. Similar to previous reports [188, 192, 193], a range of benzoic acid derivatives was utilised to get a full picture of the contribution of such effects to the overall retention mechanism.

The effect of ionic strength on the retention of seven benzoic acids was investigated by varying the concentration of ammonium acetate buffer (pH 5) from 10 to 50 mM in a constant 90% ACN. pH was adjusted using acetic acid. As shown in **Figure 5.6**, the retention of all acids decreased by increasing the buffer concentration, which is characteristic of an ion-exchange retention mechanism.

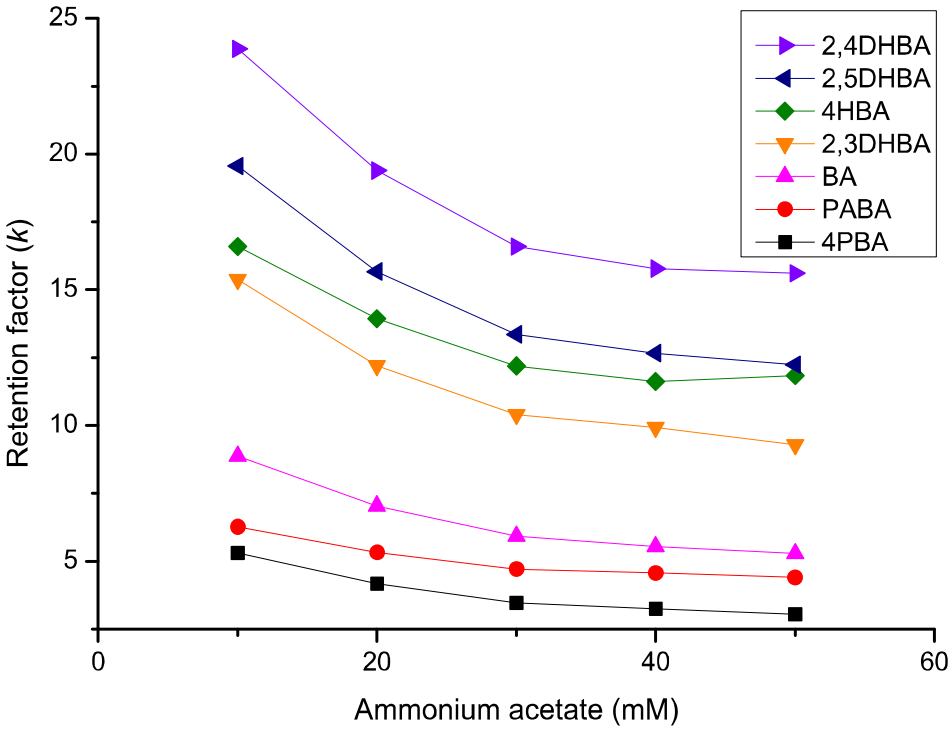


**Figure 5.6:** The influence of buffer concentration on the retention factor of benzoic acids. Conditions: diol-amino column (24 cm × 100 µm i.d.); eluent: ACN/ammonium acetate (at various concentrations) pH 5 (90:10), flow-rate, 5 µL/min; UV detection at 280 nm. Solutes: 4-propylbenzoic acid (4PBA), p-aminobenzoic acid (PABA), benzoic acid (BA), 2,3-dihydroxybenzoc acid (2,3DHBA), 4-hydroxybenzoic acid (4HBA), 2,5-dihydroxybenzoic acid (2,5DHBA), and 2,4-dihydroxybenzoic acid (2,4DHBA).

This behaviour is actually opposite to that expected from consideration of the hydrophilic partitioning mechanism [125] suggested to describe retention in the HILIC mode. In this model, hydrophilic partitioning of polar solutes between relatively less polar bulk eluent and a water-enriched layer immobilised on the hydrophilic stationary phase contributes mostly to the retention of analytes and this partitioning would be increased by increasing the electrolyte concentration, leading to greater retention of solutes [125, 127, 183, 188, 194].

The observed retention behaviour can be explained by considering the contribution of electrostatic interactions in a mixed-mode mechanism [190]. The p$K_{a1}$ values for 4-propylbenzoic acid (4PBA), p-aminobenzoic acid (PABA), benzoic acid (BA), 2,3-dihydroxybenzoc acid (2,3DHBA), 4-hydroxybenzoic acid (4HBA), 2,5-dihydroxybenzoic acid (2,5DHBA), and 2,4-dihydroxybenzoic acid (2,4DHBA) are 4.4, 4.9, 4.2, 3.0, 4.6, 3.0 and 3.3, respectively [195].

At pH 5 they will be partially or fully deprotonated, thus interacting electrostatically with the protonated primary and secondary amine functionalities on the surface of the monolith in a mixed HILIC-WAX mode. Decreases in solute retention by increasing the buffer concentration at such a high content of ACN therefore reflects that the ion-exchange retention is more significant than the HILIC mode.

The effect of buffer pH on the HILIC separation of benzoic acids was also investigated. Buffer pH was adjusted from 5 to 3.5 by adding acetic acid to the buffer solution before mixing with ACN. The content of ACN in the eluent and the concentration of buffer were kept constant at 90% and 40 mM, respectively. As can be seen in **Figure 5.7**, the retention of 2,3DHBA, 2,4DHBA and 2,5DHBA, having p$K_{a1}$ < 3, increased continuously by decreasing the pH. Since there were no significant changes in their ionisation states within the studied pH range, the observed trends might occur because with decreasing eluent pH, WAX sites on the stationary phase (estimated p$K_a$ ~ 8 and 9) became even more

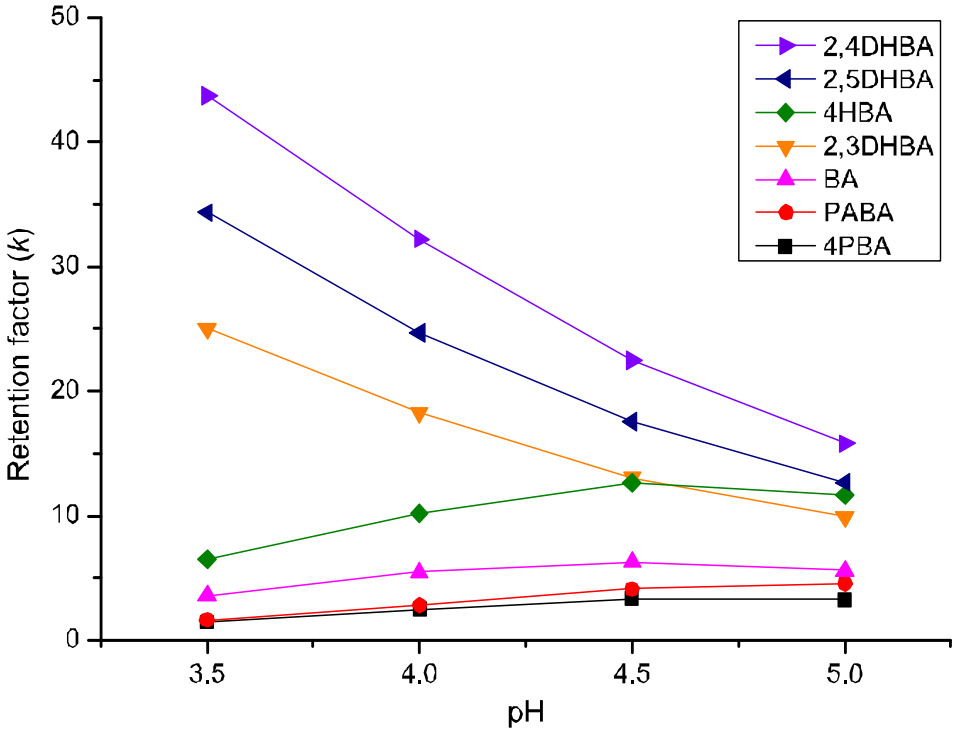


**Figure 5.7:** The influence of buffer pH on retention factor of benzoic acids. Eluent: ACN/40 mM ammonium acetate with various pH (90:10). Other conditions as in Figure 5.6.

protonated. This in turn would lead to stronger electrostatic interaction and therefore longer retention times.

On the other hand, the retention factors of the other four acids remained virtually unchanged between pH 5 and 4.5. Also, in this pH range the elution order of 2,3DHBA and 4HBA was reversed, with a crossover point around pH 4.6. Retention factors then decreased modestly when the pH was decreased further to 3.5. This can be attributed to the fact that when the pH approached the p$K_{a1}$ values of the acids, they became more protonated and the retention was governed by the hydrophilicity of their undissociated forms [128]. Since hydrophilic

interaction is mainly independent of pH [190], retention remained relatively unaltered, except for 4HBA which showed a considerable decrease in retention, possibly because of more polarity difference between its dissociated and undissociated forms. Similar observations were reported by Bui *et al.* for HILIC of organic acids using a column packed with modified silica particles bearing both hydroxyl and amine functionalities [183].

The aforementioned experimental data substantiate the key role of electrostatic interactions in the HILIC mode. However, the contribution of this effect to the overall retention also varies with the content of ACN in the eluent. **Figure 5.8** demonstrates a typical "U"-shaped retention *versus* solvent content curve, being reported frequently for mixed-mode chromatography [179, 188, 190]. The percentage of 40 mM ammonium acetate buffer at pH 5 was changed in the eluent within the 10-50% range.

As can be seen, the retention time of all seven acids decreased by decreasing the ACN concentration from 90 to 80%, which clearly demonstrates the hydrophilic partitioning effect. Also, the elution order of 2,3DHBA and 4HBA changed once again. Worth noting is the similarity of retention behaviour of solutes with similar acidity ($pK_{a1}$). This retention *versus* solvent dependency might also be explained by an ion-exchange effect.

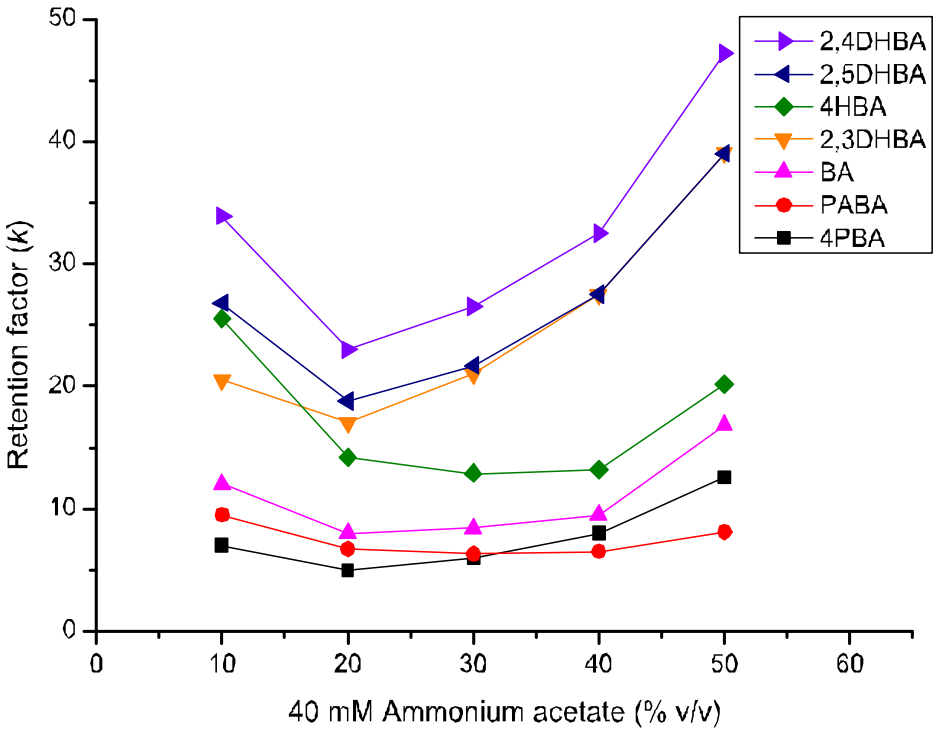


**Figure 5.8:** The influence of ACN content on retention factor of benzoic acids. Eluent: 40 mM ammonium acetate, pH 5 with various concentrations of ACN, flow-rate, 3 µL/min. Other conditions as in Figure 5.6.

Although the pH and concentration of the buffer were kept constant, a decrease in the concentration of the organic solvent would lead to an increase in the activity of eluent ions, ammonium and acetate, due to solvation enhancement, or as suggested by Liu and Pohl [190] an increase in the ionisation of eluent ions, which in turn causes a decrease in the retention of solutes. In fact, the content of organic solvent in the eluent also affects the extent of ionisation of both solutes and stationary phase; and therefore, the electrostatic attraction between them. With a further decrease in ACN content from 80 to 60%, the retention behaviour of benzoic acids with p$K_{a1}$ values around 4, i.e., 4PBA, PABA, BA and 4HBA suggests a compromise between the attraction forces and the

aforementioned ion-exchange effect, demonstrated by an almost constant (PABA) or marginally increased retention over this range. A change in selectivity is also apparent for PABA and 4PBA, with a crossover point at 70% ACN. By comparison, the retention of the remaining three acids ($pK_{a1} \sim 3$) was increased markedly by this change, suggesting an ion-exchange effect superimposed by electrostatic attractions. This might be because the extent of deprotonation of these relatively stronger acids is greater than the first group. Further decreasing the concentration of ACN to 50% showed almost similar upward trends in retention of all benzoic acids, possibly due to even stronger electrostatic attractions.

Column temperature has been well known as an influential parameter in HPLC separations, significantly affecting both mobile phase viscosity as well as solute diffusivity, and its partial molar enthalpy of transfer between mobile and stationary phases [196-198]. Gradient elution in combination with temperature programming also showed an improvement in resolution and separation efficiency of phenolic acids in the HILIC mode [193]. Very recently, Causon *et al.* demonstrated the usefulness of temperature programming, and particularly temperature pulsing, for separation optimisation in capillary LC [199]. The effect of temperature on retention and selectivity of benzoic acids in HILIC conditions was briefly investigated at column temperatures of 30, 45 and 60 ˚C.

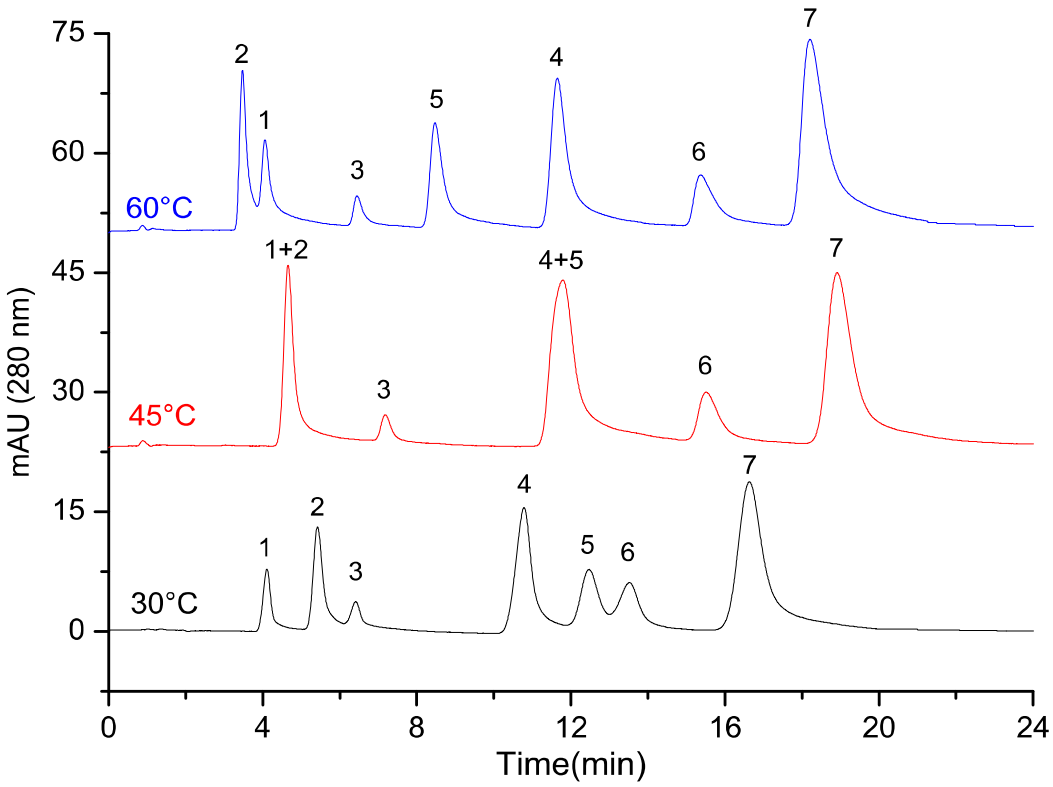


**Figure 5.9:** Effect of column temperature on separation of benzoic acids. Conditions: eluent, ACN/40 mM ammonium acetate pH 5 (90:10); solutes, (1) 4PBA, (2) PABA, (3) BA, (4) 2,3DHBA, (5) 4HBA, (6) 2,5DHBA, and (7) 2,4DHBA; other conditions as in Figure 5.6.

As seen in **Figure 5.9**, the expected decrease in retention with increasing temperature was observed only for PABA and 4HBA, with a more significant decrease for the latter. In comparison, the behaviour of other solutes appeared to be more complicated; the retention increased when increasing the temperature to 45 ˚C, then remained unchanged or decreased slightly when the temperature increased further to 60 ˚C.

This seemingly anomalous behaviour has been attributed to the nature of solutes and differences in their interactions with the mobile and stationary phases [197]. Generally speaking, when retention remains

independent of temperature, the slope of the van't Hoff plots (log *k versus* 1/T), which corresponds to the contribution of the solute transferring enthalpy from mobile to stationary phases, would be close to zero, suggesting that the retention is probably governed entropically [193]. This is also another indication of the involvement of ionic interactions in the overall retention mechanism of the acids studied in this work.

Improvements in separation efficiency at elevated temperatures were also observed, although this was at the cost of an increase in peak tailing for some of the solutes. Theoretical plate numbers as high as 17,000 plates/m were obtained for the last eluted peak (2,4DHBA) at 60 ˚C, demonstrating about 17% enhancement in comparison to 30 ˚C. Although the observed separation efficiency of the polymer-based columns for small molecules was relatively low, particularly in the HILIC mode, these values are still superior to the best plate numbers previously reported for HILIC of phenolic acids (N/m = 11,600 for 4-hydroxyphenyl acetic acid at 80 ˚C) utilizing zwitterionic monoliths [193].

### 5.3.3 Separation of peptides

The suitability of the prepared monolith for the separation of the medium size molecules was examined *via* analysis of peptides released from a tryptic digest of cytochrome c. The analysis of peptides in the HILIC mode has become popular due to the intrinsic advantages of the technique, such as the compatibility of the mobile phase with ESI-MS which results in enhanced detection sensitivity, and the equivalent or

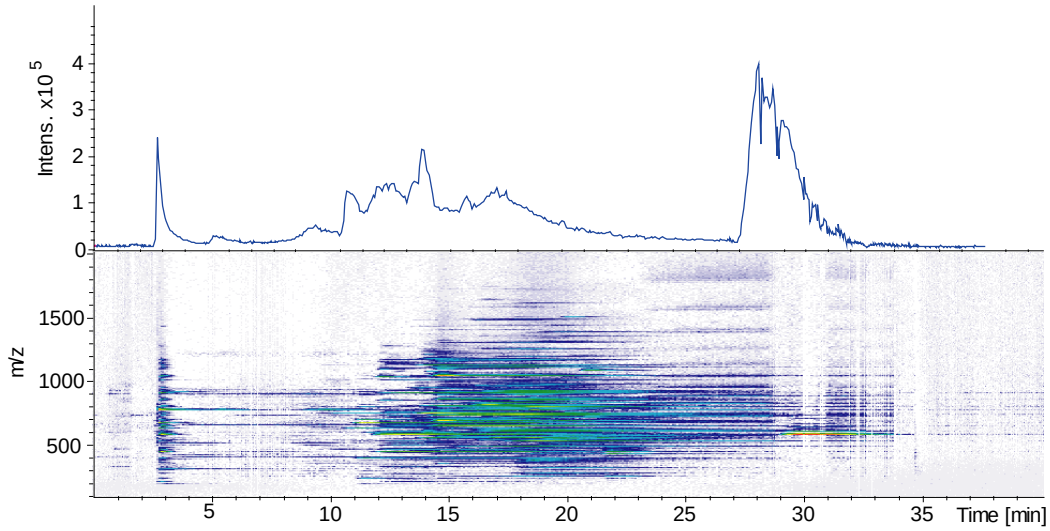


**Figure 5.10:** Base peak chromatogram (upper panel) and the corresponding density view of cytochrome c tryptic digest analysed by HILIC-ESI-qTOF-MS. Conditions: diol-amino column (24 cm × 100 μm i.d.); eluent (A) 0.1 % (v/v) formic acid in ACN, (B) 0.1 % formic acid in water; elution, 5-70 % B in 25 min, 70 % B for 5 min. Sample concentration, 0.5 mg/mL; injection vol., 100 nL; constant column pressure of 100 bar was employed.

better orthogonality of HILIC with RPLC (compared to SCX) in multi-dimensional approaches [130].

The performance of the diol-amino column was therefore evaluated for the peptide fragment fingerprinting. The separation was carried out by running a linear gradient of 0.1% formic acid in ACN to 0.1% formic acid in water. Since most peptides are positively charged at low pH due to the presence of basic amino acids, such as arginine and lysine as well as the terminal amino groups, and because of the expected positive charge on the monolith surface due to the protonation of amino groups, electrostatic repulsion-hydrophilic interaction is likely to govern the separation mechanism here, as suggested by Alpert [126].

The base peak chromatogram as well as the corresponding density view is shown in **Figure 5.10**. The various peptides with diverse charge states and m/z values, derived from the tryptic digested cytochorme c, were detected over the mass range of 400 to 1800 Da with different retention times varying from 7 to 25 min. Additionally, the presence of the undigested protein was also observed with its typical charge state ladder, being eluted between 24 and 29 min. The peptides and their amino acid sequence were identified in a consecutive LC-MS/MS run. Despite a restricted number of selected precursor ions (2) per scan, the obtained MS/MS results showed a high sequence coverage of 80%, when the results were elaborated with MASCOT. The identified peptide fragments are listed in **Table 5.2**.

Although not optimised for chromatographic resolution, this separation demonstrated the potential of this column type for peptide separations. Further investigation on analysis of the tryptic digest was performed employing the amino column. The base peak chromatogram (BPC) corresponding to the separation of tryptic peptides at neutral pH is indicated in **Figure 5.11**. Nearly baseline separation of more than ten peptides was obtained, with sharp and symmetrical peak shape. This separation is clearly superior to that obtained with the diol-amino column under acidic pH. This result might be explained by considering the fact that under the less acidic conditions when employing neutral buffer, the positive charge density on the surface of the column decreases. Together with using a higher ionic strength in the composition of the eluent, this results in weaker ionic interactions between the positively

**Table 5.2:** Identified tryptic peptides from the digestion of horse cytochrome c by HILIC-ESI-MS/MS.

| Observed mass (Da) | Calculated mass $MH^+$ (Da) | Residue | Sequence |
|---|---|---|---|
| 634.3876 (+1) | 633.3850 | 10-14 | IFVQK |
| 584.8068 (+2) | 1167.6149 | 29-39 | TGPNLHGLFGR |
| 648.8550 (+2) | 1295.7099 | 29-40 | TGPNLHGLFGRK |
| 920.9538 (+2) | 1839.9115 | 40-56 | KTGQAPGFTYTDANKNK |
| 614.3055 (+3) | 1839.9115 | 40-56 | KTGQAPGFTYTDANKNK |
| 735.8397 (+2) | 1469.6787 | 41-54 | TGQAPGFTYTDANK |
| 856.9067 (+2) | 1711.8166 | 41-56 | TGQAPGFTYTDANKNK |
| 1041.0071 (+2) | 2080.0186 | 57-73 | GITWKEETLMEYLENPK |
| 694.3409 (+3) | 2080.0186 | 57-73 | GITWKEETLMEYLENPK |
| 737.0375 (+3) | 2208.1136 | 57-74 | GITWKEETLMEYLENPKK |
| 678.3731 (+1) | 677.3748 | 75-80 | YIPGTK |
| 779.4364 (+1) | 778.4411 | 81-87 | MIFAGIK |
| 454.2682 (+2) | 906.5361 | 81-88 | MIFAGIKK |
| 907.5301 (+1) | 906.5361 | 81-88 | MIFAGIKK |
| 493.6064 (+3) | 1477.8140 | 89-100 | KTEREDLIAYLK |
| 739.9063 (+2) | 1477.8140 | 89-100 | KTEREDLIAYLK |
| 803.9525 (+2) | 1605.9090 | 89-101 | KTEREDLIAYLKK |
| 536.3045 (+3) | 1605.9090 | 89-101 | KTEREDLIAYLKK |
| 675.8589 (+2) | 1349.7190 | 90-100 | TEREDLIAYLK |

charged stationary phase and peptides with net negative charges, leading to peaks with less tailing and improved resolution. These observations are also in accordance with the results reported previously by others, and verify significant enhancement in the separation of complex peptide mixtures resulting from an increase in the eluent pH [130].

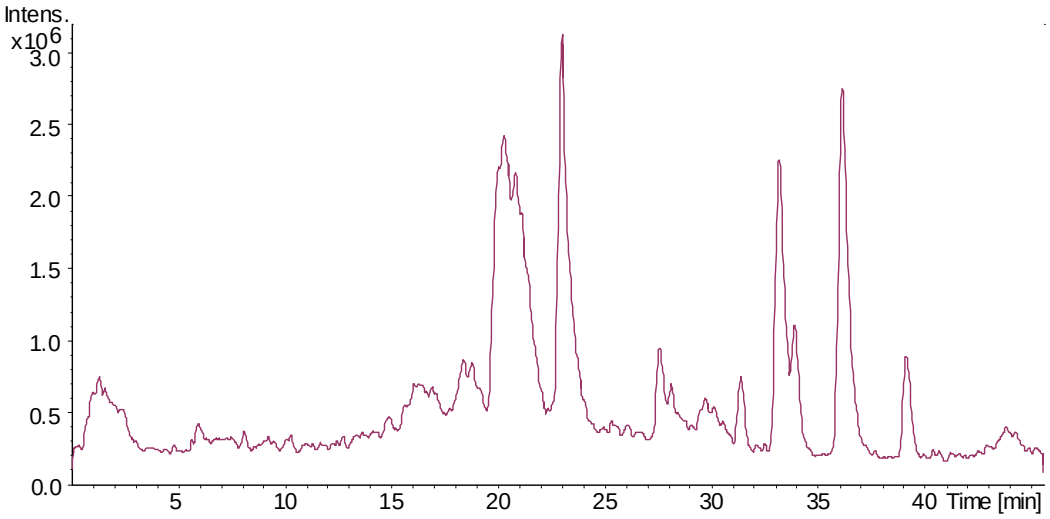


**Figure 5.11:** BPC for HILIC-ESI-IT-MS of cytochrome c tryptic digest. Conditions: amino column (23 cm × 100 μm i.d.); eluent (A) ACN, (B) 20 mM ammonium formate pH 6.2; elution, 5-60 % B in 30 min, 60 % B for 5 min. Flow-rate, 1 μL/min; Sample concentration, 0.3 mg/mL; injection vol., 100 nL.

### 5.3.4 Separation of proteins

One particularly attractive feature of the epoxy-based monoliths is that once polymerisation conditions are optimised for the desired porous properties, pendant reactive groups on the surface can be exploited for incorporating different chemistries through a wide variety of reactions (such as aminolysis or hydrolysis) without the need for re-optimisation of polymerisation conditions. While simple hydrolysis of residual epoxide groups resulted in chemistries suitable for separation of small molecules, the same residual epoxides were targeted for introducing chemistries appropriate for the separation of proteins.

Unlike for peptides, protein denaturation is a common issue in RPLC due to the addition of organic solvents and the strong hydrophobic

interactions involved [74]. An appreciable level of organic solvents also reduces the solubility of biomolecules by decreasing the dielectric constant of the mobile phase [200]. Due to the mild separation conditions involved, IEC, HIC and SEC are therefore methods of choice when preserving proteins in their native conformations is important. While the absence of any kind of interaction between the analytes and the stationary phase is an ideal situation for SEC, hydrophilicity of the separation matrix in HIC, and pore surface in IEC, are preferred in order to prevent non-specific interactions [74, 94].

The developed epoxy-based monoliths were found to possess sufficient hydrophilicity in the monolith scaffold to be suitable for the separation of biomolecules. By taking into account the mole ratio of 2:1 for epoxide to amine in the monomers, an epoxy value of 0.68 mol/100g for GE-100 and a reaction efficiency of 90%, and assuming that both amino groups of EDA were incorporated into the condensation reaction, the content of the residual epoxides in the obtained monolith would roughly be 3.6 mmol/g, which is only 16% lower than the classic poly(GMA-*co*-EDMA) monolith containing 24% GMA. SCX functionalities were then incorporated into the pores through a ring-opening modification of residual epoxides. Because of the presence of amino functionalities in both the monolith skeleton and on the pore surface, the resultant monolith would in fact exhibit a mixed WAX-SCX chemistry.

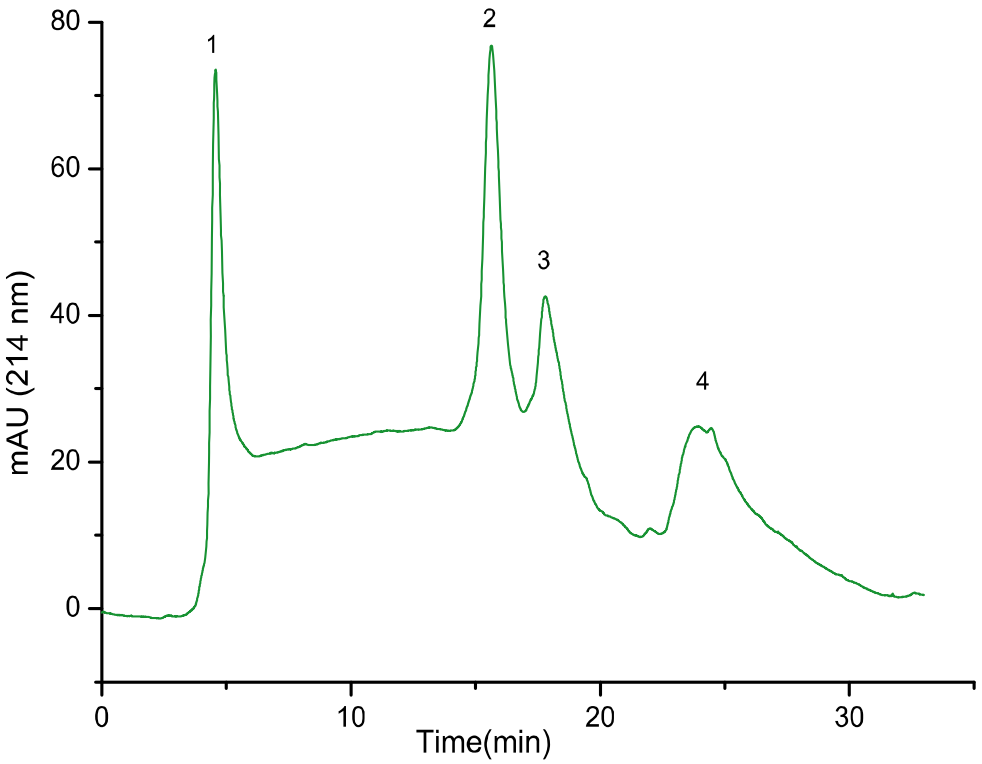


**Figure 5.12:** IEC separation of proteins; conditions: eluent (A) 10 mM phosphate buffer pH 6, (B) 1 M sodium chloride in A; elution, 1-99 % B in 15 min; flow-rate, 1 μL/min; column (WAX-SCX), 15 cm × 100 μm i.d.; peaks are (1) myoglobin, (2) *α*-chymotrypsinogen, (3) cytochrome c, (4) lysozyme; protein concentrations, 0.2 mg/mL each; UV detection at 214 nm.

**Figure 5.12** shows a typical separation of four protein standards using this column. Due to the swelling of the monolith in aqueous eluent (10 mM phosphate buffer, pH 7), the permeability of the column was decreased by this modification, leading to a marked increase in the column back-pressure. A significant shift in the baseline was also observed between ~5-20 min which is assumed to be due to column contamination during the modification process. Nevertheless, the separation efficiency was still satisfactory.

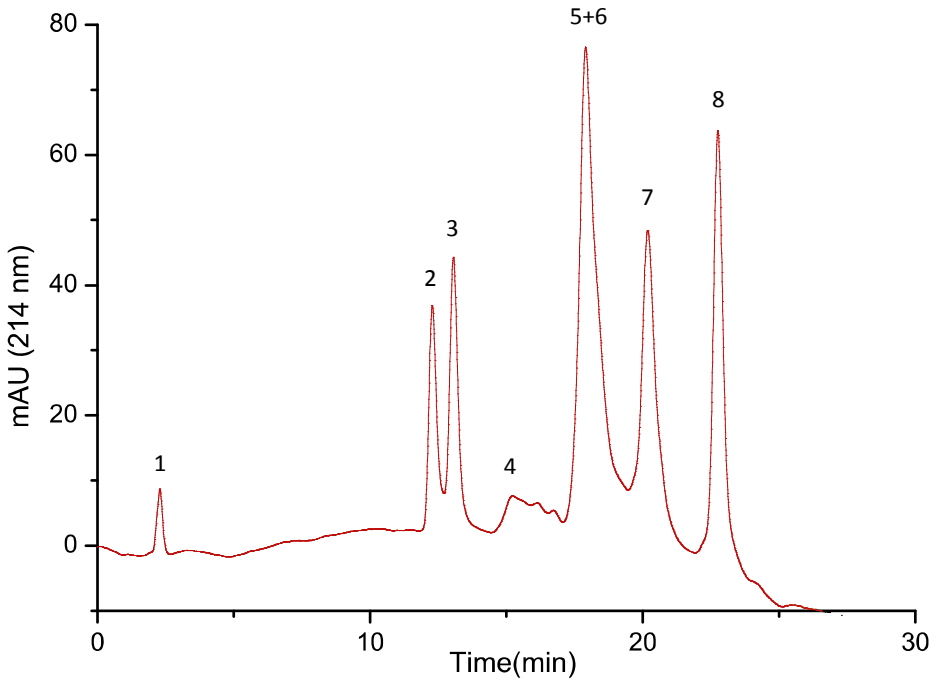


**Figure 5.13:** HIC separation of proteins; conditions: HIC column (18 cm × 100 μm i.d.); eluent (A) 3 M ammonium sulfate in B, (B) 100 mM phosphate buffer pH 7; elution, 0-100 % B in 15 min, 100 % B for 5 min; flow-rate, 0.8 μL/min; peaks: (1) cytochrome c, (2) myoglobin, (3) ribonuclease A, (4) β-lactoglobulin a&b, (5) transferrin, (6) ovalbumin, (7) trypsin, (8) α-chymotrypsinogen; protein concentrations, 0.2 mg/mL each; UV detection at 214 nm.

Usually in HIC stationary phases, mildly hydrophobic ligands are incorporated in a hydrophilic matrix at a concentration of about 10-100 times lower than RP sorbents [81]. The hydrophilicity of the scaffold in the monoliths developed in this work was therefore exploited by integrating hydrophobic chains on the pore surface through a grafting approach. Separation of a test mixture consisting of eight protein standards in the HIC mode is shown in **Figure 5.13**. This column demonstrated superior separation efficiency than its IEX counterpart over the same retention timeframe. Noteworthy is the high concentration of

weak eluent (3 M ammonium sulfate) utilised in order to retain all solutes.

Although cytochrome c was not retained and was eluted at the void time, its peak was not broad or distorted, as seen before under the same conditions [81]. These observations, along with the narrow peak shapes found for other proteins, would suggest a mild hydrophobicity of the modified monolith along with the absence of non-specific interactions, giving suitability for separations in the HIC mode.

### 5.3.5 Reproducibility

The batch-to-batch reproducibility and run-to-run repeatability were evaluated utilising two independently prepared and modified columns for HIC separation of proteins. Since a multi-step process is involved in preparing this type of chemistry and two different people prepared the columns, this approach offered a good test of the column reproducibility. Separation parameters, including retention factor ($k$), peak area ($A$) and resolution ($R_s$) were determined for four well-resolved proteins, namely, myoglobin, ribonuclease A, trypsinogen and $\alpha$-chymotrypsinogen A, from five runs (n = 5). Average relative standard deviations (RSDs) of 0.7, 1.7 and 0.4% were obtained for $k$, $A$ and $R_s$, respectively, suggesting a high reproducibility of column preparation and modification procedures.

One important qualification for HILIC stationary phases is their water retaining property, which reflects the chemical stability of the

material. Inter-day reproducibility of the developed monolith for the HILIC separation of small molecules was also tested by using a diol-amino column continuously for several days and then storing it in aqueous mobile phase for a few weeks. Resuming chromatography of nucleobases and nucleosides using this column showed only minor changes in retention factors of solutes, indicating good chemical stability of the prepared monolith.

## 5.4 Conclusion

Homogenous, highly hydrophilic epoxy-based monoliths were prepared using a polycondensation polymerisation approach. The materials showed high mechanical and chemical stability. Although a decrease in permeability was observed when the polarity of eluents was increased, this did not affect the stability or reproducibility of the column. Diol functionalities, incorporated with simple acid hydrolysis of residual epoxide groups, together with residual amino groups, afforded a unique chemistry for HILIC or mixed-mode separations, depending on the type of analyte and separation conditions. While hydrophilic partitioning appeared to be the primary mechanism involved in retention of highly polar neutral solutes, it was accompanied by electrostatic interactions for charged solutes. The extent of contribution of each effect on the retention and selectivity of acids was shown to be influenced by separation conditions, such as the content of ACN in the eluent, buffer concentration and pH, and the temperature, offering a wider application range with

more flexibility for retention and selectivity tuning during method development.

The HILIC separation of tryptic peptides using this chemistry was also promising. In this case, due to the presence of positive charge on the surface of both analytes and stationary phase, the separation mechanism seemed to be a compromise between electrostatic repulsion and hydrophilic interactions. Surface modification of the monolith also enabled efficient separation of proteins under IEC and HIC modes, with absence of non-specific interactions stemming from the inherent hydrophilicity of the monolith scaffold.

The aforementioned qualities, along with the possibility of incorporating functionalities with a wide variety of properties, can actually widen the applicability of epoxy-based monoliths, especially for bioseparations, which is the focus of future investigations.

# *Chapter 6*

## General Conclusions and Future Directions

The suitability of polymer monolith for bioseparations has been well accepted and demonstrated in a considerable number of publications. In this regard, developing biocompatible monolithic materials featuring minimal non-specific interactions is desirable in order to achieve higher separation efficiency, as a result of better peak shapes, and to preserve the structure of the biomolecules. Two new polymer monoliths were developed in this study possessing this particular feature (hydrophilicity).

A poly(GMA-*co*-PETA) monolith was prepared in 100 μm i.d. capillaries *via* thermally-initiated radical co-polymerisation. PETA as a hydrophilic cross-linker supplied the desired hydrophilicity to the monolith, whereas GMA as a reactive monomer provided the epoxide groups that were exploited for post-polymerisation modification of the monolith. The resulting WCX column containing phosphoric acid functionality, and SCX column containing sulfonic acid functionality demonstrated good separation performance for standard proteins with acceptable dynamic binding capacities compared to the previously reported monoliths used for the same purpose. Ion-exchange capacity and resulting separation performance enhancement for these columns was predicted by further improvement in the quality of the post-polymerisation reactions. For example, the epoxide groups can be

converted to more reactive aldehyde groups, which react readily with amines even in aqueous media and at room temperature [201, 202]. Another possibility is conducting the modification reaction at a pH of 14. In one report, published in 1977 [203], it was shown that at pH 14 (1 M sodium hydroxide) 60% of the epoxide groups in a co-polymer of GMA-EDMA remained preserved even after 9 h at 90 ˚C. Very recently, the suitability of this approach was demonstrated by surface modification of a poly(GMA-*co*-EDMA) capillary monolithic column with cystamine [204]. The reaction was performed twice at 50 ˚C for only 1h each time, probably in order to prevent hydrolysis of siloxane bonds.

Grafting of functionalised monomers is a widely used approach to increase the density of functional groups on the surface of polymers leading to an increase in loading capacity. In this regard, a *"grafting from"* approach through which polymer chains are grown from a surface that was functionalised previously with initiator moieties is particularly suitable for controlling the density of the grafted layer and the prevention of homopolymerisation of the grafting monomer in solution. In monolithic materials, such homopolymerisation can cause a decrease in the permeability of the monolith. Among all *"grafting from"* approaches, attachment of an azo initiator to the pore surface of the monolith appears to be the most convenient and straightforward approach. Commercially available initiators, such as 4,4'-azobis(4-cyanovaleric acid) (ACVA), can be attached directly to the monoliths containing, for example, benzyl chloride functionalities *via* nucleophilic displacement of the chloride groups [205]. Alternatively, ACVA can be first derivatised to 4,4'-

azobis(4-cyanovaleric acid chloride) before attachment to a monolith containing nucleophilic groups, such as amine or thiol functionalities [206].

The application of polymer monoliths for the efficient separation of small molecules has still remained a challenge, mostly due to their monomodal pore size distribution and the absence of mesopores, or alternatively, due to the significant gel porosity in the monolith scaffold in the swollen state [54, 178]. Several attempts have been made to address these limitations, but the more straightforward ones are probably the low density polymerisation [55] and incomplete polymerisation [178]. Low density polymerisation can be achieved by lower percentage of monomers in the polymerisation mixture (typically 20% wt.), whereas incomplete polymerisation is accomplished by termination of polymerisation reaction shortly after starting the reaction (30 min in a typical example [178]. Both approaches resulted in smaller domain size, represented by the combined average size of the macropores and microglobules, leading to significant improvement in the separation of small molecules.

Polycondensation polymerisation is a relatively new approach in making monolithic materials. Using this approach, homogeneous and highly hydrophilic epoxy-based monoliths were developed for the separation of small molecule probes and peptides as well as proteins as large biomolecules. Diol functionalities incorporated with simple acid hydrolysis of residual epoxide groups, together with residual amino

groups, afforded a unique chemistry for HILIC or mixed-mode separations, depending on the type of analyte and separation conditions. Due to the presence of residual amino groups, their density can be increased through the reaction of residual epoxide groups with amines, such as ethylenediamine. Further investigation on modification of the surface chemistry of these materials can be performed *via* a *"grafting from"* approach, as described above. A wide range of monomers with a variety of chemical properties can be incorporated into the pores. For example, incorporation of zwitterionic monomers, which are highly suitable for HILIC of small molecules and peptides [122, 131, 188, 192], can be grafted to the pores of the developed epoxy-based monolith. Because of the hydrophilicity of the monolith scaffold, very hydrophilic monoliths are expected after grafting, which together with the high permeability of these materials can serve as a suitable platform for proteomics studies.

There is an increasing interest on mixed-mode stationary phases, featuring multiple functionalities which enable, for example, comprehensive analysis of complex samples by taking advantage of more than one-type of interactions between solutes and stationary phase [207]. While the developed epoxy-based monolith is mixed-mode by nature, other mixed chemistries than HILIC-IEX can also be feasible to introduce, such as RP-HILIC. RP chemistry can be added to the monolith backbone *via* substituting EDA with a hydrophobic amine such as BACM, or through reacting the residual epoxide groups with hydrophobic reagents. While the former approach requires re-optimisation of the monolith

recipe, due to the difference in reactivity of amine curing agents, the latter approach is a post-polymerisation modification and seems to be more straightforward.

As mentioned earlier, the efficiency of monolithic stationary phases for the separation of small molecules can be increased by decreasing the monolith domain size, i.e., the combined average size of the macropores and microglobules. Further enhancement in the morphology of the developed epoxy-based monolith thus recommended for this purpose. It was shown theoretically that domain geometry can also have a significant contribution into the column efficiency, with more efficiency was suggested for honeycomb-like structure in comparison to hexagonal or circular shapes [208]. This was attributed to the perfect homogeneity of the flow-through pore network leading to up to 10 times smaller Eddy dispersion (the *A* term in the Van Deemter equation).

Unfortunately, attempts at making the developed polymer monoliths in conventional bore format were unsuccessful due mostly to the considerable post-polymerisation shrinkage of the materials. Among all approaches tried, mechanical compression of the monolith provided a more promising column. As mentioned in Chapter 4, this approach has been successfully used by Dionex for making its polymer monolithic columns inside 4.6 mm i.d. PEEK and stainless steel tubes. Special hardware is required, which is commercially available. **Figure 6.1** shows the model provided by Grace (www.discoverysciences.com). Standard HPLC column end-fittings can also be used but the insert (piston) has to

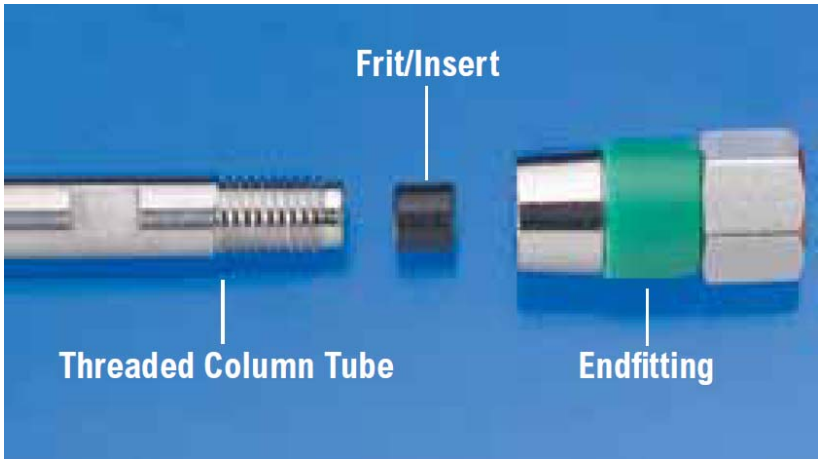


**Figure 6.1:** The empty HPLC column hardware provided by Grace.

be made in-house. To be successful with this approach, the monolith needs to demonstrate enough swelling upon elution with some solvents (chosen based on the polarity of the monolith) to fill the gaps between the monolith body and the column wall. Optimisation of the polymerisation recipe is needed to obtain monoliths with adequate swelling propensity (for more information about swelling propensity of packing materials see, for example, [209]).

Both polymer-based monoliths, prepared by free radical polymerisation approach, and silica-based monoliths are suffer from structural inhomogeneity [54], which can adversely affect their separation efficiency by increasing the Eddy dispersion in the column. More homogeneous structures can be obtained by employing other polymerisation approaches, such as polycondensation, which was performed in this study for the preparation of epoxy-based monoliths. Another approach can be unidirectional freezing. Kim *et al.* [210] reported

on preparation of honeycomb-structured porous monoliths of poly(L-lactic acid) by combining *pseudo*-steady state unidirectional freezing and freeze-drying techniques. Unfortunately, they didn't report any chromatographic study on these materials, but as mentioned before separation enhancement owing to significant reduction in Eddy dispersion is expected from these monoliths.

It is known that a pH gradient IEC can provide superior separation efficiency for biomolecules in terms of peak capacity and resolution compared to its salt-gradient counterpart. This technique has been well accepted as an alternative to preparative gel electrophoresis for isolation and purification of large proteins, such as antibodies from biological matrices [45]. Recently, the suitability of the pH gradient approach for quality control applications, such as resolving charge heterogeneity of mAbs was also demonstrated [17, 21]. Similarly, the same application was targeted, by developing single component buffer systems based on a novel concept called shallow pH gradient over cation-exchange (CEX) monolithic columns. Unlike previous reports, a very low concentration of eluents also enabled direct connection of the separation system to MS for further characterisation.

Although very promising for the investigated purpose, the developed pH gradient approach may suffer from some limitations, such as gradual pH transition of eluents due to the very low concentrations (typically < 5 mM). Combinations of buffer components that cover a wider pH range and provide more stable buffer capacities are therefore

recommended. Due to the ongoing increase of the importance of miniaturisation, further investigations in this area can also be performed by employing capillary IEX columns. The author is aware of only two reports on pH gradient separations using microbore (0.32 mm i.d.) columns [32, 211].

Unfortunately, one issue here is the difficulty of monitoring the pH profile for capillary columns during the elution. Monitoring the pH profile is usually performed to ensure its linearity. However, it has also been shown that high resolution pH gradient separation can still be achieved when the pH profile is not linear, provided the profile has an appropriate slope [36]. Given that the slope of the pH profile can be manipulated by changing the concentration (and pH) of eluents, optimisation of the separation can still be achieved by trial and error without knowing the shape of the pH profile.

An external pH gradient was proposed to address some of the limitations associated with its traditional internal counterpart. As discussed in Chapter 3, the main concerns with CF originate from the polyampholyte elution buffers. Some studies have shown that comparable separations can also be achieved by substituting polyampholytes with simple buffer mixtures (see for example [36]). One great advantage of CF is that it is performed isocraticaly and the composition of both retaining (equilibrating) and eluting buffers can be optimised separately. Also, similar buffer mixtures to those employed in external pH gradients can be used with weak ion-exchange stationary

phases. Thus, employing capillary monolithic columns in the CF approach appears to offer new opportunities for bioseparation, which can be targeted for future investigations.

# References


[1] O'Keefe, D. O., in: Ahuja, S. (Ed.), *Handbook of Bioseparations*, Academic Press 2000, pp. 23-70.

[2] Reichert, J. M., Valge-Archer, V. E., *Nature Reviews* 2007, *6*, 349-356.

[3] Dibner, M. D., *BioPharm* 1997, *10*, 24-30.

[4] Bischoff, R., Bouchon, B., in: Aboul-Enein, H. Y. (Ed.), *Analytical and Preparative Separation Methods of Biomacromolecules*, Marcel Dekker, New York 1999, pp. 13-37.

[5] Aguilar, M.-I., in: Aguilar, M.-I. (Ed.), *HPLC of Peptides and Proteins*, Humana Press 2004, pp. 3-8.

[6] Mant, C. T., Hodges, R. S., *High-Performance Liquid Chromatography of Peptides and Proteins: Separation, Analysis, and Conformation*, Taylor & Francis 1991.

[7] *Ion-Exchange Chromatography: Principles and Methods*, Amersham Biosiences, Uppsala, Sweden 1999.

[8] Wang, F., Dong, J., Jiang, X., Ye, M., Zou, H., *Anal. Chem.* 2007, *79*, 6599-6606.

[9] Chen, X., Tolley, H. D., Lee, M. L., *J. Sep. Sci.* 2011, *34*, 2063-2071.

[10] Stanton, P., in: Aguilar, M.-I. (Ed.), *HPLC of Peptides and Proteins*, Humana Press 2004, pp. 23-43.

[11] Ajit, S., in: Ahuja, S. (Ed.), *Bioseparation of Proteins-Unfolding/Folding and Validations*, Academic Press 1998, pp. 135-176.

[12] Lesins, V., Ruckenstein, E., *J. Colloid Interf. Sci.* 1989, *132*, 566.

[13] Kopaciewicz, W., Regnier, F. E., *Anal. Biochem.* 1983, *133*, 251-259.

[14] Rounds, M. A., Regnier, F. E., *J. Chromatogr.* 1984, *283*, 37.

[15] Regnier, F. E., *Science* 1987, *238*, 319-323.

[16] Ahamed, T., Chilamkurthi, S., Nfor, B. K., Verhaert, P. D., van Dedem, G. W., van der Wielen, L. A., Eppink, M. H., van de Sandt, E. J., Ottens, M., *J. Chromatogr., A* 2008, *1194*, 22-29.

[17] Farnan, D., Moreno, G. T., *Anal. Chem.* 2009, *81*, 8846-8857.

[18] Pabst, T. M., Antos, D., Carta, G., Ramasubramanyan, N., Hunter, A. K., *J Chromatogr A* 2008, *1181*, 83-94.

[19] Pabst, T. M., Carta, G., *J. Chromatogr., A* 2007, *1142*, 19-31.

[20] Perez, J. S., Frey, D. D., *Biotechnol. Prog.* 2005, *21*, 902.

[21] Rozhkova, A., *J. Chromatogr., A* 2009, *1216*, 5989-5994.

[22] Yamamoto, S., Ishihara, T., *J. Chromatogr., A* 1999, *852*, 31.

[23] Kang, X., Frey, D., *J. Chromatogr., A* 2003, *991*, 117-128.

[24] Tsonev, L. I., Hirsh, A. G., *Am. Biotechnol. Lab.* 2009, *27*, 10-12.

[25] Moorhouse, K. G., Nashabeh, W., Deveney, J., Bjork, N. S., Mulkerrin, M. G., Ryskamp, T., *J. Pharm. Biomed. Anal.* 1997, *16*, 593-603.

[26] Teshima, G., Stults, J. T., Ling, V., Canova-Davis, E., *J. Biol. Chem.* 1991, *266*, 13544-13547.

[27] Sluyterman, L. A. Æ., Kooistra, C., *J. Chromatogr., A* 1989, *470*, 317-326.

[28] Sluyterman, L. A. Æ., Wijdenes, J., *J. Chromatogr., A* 1981, *206*, 441-447.

[29] Sluyterman, L. A. Æ., Wijdenes, J., *J. Chromatogr., A* 1981, *206*, 429-440.

[30] Sluyterman, L. A. A. E., Elgersma, O., *J. Chromatogr., A* 1978, *150*, 17-30.

[31] Sluyterman, L. A. A. E., Wijdenes, J., *J. Chromatogr., A* 1978, *150*, 31-44.

[32] Andersen, T., Pepaj, M., Trones, R., Lundanes, E., Greibrokk, T., *J. Chromatogr., A* 2004, *1025*, 217-226.

[33] Liu, Y., Anderson, D. J., *J. Chromatogr., A* 1997, *762*, 207-217.

[34] Kang, X., Frey, D. D., *Anal. Chem.* 2002, *74*, 1038-1045.

[35] Shan, L., Anderson, D. J., *Anal. Chem.* 2002, *74*, 5641-5649.

[36] Kang, X., Bates, R. C., Frey, D. D., *J. Chromatogr., A* 2000, *890*, 37-43.

[37] Kang, X., Frey, D. D., *Biotechnol. Bioeng.* 2004, *87*, 376-387.

[38] Shan, L., Anderson, D. J., *J. Chromatogr., A* 2001, *909*, 191-205.

[39] Shan, L., Hribar, J. A., Zhou, X., Anderson, D. J., *J. Am. Soc. Mass. Spec.* 2008, *19*, 1132-1137.

[40] Waldrep, J. C., Schulte, J. R., *Reg. Immunol.* 1989, *2*, 22-32.

[41] Khawli, L. A., Goswami, S., Hutchinson, R., Kwong, Z. W., Yang, J., Wang, X., Yao, Z., Sreedhara, A., Cano, T., Tesar, D., Nijem, I., Allison, D. E., Wong, P. Y., Kao, Y. H., Quan, C., Joshi, A., Harris, R. J., Motchnik, P., *MAbs* 2010, *2*, 613-624.

[42] Vlasak, J., Ionescu, R., *Curr. Pharm. Biotechnol.* 2008, *9*, 468-481.

[43] Liu, H., Gaza-Bulseco, G., Faldu, D., Chumsae, C., Sun, J., *J. Pharm. Sci.* 2008, *97*, 2426-2447.

[44] Rea, J. C., Moreno, G. T., Lou, Y., Farnan, D., *J. Pharm. Biomed. Anal.* 2011, *54*, 317-323.

[45] Mhatre, R., Nashabeh, W., Schmalzing, D., Yao, X., Fuchs, M., Whitney, D., Regnier, F., *J. Chromatogr., A* 1995, *707*, 225-231.

[46] Lyubarskaya, Y., Houde, D., Woodard, J., Murphy, D., Mhatre, R., *Anal. Biochem.* 2006, *348*, 24-39.

[47] Pristatsky, P., Cohen, S. L., Krantz, D., Acevedo, J., Ionescu, R., Vlasak, J., *Anal. Chem.* 2009, *81*, 6148-6155.

[48] Santora, L. C., Krull, I. S., Grant, K., *Anal. Biochem.* 1999, *275*, 98-108.

[49] Tao, D., Zhang, L., Shan, Y., Liang, Z., Zhang, Y., *Anal. Bioanal. Chem.* 2011, *399*, 229-241.

[50] Freitag, R., Allington, R. W., Brüggemann, O., Frechet, J. M. J., Imamoglu, S., Necina, R., Podgornik, A., Strancar, A., Svec, F., *Modern Advances in Chromatography*, Springer 2002.

[51] Giddings, J. C., *Anal. Chem.* 1984, *56*, 1258A-1260A, 1262A, 1264A passim.

[52] Rozenbrand, J., van, B. W. P., *J. Sep. Sci.* 2011, *34*, 1934-1944.

[53] Nischang, I., Teasdale, I., Brueggemann, O., *Anal. Bioanal. Chem.* 2011, *400*, 2289-2304.

[54] Nischang, I., Teasdale, I., Bruggemann, O., *Anal. Bioanal. Chem.* 2011, *400*, 2289-2304.

[55] Eeltink, S., Herrero-Martinez, J. M., Rozing, G. P., Schoenmakers, P. J., Kok, W. T., *Anal. Chem.* 2005, *77*, 7342-7347.

[56] Gritti, F., Guiochon, G., *J. Chromatogr., A* 2009, *1216*, 4752-4767.

[57] Aoki, H., Tanaka, N., Kubo, T., Hosoya, K., *J. Sep. Sci.* 2009, *32*, 341-358.

[58] Hjertén, S., Liao, J.-L., Zhang, R., *J. Chromatogr., A* 1989, *473*, 273-275.

[59] Svec, F., Frechet, J. M. J., *Anal. Chem.* 1992, *64*, 820-822.

[60] Svec, F., Frechet, J. M., *J. Chromatogr., A* 1995, *702*, 89-95.

[61] Wang, Q. C., Svec, F., Frechet, J. M., *Anal. Chem.* 1995, *67*, 670-674.

[62] Deverell, J. A., Rodemann, T., Smith, J. A., Canty, A. J., Guijt, R. M., *Sensors and Actuators B: Chemical* 2011, *155*, 388-396.

[63] Ott, S., Niessner, R., Seidel, M., *J. Sep. Sci.* 2011, *34*, 2181-2192.

[64] Peskoller, C., Niessner, R., Seidel, M., *J. Chromatogr., A* 2009, *1216*, 3794-3801.

[65] Pflegerl, K., Podgornik, A., Berger, E., Jungbauer, A., *J. Comb. Chem.* 2002, *4*, 33-37.

[66] Svec, F., *J. Chromatogr., A* 2010, *1217*, 902-924.

[67] Svec, F., Fréchet, J. M. J., *Indust. Eng. Chem. Res.* 1998, *38*, 34-48.

[68] Vazquez, M., Paull, B., *Anal. Chim. Acta* 2010, *668*, 100-113.

[69] Nordborg, A., Hilder, E. F., *Anal. Bioanal. Chem.* 2009, *394*, 71-84.

[70] Buchmeiser, M. R., *Polymer* 2007, *48*, 2187-2198.

[71] Urban, J., Jandera, P., *J. Sep. Sci.* 2008, *31*, 2521-2540.

[72] Bakry, R., Huck, C. W., Bonn, G. K., *J. Chromatogr. Sci.* 2009, *47*, 418-431.

[73] Arrua, R. D., Talebi, M., Causon, T. J., Hilder, E. F., *Anal. Chim. Acta* 2012, *738*, 1-12.

[74] Li, Y., Lee, M. L., *J. Sep. Sci.* 2009, *32*, 3369-3378.

[75] Hemstroem, P., Nordborg, A., Irgum, K., Svec, F., Frechet, J. M. J., *J. Sep. Sci.* 2006, *29*, 25-32.

[76] Kennedy, L. A., Kopaciewicz, W., Regnier, F. E., *J. Chromatogr.* 1986, *359*, 73-84.

[77] Gu, B., Li, Y., Lee, M. L., *Anal. Chem.* 2007, *79*, 5848-5855.

[78] Xie, S., Svec, F., Fréchet, J. M. J., *J. Polym. Sci. A Polym. Chem.* 1997, *35*, 1013-1021.

[79] Palm, A. K., Novotny, M. V., *Rapid Commun Mass Spectrom* 2004, *18*, 1374-1382.

[80] Peterka, M., Glover, D., Kramberger, P., Banjac, M., Podgornik, A., Barut, M., Strancar, A., *Bioprocess. J.* 2005, *4*, 79.

[81] Li, Y., Tolley, H. D., Lee, M. L., *J. Chromatogr., A* 2010, *1217*, 4934-4945.

[82] Gu, B., Armenta, J., Lee, M., *J. Chromatogr., A* 2005, *1079*, 382-391.

[83] Li, Y., Tolley, H. D., Lee, M. L., *J. Chromatogr., A* 2010, *1217*, 8181-8185.

[84] Chen, X., Tolley, H. D., Lee, M. L., *J. Chromatogr., A* 2010, *1217*, 3844-3854.

[85] Gu, B., Chen, Z., Thulin, C. D., Lee, M. L., *Anal. Chem.* 2006, *78*, 3509-3518.

[86] Chen, X., Tolley, H. D., Lee, M. L., *J. Chromatogr., A* 2011, *1218*, 4322-4331.

[87] Wang, X., Lin, X., Xie, Z., *Electrophoresis* 2009, *30*, 2702-2710.

[88] Nordborg, A., Hilder, E. F., *Anal Bioanal Chem* 2009, *394*, 71-84.

[89] Bruchet, A., Dugas, V., Mariet, C., Goutelard, F., Randon, J., *J. Sep. Sci.* 2011, *34*, 2079-2087.

[90] Cao, Q., Xu, Y., Liu, F., Svec, F., Frechet, J. M., *Anal. Chem.* 2010, *82*, 7416-7421.

[91] Preinerstorfer, B., Lindner, W., Lammerhofer, M., *Electrophoresis* 2005, *26*, 2005-2018.

[92] Wieder, W., Bisjak, C. P., Huck, C. W., Bakry, R., Bonn, G. K., *J. Sep. Sci.* 2006, *29*, 2478-2484.

[93] Bruchet, A., Dugas, V., Laszak, I., Mariet, C., Goutelard, F., Randon, J., *J. Biomed. Nanotechnol.* 2011, *7*, 415-425.

[94] Krenkova, J., Gargano, A., Lacher, N. A., Schneiderheinze, J. M., Svec, F., *J. Chromatogr., A* 2009, *1216*, 6824-6830.

[95] Hilder, E., Svec, F., Frechet, J., *J. Chromatogr., A* 2004, *1053*, 101-106.

[96] Nilsson, C., Birnbaum, S., Nilsson, S., *J. Chromatogr., A* 2007, *1168*, 212-224; discussion 211.

[97] Jackson, P. E., Haddad, P. R., *Ion Chromatography*, Elsevier Science 1990, p 60.

[98] Thayer, J. R., Flook, K. J., Woodruff, A., Rao, S., Pohl, C. A., *J. Chromatogr., B* 2010, *878*, 933-941.

[99] Xu, Y., Cao, Q., Svec, F., Fréchet, J. M. J., *Anal. Chem.* 2010, *82*, 3352-3358.

[100] Gao, H., Min, K., Matyjaszewski, K., *Macromolecules* 2007, *40*, 7763-7770.

[101] Kannurpatti, A. R., Anseth, J. W., Bowman, C. N., *Polymer* 1998, *39*, 2507-2513.

[102] Andrzejewska, E., *Prog. Polym. Sci.* 2001, *26*, 605-665.

[103] Svec, F., Frechet, J. M. J., *Chem. Mater.* 1995, *5*, 707-715.

[104] Hosoya, K., Hira, N., Yamamoto, K., Nishimura, M., Tanaka, N., *Anal. Chem.* 2006, *78*, 5729-5735.

[105] Xin, P., Shen, Y., Qi, L., Yang, G., Chen, Y., *Talanta* 2011, *85*, 1180-1186.

[106] Tsujioka, N., Hira, N., Aoki, S., Tanaka, N., Hosoya, K., *Macromolecules* 2005, *38*, 9901-9903.

[107] Nguyen, A. M., Irgum, K., *Chem. Mater.* 2006, *18*, 6308-6315.

[108] Tsujioka, N., Ishizuka, N., Tanaka, N., Kubo, T., Hosoya, K., *J. Polym. Sci. A Polym. Chem.* 2008, *46*, 3272-3281.

[109] Liu, J., Ren, L., Liu, Y., Li, H., Liu, Z., *J. Chromatogr., A* 2012, *1228*, 276-282.

[110] Nischang, I., Svec, F., Frechet, J. M. J., *J. Chromatogr., A* 2009, *1216*, 2355-2361.

[111] Hosoya, K., Mori, T., Sakamoto, M., Kubo, T., Kaya, K., *Chromatographia* 2009, *70*, 699-704.

[112] Wang, F., Chen, R., Zhu, J., Sun, D., Song, C., Wu, Y., Ye, M., Wang, L., Zou, H., *Anal. Chem.* 2010, *82*, 3007-3015.

[113] Shen, Y., Zhao, R., Berger, S. J., Anderson, G. A., Rodriguez, N., Smith, R. D., *Anal. Chem.* 2002, *74*, 4235-4249.

[114] Tao, D., Zhu, G., Sun, L., Ma, J., Liang, Z., Zhang, W., Zhang, L., Zhang, Y., *Proteomics* 2009, *9*, 2029-2036.

[115] Giddings, J. C., *Anal Chem* 1984, *56*, 1258A-1260A, 1262A, 1264A passim.

[116] Nischang, I., Svec, F., Frechet, J. M., *Anal. Chem.* 2009, *81*, 7390-7396.

[117] Guiochon, G., *J. Chromatogr., A* 2007, *1168*, 101-168; discussion 100.

[118] Ivanov, A. R., Zang, L., Karger, B. L., *Anal. Chem.* 2003, *75*, 5306-5316.

[119] Zhang, J., Wu, S.-L., Kim, J., Karger, B. L., *J. Chromatogr., A* 2007, *1154*, 295-307.

[120] Ro, K. W., Nayak, R., Knapp, D. R., *Electrophoresis* 2006, *27*, 3547-3558.

[121] Moravcova, D., Kahle, V., Rehulkova, H., Chmelik, J., Rehulka, P., *J. Chromatogr., A* 2009, *1216*, 3629-3636.

[122] Di Palma, S., Boersema, P. J., Heck, A. J., Mohammed, S., *Anal. Chem.* 2011, *83*, 3440-3447.

[123] Wang, F., Dong, J., Jiang, X., Ye, M., Zou, H., *Anal Chem* 2007, *79*, 6599-6606.

[124] Link, A. J., Eng, J., Schieltz, D. M., Carmack, E., Mize, G. J., Morris, D. R., Garvik, B. M., Yates, J. R., 3rd, *Nature Biotechnol.* 1999, *17*, 676-682.

[125] Alpert, A. J., *J. Chromatogr.* 1990, *499*, 177-196.

[126] Alpert, A. J., *Anal. Chem.* 2008, *80*, 62-76.

[127] Guo, Y., Gaiki, S., *J. Chromatogr., A* 2005, *1074*, 71-80.

[128] Hatambeygi, N., Abedi, G., Talebi, M., *J. Chromatogr., A* 2011, *1218*, 5995-6003.

[129] Alpert, A. J., Shukla, M., Shukla, A. K., Zieske, L. R., Yuen, S. W., Ferguson, M. A., Mehlert, A., Pauly, M., Orlando, R., *J. Chromatogr., A* 1994, *676*, 191-122.

[130] Yang, Y., Boysen, R. I., Hearn, M. T., *J. Chromatogr., A* 2009, *1216*, 5518-5524.

[131] Boersema, P. J., Mohammed, S., Heck, A. J., *Anal. Bioanal. Chem.* 2008, *391*, 151-159.

[132] Scott, N. E., Parker, B. L., Connolly, A. M., Paulech, J., Edwards, A. V., Crossett, B., Falconer, L., Kolarich, D., Djordjevic, S. P., Hojrup, P., Packer, N. H., Larsen, M. R., Cordwell, S. J., *Mol. Cell Proteomics* 2011, *10*, M000031-MCP000201.

[133] Wu, C. J., Chen, Y. W., Tai, J. H., Chen, S. H., *J. Proteome Res.* 2011, *10*, 1088-1097.

[134] Gilar, M., Olivova, P., Daly, A. E., Gebler, J. C., *Anal. Chem.* 2005, *77*, 6426-6434.

[135] Boersema, P. J., Divecha, N., Heck, A. J., Mohammed, S., *J. Proteome Res.* 2007, *6*, 937-946.

[136] Ahamed, T., Nfor, B. K., Verhaert, P. D., van Dedem, G. W., van der Wielen, L. A., Eppink, M. H., van de Sandt, E. J., Ottens, M., *J. Chromatogr., A* 2007, *1164*, 181-188.

[137] Dean, J. A., *Lange's Handbook of Chemistry*, McGraw-Hill, New York 1999.

[138] Rohr, T., Hilder, E. F., Donovan, J. J., Svec, F., Fréchet, J. M. J., *Macromolecules* 2003, *36*, 1677-1684.

[139] Smirnov, K. N., Dyatchkov, I. A., Telnov, M. V., Pirogov, A. V., Shpigun, O. A., *J. Chromatogr., A* 2010, *1218*, 5510-5519.

[140] Urban, J., Svec, F., Frechet, J. M., *J. Chromatogr., A* 2010, *1217*, 8212-8221.

[141] Etzel, M. R., Riordan, W. T., *J. Chromatogr., A* 2009, *1216*, 2621-2624.

[142] Perkins, M., Theiler, R., Lunte, S., Jeschke, M., *Pharm. Res.* 2000, *17*, 1110-1117.

[143] Harris, R. J., Kabakoff, B., Macchi, F. D., Shen, F. J., Kwong, M., Andya, J. D., Shire, S. J., Bjork, N., Totpal, K., Chen, A. B., *J. Chromatogr., B* 2001, *752*, 233-245.

[144] *Q6B: Specifications: Test procedures and acceptance criteria for biotechnology, Federal Register* 1996, *63*, 31506-31513.

[145] Tsonev, L. I., Hirsh, A. G., *J. Chromatogr., A* 2008, *1200*, 166-182.

[146] Sosic, Z., Houde, D., Blum, A., Carlage, T., Lyubarskaya, Y., *Electrophoresis* 2008, *29*, 4368-4376.

[147] He, Y., Lacher, N. A., Hou, W., Wang, Q., Isele, C., Starkey, J., Ruesch, M., *Anal. Chem.* 2010, *82*, 3222-3230.

[148] Xie, S., Allington, R. W., Svec, F., Frechet, J. M. J., *J. Chromatogr., A* 1999, *865*, 169-174.

[149] Nordborg, A., Zhang, B., He, X. Z., Hilder, E. F., Haddad, P. R., *J. Sep. Sci.* 2009, *32*, 2668-2673.

[150] Liu, Y., Anderson, D. J., *J. Chromatogr., A* 1997, *762*, 47-54.

[151] Rehder, D. S., Dillon, T. M., Pipes, G. D., Bondarenko, P. V., *J. Chromatogr., A* 2006, *1102*, 164-175.

[152] Chen, X., Tolley, H. D., Lee, M. L., *J Chromatogr A* 2010, *1217*, 3844-3854.

[153] Wolters, D. A., Washburn, M. P., Yates, J. R., 3rd, *Anal. Chem.* 2001, *73*, 5683-5690.

[154] Alpert, A. J., Andrews, P. C., *J. Chromatogr.* 1988, *443*, 85-96.

[155] Chen, X., Tolley, H. D., Lee, M. L., *J. Sep. Sci.* 2009, *32*, 2565-2573.

[156] Peters, E. C., Petro, M., Svec, F., Frechet, J. M., *Anal. Chem.* 1998, *70*, 2288-2295.

[157] Yang, G., Liu, H., Zhang, Y., Wang, S., Yin, J., Yin, B., Chen, Y., *J. Chromatogr., A* 2006, *1129*, 231-235.

[158] Bruchet, A., Dugas, V., Mariet, C., Goutelard, F., Randon, J., *J Sep Sci* 2011, n/a-n/a.

[159] Wang, M., Xu, J., Zhou, X., Tan, T., *J. Chromatogr., A* 2007, *1147*, 24-29.

[160] Dinh, N. P., Cam, Q. M., Nguyen, A. M., Shchukarev, A., Irgum, K., *J. Sep. Sci.* 2009, *32*, 2556-2564.

[161] Hutchinson, J. P., Hilder, E. F., Shellie, R. A., Smith, J. A., Haddad, P. R., *Analyst* 2006, *131*, 215-221.

[162] Ueki, Y., Umemura, T., Li, J., Odake, T., Tsunoda, K., *Anal. Chem.* 2004, *76*, 7007-7012.

[163] Li, Y., Gu, B., Tolley, H. D., Lee, M. L., *J. Chromatogr., A* 2009, *1216*, 5525-5532.

[164] Krenkova, J., Lacher, N. A., Svec, F., *Anal. Chem.* 2009, *81*, 2004-2012.

[165] Chen, M. L., Wei, S. S., Yuan, B. F., Feng, Y. Q., *J. Chromatogr., A* 2012, *1228*, 183-192.

[166] Gunasena, D. N., El Rassi, Z., *J. Sep. Sci.* 2011.

[167] Lin, J., Lin, J., Lin, X., Xie, Z., *J. Chromatogr., A* 2009, *1216*, 801-806.

[168] Wang, X., Lin, X., Xie, Z., Giesy, J. P., *J. Chromatogr., A* 2009, *1216*, 4611-4617.

[169] Huang, H., Lin, Z., Lin, Y., Sun, X., Xie, Y., Zhang, L., Chen, G., *J. Chromatogr., A* 2012, *1251*, 82-90.

[170] Wang, X., Ding, K., Yang, C., Lin, X., Lu, H., Wu, X., Xie, Z., *Electrophoresis* 2010, *31*, 2997-3005.

[171] Courtois, J., Bystrom, E., Irgum, K., *Polymer* 2006, *47*, 2603-2611.

[172] Sykora, D., Svec, F., Frechet, J. M., *J. Chromatogr., A* 1999, *852*, 297-304.

[173] Allington, R. W., Xie, S., Jiang, T., Xu, M., Isco, Inc., USA; Dionex Corporation . 2004, pp. 54 pp., Cont.-in-part of U.S. Ser. No. 180,350.

[174] Greiderer, A., Trojer, L., Huck, C. W., Bonn, G. K., *J. Chromatogr., A* 2009, *1216*, 7747-7754.

[175] Lubbad, S. H., Buchmeiser, M. R., *J. Sep. Sci.* 2009, *32*, 2521-2529.

[176] Hosoya, K., Hira, N., Yamamoto, K., Nishimura, M., Tanaka, N., *Anal Chem* 2006, *78*, 5729-5735.

[177] Liu, K., Tolley, H. D., Lee, M. L., *J. Chromatogr., A* 2012, *1227*, 96-104.

[178] Nischang, I., Bruggemann, O., *J. Chromatogr., A* 2010, *1217*, 5389-5397.

[179] Urban, J., Svec, F., Frechet, J. M., *Anal. Chem.* 2010, *82*, 1621-1623.

[180] Causon, T. J., Shellie, R. A., Hilder, E. F., *Analyst* 2009, *134*, 440-442.

[181] Greiderer, A., Ligon, S. C., Jr., Huck, C. W., Bonn, G. K., *J. Sep. Sci.* 2009, *32*, 2510-2520.

[182] Chambers, S. D., Svec, F., Frechet, J. M., *J. Chromatogr., A* 2011, *1218*, 2546-2552.

[183] Bui, T. N., Verhage, J. J., Irgum, K., *J. Sep. Sci.* 2010, *33*, 2965-2976.

[184] Peters, E. C., Svec, F., Fréchet, J. M. J., *Adv. Mater.* 1997, *9*, 630-633.

[185] Courtois, J., Byström, E., Irgum, K., *Polymer* 2006, *47*, 2603-2611.

[186] Siouffi, A. M., *J Chromatogr A* 2006, *1126*, 86-94.

[187] Chen, M. L., Li, L. M., Yuan, B. F., Ma, Q., Feng, Y. Q., *J. Chromatogr., A* 2012, *1230*, 54-60.

[188] Jiang, Z., Smith, N. W., Ferguson, P. D., Taylor, M. R., *Anal. Chem.* 2007, *79*, 1243-1250.

[189] Gilar, M., Yu, Y. Q., Ahn, J., Fournier, J., Gebler, J. C., *J. Chromatogr., A* 2008, *1191*, 162-170.

[190] Liu, X., Pohl, C. A., *J. Sep. Sci.* 2010, *33*, 779-786.

[191] Zhang, K., Dai, L., Chetwyn, N. P., *J. Chromatogr., A* 2010, *1217*, 5776-5784.

[192] Jiang, Z., Smith, N. W., Ferguson, P. D., Taylor, M. R., *J. Sep. Sci.* 2009, *32*, 2544-2555.

[193] Skerikova, V., Jandera, P., *J. Chromatogr., A* 2010, *1217*, 7981-7989.

[194] Hemstrom, P., Irgum, K., *J. Sep. Sci.* 2006, *29*, 1784-1821.

[195] Dean, J. A., McGraw-Hill, New York 1999.

[196] Horvath, C. G., Preiss, B. A., Lipsky, S. R., *Anal. Chem.* 1967, *39*, 1422-1428.

[197] Hao, Z., Xiao, B., Weng, N., *J. Sep. Sci.* 2008, *31*, 1449-1464.

[198] Padivitage, N. L., Armstrong, D. W., *J. Sep. Sci.* 2011, *34*, 1636-1647.

[199] Causon, T. J., Cortes, H. J., Shellie, R. A., Hilder, E. F., *Anal. Chem.* 2012, *84*, 3362-3368.

[200] Chen, X., Tolley, H. D., Lee, M. L., *J Sep Sci* 2011.

[201] Dong, X., Dong, J., Ou, J., Zhu, Y., Zou, H., *Electrophoresis* 2007, *28*, 2606-2612.

[202] Gunasena, D. N., El, R. Z., *J. Sep. Sci.* 2011, *34*, 2097-2105.

[203] Hrudkova, H., Svec, F., Kalal, J., *Brit. Polym. J.* 1977, *9*, 238-240.

[204] Lv, Y., Lin, Z., Svec, F., *Analyst* 2012, *137*, 4114-4118.

[205] Tripp, J. A., Svec, F., Frechet, J. M., *J. Comb. Chem.* 2001, *3*, 216-223.

[206] Peng, X. T., Yuan, B. F., Feng, Y. Q., *J. Sep. Sci.* 2011, *34*, 3123-3130.

[207] Lammerhofer, M., Richter, M., Wu, J., Nogueira, R., Bicker, W., Lindner, W., *J Sep Sci* 2008, *31*, 2572-2588.

[208] Gzil, P., De Smet, J., Vervoort, N., Verelst, H., Baron, G. V., Desmet, G., *J Chromatogr A* 2004, *1030*, 53-62.

[209] Nevejans, F., Verzele, M., *J. Chromatogr.* 1985, *350*, 145.

[210] Kim, J.-W., Taki, K., Nagamine, S., Ohshima, M., *Chemical Engineering Science* 2008, *63*, 3858-3863.

[211] Li, Y. M., Liao, J. L., Zhang, R., Henriksson, H., Hjerten, S., *Anal. Biochem.* 1999, *267*, 121-124.